Matter-Only Cosmology: A Unified Origin for Inflation and Dark Energy

Hyoyoung Choi[1*]

1 Independent Researcher, Gunsan, Republic of Korea.

∗ E-mail:7icarus7@gmail.com

Abstract

The standard cosmological model, ΛCDM, successfully describes cosmic acceleration, but it treats dark energy as an independent and poorly understood component of the universe. In this paper, we show that dark energy is not a fundamental entity separate from matter, but is instead the total gravitational self-energy (GSE) inherent to matter itself. Matter-Only Cosmology (MOC) expresses the dark energy density solely as a function of the matter density ρ_m and the compactness ratio R_S/χ_p, without introducing new fundamental fields. The matter-induced dark energy density is given by $\rho_{\Lambda_m} = \frac{\beta\rho_m}{2}\frac{R_S}{\chi_p}\left(\frac{5\beta}{14}\frac{R_S}{\chi_p} - 1\right)$, where $R_S = 2GM/c^2$ is the Schwarzschild radius of the causally connected mass and χ_p is the comoving particle horizon. Thus, the compactness ratio determines the transition between the attractive and repulsive GSE regimes. Because ρ_{Λ_m} is explicitly tied to ρ_m, dark energy is reinterpreted as a matter-induced form of energy rather than as an independent energy component. The dark energy density is negative in the early universe, thereby enhancing structure formation, before later transitioning to a positive phase that drives cosmic acceleration. In this way, MOC naturally addresses the Hubble tension, the existence of massive galaxies in the early universe, the observed present-day dark energy density, its late-time quasi-constant behavior, recent indications of a weakening dark energy component, and the cosmological constant coincidence problem. Moreover, MOC unifies inflation and late-time cosmic acceleration under the same GSE principle, and it provides a natural built-in termination mechanism for primordial inflation. Finally, by predicting macroscopic non-singular cores inside black holes, MOC offers a physically motivated route toward resolving the black hole information paradox. By expressing dark energy as an explicit function of the matter density ρ_m and the compactness R_S/χ_p , the MOC framework transforms it from a phenomenological parameter into a predictive and falsifiable physical quantity.

Contents

Part I. Core Theory

1 Introduction

The discovery of the accelerated expansion of the universe [1,2] marked a monumental turning point in modern cosmology. To account for this unexpected cosmic acceleration, the standard cosmological model, ΛCDM, introduced an additional component commonly referred to as dark energy [3,4]. Characterized phenomenologically by a positive energy density and a negative pressure, the cosmological constant Λ has proven remarkably successful in reproducing the observed large-scale dynamics of the universe [5].

However, despite its empirical success, the ΛCDM framework faces several deep and persistent conceptual challenges [6,7]. In particular, the physical origin of dark energy remains unknown, indicating that our current description of the cosmic energy budget may be incom-

plete.

In this work, we argue that the origin of these difficulties does not necessarily require the introduction of new particles, exotic fields, or modifications of gravity, but instead points to an incomplete accounting of the total energy density in gravitating systems, whose consequences become manifest in the Friedmann equations.

Within the standard cosmological framework, dark energy is modeled as a perfect fluid with a constant equation-of-state parameter $w = -1$ [3,4]. While this assumption provides an excellent phenomenological fit to current data, it is not derived from first principles. The most widely discussed candidate, vacuum energy, leads to the well-known cosmological constant problem, namely a discrepancy of order 10^{60}–10^{120} between theoretical expectations from quantum field theory and the observed value of Λ [7,8]. In addition, the model suffers from the so-called coincidence problem, which asks why the dark energy density becomes dynamically relevant only in the current cosmological epoch [3,9].

Beyond these theoretical concerns, recent observational results have motivated renewed scrutiny of the simplest ΛCDM scenario and of possible extensions with evolving dark energy [10–12]. In particular:

1) **The Hubble tension:** A persistent discrepancy exists between the Hubble constant inferred from early-universe observations of the cosmic microwave background (CMB) and that measured directly in the local universe. This tension may indicate physics beyond a strictly constant dark energy component [5,10,13]. Quantitatively, $H_0(\mathrm{CMB}) \approx 67.36$ $\mathrm{km\,s^{-1}\,Mpc^{-1}}$ compared to $H_0(\mathrm{local}) \approx 74.0\,\mathrm{km\,s^{-1}\,Mpc^{-1}}$ [5,13].

2) **Supernova constraints:** Recent analyses of nearly 1500 Type Ia supernovae by the Dark Energy Survey (DES) collaboration suggest that a time-independent cosmological constant may not provide the best fit to the data, allowing room for a dynamical dark energy component [12].

3) **Spectroscopic measurements:** Independent results from the Dark Energy Spectroscopic Instrument (DESI) have likewise increased interest in models with evolving dark energy, further challenging the assumption of a strictly constant Λ [11].

Taken together, these theoretical and observational tensions motivate a reassessment of the physical origin of cosmic acceleration. In this paper, we propose that these issues arise from a long-standing omission in the standard treatment of gravitating systems: the failure to explicitly account for gravitational self-energy (GSE) as a contribution to the gravitational source term, as required by the equivalence principle of General Relativity.

1.1 Components of total mass or equivalent mass in a gravitational system

In gravitational physics, it is customary to characterize a gravitating system by an effective or equivalent energy (or mass) that reproduces its external gravitational influence [14–16]. Even when the detailed composition of the source's internal energy is unknown, one may treat the system as possessing an equivalent mass that implicitly incorporates all internal energy contributions, thereby enabling a consistent description of its external gravitational interactions within a given approximation scheme [14,15].

Because this equivalent energy–mass framework has been remarkably successful for analyzing external gravitational fields, it is often unnecessary to specify how the equivalent mass is decomposed into its microscopic or internal energy components.

However, this simplification becomes conceptually insufficient when one attempts to analyze the internal energy composition of a gravitating system itself, rather than merely its external gravitational influence.

In cosmology, this distinction becomes particularly important. The system under consideration is not an isolated object embedded in an external spacetime, but the universe itself, within which matter and galaxies reside. Consequently, questions concerning the internal energy structure and self-gravitating dynamics of the cosmic matter distribution can no longer be avoided when interpreting the total gravitating energy budget.

For a generic bound system, the total mass, or more precisely the total energy E_T, can be expressed as the sum of the free-state rest-mass energy of its constituents and all internal binding and interaction energies [14, 16]:

$$E_T = M_{fr}c^2 + \sum_i U_{\mathrm{BE},i} + \sum_{i>j} U_{\mathrm{int},ij}. \tag{1}$$

Here $M_{fr}c^2$ denotes the sum of the rest-mass energies of the constituents in their free states. The terms $U_{\mathrm{BE},i}$ represent binding energies associated with composite structures, including gravitational, electromagnetic, weak, and strong interactions. The quantities $U_{\mathrm{int},ij}$ denote interaction energies between different constituents or subsystems.

Dividing by c^2 yields the corresponding total equivalent mass $M_T \equiv E_T/c^2$, which is the quantity that acts as the effective gravitational source in many external-field problems [14–16].

1.2 A conceptual analogy: Binding energy in the hydrogen atom and a missing term in the Friedmann equation

A useful analogy for understanding the role of GSE in cosmology is provided by the hydrogen atom. A hydrogen atom is a composite system consisting of a proton and an electron bound together by electromagnetic interaction. Likewise, the universe may be regarded as a composite gravitating system composed of many constituents, such as matter, galaxies, and large-scale structures, which interact gravitationally over cosmological scales.

The total energy of a hydrogen atom is given by

$$E_H = E_p + E_e + U_{\mathrm{binding}}. \tag{2}$$

Here E_p and E_e are the rest-mass energies of the proton and electron in their free states.

The quantity $U_{\mathrm{binding}} < 0$ denotes the electromagnetic binding energy. Because the binding energy is negative, the total energy and hence the invariant mass of the hydrogen atom is smaller than the sum of the free-state particle masses. When a hydrogen atom acts as a gravitational source, the gravitating mass is, in principle, determined by its total energy content, including the contribution from binding energy, rather than by the free-state particle masses alone.

Correspondingly, one may express the total equivalent mass density schematically as

$$\rho_T = \rho_p + \rho_e + \rho_{\mathrm{binding}}. \tag{3}$$

Here $\rho_{\mathrm{binding}} \equiv U_{\mathrm{binding}}/(Vc^2)$ represents the contribution of binding energy per unit volume V. This viewpoint, namely that internal binding energy contributes to the total mass-energy of a bound system, is standard in atomic, nuclear, and particle physics [14].

Let us now examine what is effectively assumed in standard cosmology. Neglecting the spatial curvature term for simplicity, the Friedmann equation is written as

$$H^2 = \frac{8\pi G}{3}\rho_T = \frac{8\pi G}{3}(\rho_m + \rho_\Lambda). \tag{4}$$

Here ρ_m denotes the matter density.

The quantity ρ_Λ is introduced as a separate dark energy component [3, 5]. In practice, ρ_m is constructed from the free-state mass densities of matter constituents (baryons and dark matter), analogous to using $\rho_p + \rho_e$ for the hydrogen atom. Observationally, however, the inferred matter density alone is subcritical at late times, while the expansion history indicates a total energy density close to the critical value. This motivates the introduction of an additional energy density component ρ_Λ within the standard cosmological interpretation [1, 2, 5, 8].

We argue that this procedure may reflect an incomplete accounting of the total gravitating energy budget. From the standpoint of General Relativity, the source term governing cosmic expansion is the total stress-energy content, which suggests that all relevant contributions to the system's energy, including those associated with self-gravitating interactions, should in principle be taken into account [14–17].

In a cosmological context, this motivates considering a decomposition of the form

$$\rho_T = \rho_{\text{free}} + \rho_{\text{GSE}}. \tag{5}$$

Here ρ_{GSE} represents an effective contribution associated with GSE. This term arises from the mutual gravitational interactions of matter within the causally connected region.

By omitting such a contribution and modeling the additional required energy density as an independent fluid component, standard cosmology introduces ρ_Λ phenomenologically. We argue that the physical origin of dark energy lies in GSE itself, and that the introduction of ρ_Λ in standard cosmology reflects a systematic omission of this contribution from the total gravitating energy density.

Finally, we note an important conceptual point. Gravitational binding energy is conventionally negative, as it represents the energy required to disassemble a bound system into free components [14–16]. However, as will be shown in the following sections, the self-gravitating contribution to the cosmological energy budget is not restricted to being purely negative. Depending on the scale and compactness of the causally connected system, the net contribution associated with GSE can become positive and thereby act as a source of repulsive cosmic dynamics.

This perspective suggests that what is conventionally identified as dark energy may instead reflect an intrinsic manifestation of GSE, consistently included in the total energy accounting as required by the principles of General Relativity.

1.3 Gravitational field energy vs. gravitational self-energy

A frequent source of confusion in discussions of GSE arises from conflating it with the energy of the gravitational field itself. In General Relativity, it is well established that the energy of the gravitational field cannot be localized in a coordinate-independent manner [14, 15, 18]. Because the gravitational field extends beyond the material source and depends on the choice of coordinates, no unique local energy density can be assigned to it. For this reason, gravitational field energy does not appear explicitly as a source term in the Einstein field equations, but is instead encoded implicitly through their nonlinear structure [14, 15, 18].

GSE, however, represents a conceptually distinct physical quantity. It does not correspond to the energy of the gravitational field in empty space, but rather to the gravitational potential energy associated with interactions among the constituents of a gravitating system [14, 16]. As such, GSE is defined with respect to the finite mass distribution and finite spatial extent of the system itself.

In contrast to gravitational field energy, GSE is defined with respect to the finite mass distribution and finite spatial extent of the system, and therefore contributes to the total energy characterizing that system in a well-defined manner [14, 16].

> *The mass energy of a gravitating system includes the negative binding energy, such that the total gravitational mass is less than the sum of the constituent rest masses.* [16]

The distinction between gravitational field energy and gravitational self-energy is also reflected in tests of the strong equivalence principle. Nordtvedt-effect analyses ask whether the gravitational self-energy contained in an extended body contributes to its gravitational mass in the same way as other forms of energy [16, Sec. 1.6]. The absence of an observed Nordtvedt effect in the Earth–Moon system supports the standard GR expectation that gravitational self-energy gravitates normally [16, Sec. 1.6]. Thus, the GSE term used here is best understood as a contribution to the equivalent mass of a finite matter distribution, not as a local energy density of the gravitational field.

This distinction is familiar in other areas of physics. In atomic physics, for example, the mass of a hydrogen atom is smaller than the sum of the rest masses of a free proton and electron. The difference corresponds to the negative electromagnetic binding energy, which contributes to the invariant mass of the bound system. The atom is therefore treated as a single object whose total mass already incorporates its internal binding energy.

There is no compelling physical reason to treat gravity differently in this respect. Although gravitational field energy itself cannot be represented as a local density, the binding energy associated with gravitational interactions among matter constituents contributes to the total energy of a self-gravitating system. In a cosmological setting, this contribution is therefore relevant to the effective energy density that governs the expansion dynamics. Neglecting GSE in this context corresponds to describing the system using only free-state mass densities, rather than the total equivalent mass required by a consistent accounting of energy in General Relativity.

2 Gravitational Self-Energy as the Origin of Dark Energy

In a cosmological context, the binding energies associated with the strong, weak, and electromagnetic interactions are confined to microscopic and effectively time-independent scales, and may therefore be regarded as part of the free-state mass M_{fr}. In contrast, GSE is determined by the macroscopic distribution of matter M and by the evolving spatial scale of the universe R. As cosmic expansion proceeds, GSE is not constant but evolves dynamically, actively participating in the global energy budget of the universe. This observation leads to the central thesis of this work, namely that the phenomenon conventionally labeled as dark energy is not a new exotic component, but rather the manifestation of the universe's own dynamical GSE.

2.1 The equivalent gravitational source

The calculation of gravitational potential energy involves integrating the contributions of infinitesimal mass elements dm as they are assembled within the gravitational field generated by the interior mass $M'(r)$. In its standard form, the differential contribution is written as

$$dU_{gs} = -G\frac{M'(r)}{r}\,dm. \tag{6}$$

A fundamental principle of General Relativity is that all forms of energy contribute to gravitation [14, 16]. It is then natural, within the present framework, to treat GSE itself as contributing to the effective gravitational source. In conventional treatments, however, the gravitational

influence of self-energy is not incorporated explicitly, since the source mass is taken to be the free-state mass alone.

The central postulate of this work is that the interior source term $M'(r)$ should instead be replaced by an equivalent gravitational source $M_{\rm eq}(r)$, which includes both the material mass and the equivalent mass associated with GSE, denoted by $M'_{gs}(r)$.

$$M_{\rm eq}(r) = M'(r) - M'_{gs}(r). \tag{7}$$

For a general mass distribution, the GSE of the interior sphere of radius r and mass $M'(r)$ is parameterized by a structure coefficient β, which encapsulates the effects of mass geometry and relativistic corrections. For a uniform sphere in Newtonian gravity, $\beta = 3/5$. More centrally condensed or relativistic configurations generally correspond to larger effective coefficients multiplying GM^2/R. For example, the classical $n = 3$ polytrope yields $\beta = 1.5$ [19], while relativistic compact-star estimates often write the binding energy in the order-of-magnitude form $E_{\rm grav} \sim GM^2/R$, which corresponds to an effective coefficient of order unity [20].

$$U_{gs}(r) = -\beta \frac{GM'(r)^2}{r}. \tag{8}$$

The equivalent mass associated with this self-energy is therefore given by

$$-M'_{gs}(r) = \frac{U_{gs}(r)}{c^2} = -\beta \frac{GM'(r)^2}{rc^2}. \tag{9}$$

Substituting this back into the equivalent source equation yields

$$M_{\rm eq}(r) = M'(r)\left(1 - \beta \frac{GM'(r)}{rc^2}\right). \tag{10}$$

A formally similar inclusion of the equivalent mass associated with GSE in the interior source term was already considered in Ref. [21].

The **total GSE,** $U_{\text{gs-T}}$, is the integral of the differential energy contributions from $r = 0$ to the final radius R:

$$U_{\text{gs-T}} = \int_0^R dU_{\text{gs-T}} = \int_0^R -G\frac{M_{\rm eq}(r)}{r}\, dm. \tag{11}$$

Assuming a uniform density ρ for analytical clarity, we have $M'(r) = \frac{4}{3}\pi r^3\rho$ and the differential mass shell is $dm = 4\pi r^2\rho\, dr$. Substituting these into the integral gives

$$U_{\text{gs-T}} = \int_0^R -G\frac{1}{r}\left[M'(r)\left(1 - \beta\frac{GM'(r)}{rc^2}\right)\right](4\pi r^2\rho\, dr) \tag{12}$$

$$= -4\pi G\rho \int_0^R r\left[M'(r) - \frac{\beta G}{c^2}\frac{M'(r)^2}{r}\right]dr. \tag{13}$$

We now substitute $M'(r) = \frac{4}{3}\pi r^3\rho$:

$$U_{\text{gs-T}} = -4\pi G\rho \int_0^R r\left[\left(\frac{4\pi}{3}\rho r^3\right) - \frac{\beta G}{c^2 r}\left(\frac{4\pi}{3}\rho r^3\right)^2\right]dr \tag{14}$$

$$= \int_0^R \left(-\frac{16\pi^2 G\rho^2}{3}r^4 + \frac{64\pi^3\beta G^2\rho^3}{9c^2}r^6\right)dr. \tag{15}$$

$$U_{\text{gs-T}} = \frac{3}{5}\left[-\frac{16\pi^2 G\rho^2 R^5}{9} + \frac{320\pi^3\beta G^2\rho^3 R^7}{189c^2}\right]. \tag{16}$$

To account for the relativistic contributions and the geometric distribution of mass in a general self-gravitating system, we generalize the Newtonian coefficient 3/5 to the structure coefficient β:

$$U_{\text{gs-T}} = \beta \left[-\frac{16\pi^2 G\rho^2 R^5}{9} + \frac{320\pi^3 \beta G^2 \rho^3 R^7}{189c^2} \right]. \tag{17}$$

Performing the definite integration yields the final expression for the total GSE:

$$U_{\text{gs-T}} = -\beta \frac{GM^2}{R} + \frac{5}{7}\beta^2 \frac{G^2 M^3}{c^2 R^2} = -\beta \frac{GM^2}{R}\left(1 - \frac{5\beta}{7}\frac{GM}{c^2 R}\right). \tag{18}$$

This can also be written in a factored form to highlight the repulsive correction:

$$\boxed{U_{\text{gs-T}} = \beta \frac{GM^2}{R}\left(\frac{5\beta}{7}\frac{GM}{c^2 R} - 1\right)} \tag{19}$$

2.2 Connection to post-Newtonian gravity: Validation and reinterpretation

It is important to emphasize that the functional form of the self-energy correction derived in Eq. (19) is not an ad hoc assumption, but is structurally consistent with results obtained within General Relativity. In the post-Newtonian approximation, the total energy of a self-gravitating system contains relativistic corrections arising from the nonlinear structure of the Einstein field equations. At first post-Newtonian order, the gravitational binding energy of a static spherical mass distribution acquires a relativistic correction at order $1/c^2$. Schematically, this correction can be written in the form [15, 22]

$$U_{PN} \approx -\frac{3}{5}\frac{GM^2}{R}\left(1 - \kappa \frac{GM}{Rc^2}\right), \tag{20}$$

where κ is a dimensionless coefficient of order unity whose value depends on the internal structure and pressure distribution of the system.

The close correspondence between the nonperturbative GSE resummation $U_{\text{gs-T}}$ and the formal post-Newtonian expansion U_{PN} serves two essential roles:

1) **Validation:** It suggests that treating GSE as an effective contribution to the gravitational source captures the leading nonlinear corrections predicted by General Relativity, without requiring an explicit tensorial expansion.

2) **Reinterpretation in a cosmological context:** In standard post-Newtonian theory, this term is interpreted as a small correction to the binding energy relevant for stellar structure. In contrast, we identify the total GSE as the physical origin of dark energy. When applied to cosmology, where M represents the mass contained within the causally connected region, the cumulative GSE is no longer negligible and can dominate the large-scale dynamics, thereby driving accelerated expansion.

By deriving this contribution from a physical principle rather than from a truncated perturbative expansion, the GSE framework elevates what appears as a small correction in the post-Newtonian approach to a central dynamical ingredient. This provides a transparent mechanism for effective repulsive gravity that remains implicit in the standard post-Newtonian formulation.

1) **Approximation versus principle:** Chandrasekhar's result is obtained through a perturbative expansion of the Einstein field equations and is strictly valid only in the weak-field regime where $GM/(Rc^2) \ll 1$ and in the slow-motion limit. Higher-order contributions

are therefore systematically neglected [15, 22]. In contrast, the present derivation is nonperturbative and self-consistent, arising from a closed-form resummation of GSE based on energy conservation rather than on a truncated weak-field expansion. This suggests that the framework may remain applicable in regimes where standard post-Newtonian methods lose accuracy, including the early universe or strongly gravitating environments.

2) **Static versus dynamic applicability:** Post-Newtonian analyses typically assume quasi-static equilibrium, such as hydrostatic or virial balance, which is appropriate for stellar configurations [22–24]. The core mechanism of the GSE framework, namely the replacement of bare mass by equivalent mass through $M \to M_{\rm eq}$, relies instead on local energy conservation and does not require static equilibrium. The approach is therefore naturally suited to dynamic cosmological settings, including phases of rapid expansion or contraction where hydrostatic assumptions are invalid.

Accordingly, the present result should not be regarded as a mere reproduction of the post-Newtonian approximation, but rather as an effective resummation that captures the essential physics of gravitational self-repulsion in a compact analytical form applicable across a wide range of cosmic epochs.

2.3 The necessity of the GSE framework in cosmology

A common critique of semiclassical approaches is that they are not derived directly from the full formalism of General Relativity. This critique, however, overlooks the practical and mathematical limitations of exact General Relativistic solutions in a cosmological setting.

It is well established that, although a number of exact interior solutions of the Einstein field equations are known for special idealized matter distributions, no general closed-form analytic solution exists for an arbitrary gravitating system with nonzero density [23,24]. While numerical methods such as solutions of the Tolman–Oppenheimer–Volkoff (TOV) equations provide accurate descriptions of static compact objects, these approaches are both mathematically and physically unsuitable for cosmological systems, which are characterized by low density and dynamical expansion rather than hydrostatic equilibrium.

Accordingly, no exact closed-form expression derived from full General Relativity is currently available for the total GSE of a realistic expanding universe.

In contrast, the GSE framework provides a closed-form analytic expression for an effective energy contribution that incorporates self-gravitating interactions on cosmological scales. Its consistency with the first order post-Newtonian results derived by Chandrasekhar provides an important cross-check of consistency [22]. Moreover, the framework is conceptually aligned with the fact that the Friedmann equation itself admits a derivation from energy-conservation arguments within Newtonian mechanics [14, 25].

At present, the GSE framework therefore represents a viable and analytically tractable approach for investigating the role of self-gravitating energy in the dynamical evolution of the universe.

2.4 The two components of total GSE

The result derived in Eq. (19) constitutes a central element of the present framework. It shows that when GSE is computed self-consistently, it is not a single monolithic contribution, but naturally separates into two distinct components with opposite signs. This decomposition provides the physical basis for identifying GSE as the origin of dark energy.

For clarity and consistent usage throughout this paper, we explicitly define these two components according to their physical origin. We define and use the negative equivalent mass density as $-\rho_{gs}$, where $\rho_{gs} > 0$ denotes the magnitude of the attractive GSE contribution.

1) **Negative equivalent mass component ($-\rho_{gs}$):** This term corresponds to the GSE obtained at the Newtonian level. The structure factor β is a coefficient of the GSE function included to account for the geometry of the mass distribution and relativistic corrections relevant on cosmological scales. Here $\rho_{gs} > 0$ denotes the positive magnitude of this attractive GSE contribution, while the actual equivalent mass density contribution is $-\rho_{gs} < 0$.

$$-\rho_{gs} \equiv \frac{1}{Vc^2}\left(-\beta\frac{GM^2}{R}\right) < 0. \tag{21}$$

Equivalently,

$$\rho_{gs} \equiv \frac{1}{Vc^2}\left(\beta\frac{GM^2}{R}\right) > 0. \tag{22}$$

Using $V = \frac{4}{3}\pi R^3$, this expression may be written as

$$-\rho_{gs} = -\frac{3\beta}{4\pi}\frac{GM^2}{c^2R^4} = -\frac{4\pi\beta G}{3c^2}\rho_m^2 R^2. \tag{23}$$

2) **Positive equivalent mass component ($\rho_{m\text{-}gs}$):** This term arises from the interaction between matter and its own GSE. It represents a relativistic correction associated with the fact that GSE itself contributes to the effective gravitational source. In this sense, it is post-Newtonian in character, while remaining fully consistent with the nonperturbative formulation developed here.

$$\rho_{m\text{-}gs} \equiv \frac{1}{Vc^2}\left(\frac{5\beta^2}{7}\frac{G^2M^3}{c^2R^2}\right) > 0. \tag{24}$$

Using again $V = \frac{4}{3}\pi R^3$, one finds

$$\rho_{m\text{-}gs} = \frac{15\beta^2}{28\pi}\frac{G^2M^3}{c^4R^5} = \frac{80\pi^2\beta^2G^2}{63c^4}\rho_m^3 R^4. \tag{25}$$

The total mass-energy density of the universe ρ_T is therefore given by the sum of the matter density and the net contribution from GSE.

$$\rho_T = \rho_m + \rho_{\Lambda_m} = \rho_m + \rho_{m\text{-}gs} - \rho_{gs}. \tag{26}$$

We therefore identify the net total GSE density with the matter-induced dark energy density:

$$\boxed{\rho_{\Lambda_m} \equiv \left(\rho_{m\text{-}gs}\right) + \left(-\rho_{gs}\right) = \rho_{m\text{-}gs} - \rho_{gs}} \tag{27}$$

Expressed explicitly in terms of M and R, this yields

$$\rho_{\Lambda_m} = \frac{3\beta}{4\pi}\frac{GM^2}{c^2R^4}\left(\frac{5\beta}{7}\frac{GM}{c^2R} - 1\right). \tag{28}$$

In terms of the matter density ρ_m and the scale R, the same quantity may be written as

$$\rho_{\Lambda_m}(\rho_m, R) = \frac{4\pi G\beta}{3c^2}\rho_m^2 R^2\left[\left(\frac{20\pi G\beta}{21c^2}\right)\rho_m R^2 - 1\right]. \tag{29}$$

Defining the constants

$$c_1 \equiv \frac{4\pi G}{3c^2}, \qquad c_2 \equiv \frac{20\pi G}{21c^2}, \qquad R_S \equiv \frac{2GM}{c^2}. \tag{30}$$

the dark energy density can be written compactly as

$$\boxed{\rho_{\Lambda_m}(\rho_m, R) = c_1 \beta \rho_m^2 R^2 \left(c_2 \beta \rho_m R^2 - 1\right)} \tag{31}$$

Equivalently, in terms of ρ_m and $\frac{R_S}{R}$, one obtains

$$\boxed{\rho_{\Lambda_m} = \frac{\beta \rho_m}{2} \frac{R_S}{R} \left(\frac{5\beta}{14} \frac{R_S}{R} - 1\right)} \tag{32}$$

2.5 Cosmological interpretation: Attraction and repulsion

Having defined the fundamental components of GSE, we now turn to their cosmological interpretation. The dynamical role of each energy or mass component in cosmic expansion is determined by its contribution to the Friedmann acceleration equation,

$$\frac{\ddot{a}}{a} = -\frac{4\pi G}{3} \sum_i (\rho_i + 3P_i) = -\frac{4\pi G}{3} \sum_i \rho_i (1 + 3w_i). \tag{33}$$

In the standard ΛCDM framework, the dark energy component is observationally consistent with an equation-of-state parameter $w \approx -1$ and a positive energy density, which together imply a negative pressure [3, 4]. It is under this specific cosmological condition that the two components of GSE acquire their distinct roles as sources of attraction and repulsion.

- **Positive equivalent mass density $\rho_{m\text{-}gs}$:** This component has a positive equivalent energy density, $\rho > 0$. When its effective pressure satisfies $P \approx -\rho$, its contribution to the acceleration equation becomes $(\rho + 3P) \approx -2\rho < 0$. As a result, this term yields $\ddot{a} > 0$ and acts as a source of cosmic repulsion, driving accelerated expansion.

- **Negative equivalent mass density $-\rho_{gs}$:** This component corresponds to a negative equivalent energy density, $\rho < 0$. With the same effective pressure relation $P \approx -\rho$, its contribution becomes $(\rho + 3P) \approx -2\rho > 0$. Consequently, this term yields $\ddot{a} < 0$ and acts as a source of cosmic attraction, contributing to decelerated expansion.

The fundamental entities are therefore the two GSE components, $\rho_{m\text{-}gs}$ and $-\rho_{gs}$.

A point of caution in a cosmological context is that the two quantities $\rho_{m\text{-}gs}$ and $-\rho_{gs}$ should not be interpreted as independent energy components. Although these terms arise naturally from the decomposition of the total GSE, only their combined contribution corresponds to a physically meaningful and observationally relevant energy density. In cosmology, the dark energy component is therefore identified with the total GSE density, $\rho_{\Lambda_m} = \rho_{m\text{-}gs} - \rho_{gs}$.

Accordingly, the appropriate interpretation of the Friedmann acceleration equation is obtained by considering the sign and magnitude of the total equivalent mass density associated with GSE. The resulting cosmic acceleration or deceleration is therefore determined by the net contribution of the total GSE, rather than by the isolated effects of its individual constituents.

This framework, which follows directly from a consistent accounting of GSE, is referred to as **Matter-Only Cosmology (MOC)**. [1] The designation reflects the core premise of the model,

[1] Here, "Matter" includes both baryonic and dark matter. The term "Matter-Only" refers to the absence of an independent dark energy fluid. The same principle applies to radiation, with the replacement $\rho_m \to \rho_r$.

namely that cosmic acceleration and the phenomenon attributed to dark energy arise from the GSE of matter and from the interaction between matter and its own self-gravitating energy, without invoking an additional non-matter energy component.

In the following sections, we will demonstrate how this single correction based on total GSE not only provides a concrete physical origin for dark energy, but also naturally reproduces its observed magnitude in the late universe, thereby offering a self-consistent resolution of one of the central problems in modern cosmology.

3 The Total GSE and the Structure Coefficient β

As established in the previous section, the origin of dark energy in the present framework is identified with the total GSE of the universe, evaluated in a self-consistent manner. This section provides a more detailed examination of this foundational quantity, $U_{gs} = -\beta \frac{GM^2}{R}$, and clarifies the physical meaning and role of the coefficient β.

3.1 From Newtonian binding energy to a relativistic framework

The GSE U_{gs} represents the total gravitational potential energy associated with a mass distribution and arises from the mutual gravitational interaction among its constituent elements. For an object of total mass M, which may be conceptualized as an assembly of infinitesimal mass elements satisfying $M = \sum dm_i$, this energy corresponds to the work required to assemble the system from infinite separation. It is therefore a specific and fundamental form of gravitational potential energy, commonly referred to as gravitational binding energy, with a negative sign reflecting the bound nature of the system [26, 27].

Within Newtonian gravity, the GSE of a uniform sphere of mass M and radius R is given by the well-known expression [27]

$$U_{gs,\mathrm{Newton}} = -\frac{3}{5}\frac{GM^2}{R}. \tag{34}$$

Although this result provides a useful reference, it is insufficient for cosmological applications in which relativistic effects and strong self-gravity may become relevant.

In General Relativity, the evaluation of GSE for a static and spherically symmetric configuration requires integration over a curved spacetime geometry. While a general closed-form analytic expression is not available, the net result can be represented effectively by a generalized expression of the same functional form [28, 29],

$$U_{gs} = -\beta \frac{GM^2}{R}, \tag{35}$$

where the dimensionless coefficient β replaces the Newtonian value $3/5$ and summarizes the combined effects of internal density profile, pressure, and relativistic corrections. Its value is therefore not universal, but depends on the structural properties of the gravitating system.

For a uniform sphere in Newtonian gravity, $\beta = 3/5$. Relativistic compact-star estimates often raise the effective binding energy coefficient to the order-unity level by writing the leading binding energy scale as $E_{\mathrm{grav}} \sim GM^2/R$ [20, 30]. In still more centrally condensed configurations, the classical $n = 3$ polytrope gives $\beta = 3/2$ [19].

The coefficient β may also be estimated by numerically integrating the gravitational potential energy associated with the Navarro–Frenk–White (NFW) density profile, which provides

an accurate description of dark-matter haloes. The resulting values show a systematic correlation between the halo concentration parameter c and the effective structure coefficient β [31]:

- $c = 5$ gives $\beta \approx 1.02$,
- $c = 10$ gives $\beta \approx 1.25$,
- $c = 15$ gives $\beta \approx 1.45$,
- $c = 20$ gives $\beta \approx 1.62$.

A separate relativistic reference estimate can be obtained from the exact general relativistic integral expression for the binding energy of a static, spherically symmetric object with uniform density. In the author's previous analysis of this static binding energy framework, the integral was evaluated numerically under the condition that the magnitude of the negative binding energy does not exceed the rest-mass energy of the assembled object [32]. This gives the reference value

$$\beta_{\mathrm{ref}} \approx 2.039. \tag{36}$$

This value is useful as a compact-object reference scale for a static, uniform density configuration [32]. However, it should not be interpreted as a universal upper bound on the effective cosmological coefficient in the MOC framework.

The reason is that the above estimate concerns the conventional negative GSE term considered in isolation. In the total GSE framework, the negative self-energy contribution is accompanied by the positive matter–GSE interaction contribution. As shown in Sec. 4.6, the total equivalent mass density remains positive for any real value of β. Therefore, even if β exceeds the static reference value $\beta_{\mathrm{ref}} \approx 2.039$, the total GSE framework does not automatically enter a negative total density regime.

Accordingly, in the present work, the range $\beta \sim 1$–1.6 should be understood as a physically motivated reference range inferred from relativistic, centrally concentrated, and halo-like self-gravitating systems, rather than as a strict theoretical bound. Moreover, the observable universe is a horizon-scale self-gravitating system whose matter-only Schwarzschild radius exceeds its observable radius, i.e. $R_S/R > 1$. Therefore, the effective cosmological coefficient β need not be strictly limited by values inferred from ordinary localized astrophysical systems. The cosmological value of β in MOC is instead interpreted as an effective structural coefficient of the causally connected matter distribution, whose precise value should ultimately be determined by the large-scale matter distribution itself.

3.2 The structural coefficient β is not a free parameter

In the present framework, β is not introduced as an independent phenomenological parameter or as an additional dynamical degree of freedom. It is a structure coefficient associated with the gravitational self-energy integral of a given matter distribution. Once the large-scale density profile is specified, the corresponding value of β is fixed by the GSE integral.

In practice, however, a direct first-principles calculation of the cosmological value of β would require a detailed large-scale density profile for the present universe, and no unique observationally established form of such a profile is currently available. For this reason, the present work treats β as an effective structural coefficient inferred from the cosmic energy budget and compared with reference values suggested by known self-gravitating systems.

The value of β may in principle vary over the full cosmic history, because the large-scale matter distribution evolves through halo formation, void growth and virialization. However,

the direction and magnitude of this evolution cannot be fixed from the present analytic treatment alone. For fixed total mass and outer scale, more centrally concentrated or clustered distributions generally have larger gravitational binding energy in magnitude, and therefore larger effective values of β [31]. This trend is illustrated by the increase from the Newtonian uniform-sphere value $\beta = 3/5$ to the classical $n = 3$ polytropic value $\beta = 3/2$ [19], and by the monotonic increase of β with the concentration parameter in NFW-like halo profiles [31]. Nevertheless, the cosmological effective coefficient also depends on the evolving distribution of voids, collapsed structures, and the causal horizon scale. Therefore, this paper does not assume a definite monotonic time evolution of $\beta(t)$.

In the benchmark simulations below, we keep β constant after the onset of substantial structure formation. This constant-β treatment isolates the intrinsic GSE-driven evolution of $\rho_{\Lambda_m}(t)$ without introducing an additional time-dependent ansatz for $\beta(t)$. Even with fixed β, the MOC dark energy density remains dynamical, because it depends on the matter density and the horizon-scale compactness ratio $R_S(t)/\chi_p(t)$.

A slowly varying $\beta(t)$ may still arise in a more structure-resolved treatment. In such a treatment, $\beta(t)$ could be determined through direct modeling of the evolving large-scale matter distribution, for example by using cosmological N-body simulations to relate halo profiles, void structure and clustering to the effective GSE coefficient [33, 34].

3.3 Primary variables of the total GSE: matter density and horizon scale

In Newtonian gravity,

$$F = -\frac{GMm}{r^2},$$

the primary physical variables are the mass M and the distance scale r. The mass M, in turn, is determined by the matter density ρ and the characteristic radius R of the mass distribution.

The same point applies to the total GSE dynamics. The primary variables entering the GSE are the matter density and the length scale over which the mass distribution is defined. In the present horizon-scale formulation, these are $\rho_m(t)$ and the particle-horizon scale $\chi_p(t)$, since

$$M(t) = \rho_m(t)\frac{4\pi}{3}R_{\rm phys}(t)^3, \qquad R_{\rm phys}(t) = a(t)\chi_p(t),$$

and

$$R_S(t) = \frac{2GM(t)}{c^2}.$$

Thus, the compactness ratio $R_S(t)/\chi_p(t)$, which controls the total GSE density, is ultimately determined by the matter density and the horizon scale.

By contrast, β is a structural coefficient in the gravitational self-energy integral. It encodes how the same total mass is distributed within the relevant volume, but **it is not a new source of gravity and not a primary variable comparable to $\rho_m(t)$ or $\chi_p(t)$.** Once the density profile is specified, β is fixed by the corresponding GSE integral. Therefore, variations of β can modify only the detailed numerical weighting of the GSE terms, whereas the dominant time dependence of $\rho_{\Lambda_m}(t)$ is governed by $\rho_m(t)$ and the horizon-scale compactness.

4 The Friedmann Equations in the MOC Framework

The standard ΛCDM model successfully accounts for cosmic expansion by introducing dark energy as an independent component characterized by a negative pressure, $P_\Lambda = -\rho_\Lambda$ [3,4,8]. In

contrast, the Matter-Only Cosmology (MOC) framework argues that the phenomena attributed to dark energy do not arise from a new substance or exotic field, but instead emerge from the GSE of matter itself and its associated interaction energy. In this section, we reformulate the Friedmann equations within the MOC framework.

4.1 A re-examination of the gravitational source term

The first Friedmann equation in standard cosmology is

$$H^2 = \frac{8\pi G}{3}\rho - \frac{k}{a^2}, \tag{37}$$

where $H \equiv \dot{a}/a$ is the Hubble parameter, $a(t)$ is the scale factor, k is the spatial curvature parameter, and ρ denotes the total equivalent mass density sourcing cosmic expansion.

Within the Friedmann equations, all quantities denoted by ρ represent equivalent mass densities, that is, energy densities divided by c^2. As such, all ρ terms enter on equal footing as gravitational sources.

Standard cosmology has long operated on the implicit assumption that, within the matter sector, the rest-mass density ρ_m fully characterizes the gravitational source associated with matter on cosmological scales. We argue that this assumption is conceptually incomplete. The total mass density ρ_T sourcing cosmic expansion in the Friedmann equations must also include the equivalent mass density associated with the GSE of matter and its self-interaction.

The total effective mass density governing cosmic expansion therefore consists of two fundamental contributions:

1) **Matter density (ρ_m):** The observable rest-mass density of baryonic and dark matter. This term represents the material content of the universe and the origin of all gravitational interactions.

2) **Total GSE or dark energy (ρ_{Λ_m}):** The net equivalent mass density arising from the GSE of matter. This contribution is not an independent fluid, but an emergent effect generated by matter through its own self-gravity. As shown in previous sections, it consists of two components:

   - **Negative component ($-\rho_{gs}$):** The equivalent mass density associated with classical gravitational binding energy.
   - **Positive component ($\rho_{m\text{-}gs}$):** The equivalent mass density generated by the self-gravitation of GSE, consistent with the general relativistic principle that all forms of energy act as sources of gravity.

In the ΛCDM model, matter and dark energy are treated as separate and noninteracting components [3, 4, 8]. In contrast, **the MOC framework interprets dark energy as the total GSE of matter**, including both the classical self-binding contribution and the interaction energy between matter and its own GSE.

Accordingly, the total equivalent mass density entering the Friedmann equation is given by

$$\rho_T = \rho_m + \rho_{\Lambda_m} = \rho_m + \rho_{m\text{-}gs} - \rho_{gs}. \tag{38}$$

This expression does not introduce a new physical substance, but instead provides a more complete accounting of the total equivalent mass density, denoted here by ρ_T.

Including the spatial curvature parameter k, the first Friedmann equation in the MOC framework takes the form

$$H^2 = \frac{8\pi G}{3}\,\rho_T - \frac{k}{a^2} = \frac{8\pi G}{3}\,(\rho_m + \rho_{m\text{-}gs} - \rho_{gs}) - \frac{k}{a^2}. \tag{39}$$

4.2 Friedmann equations in an expanding universe

In a cosmological setting, the calculation of gravitational self-energy (GSE) requires a careful distinction between two related but physically different notions of scale. The first is the causal comoving scale that determines the particle-horizon domain whose matter content can contribute to the accumulated horizon-scale gravitational self-energy. The second is the physical volume scale that converts this global GSE contribution into an equivalent mass density sourcing the Friedmann equations.

In the MOC framework, these roles are played by the comoving particle horizon $\chi_p(t)$ and the corresponding physical horizon radius $R_{\rm phys}(t)$, respectively. As clarified below, the simultaneous appearance of $\chi_p(t)$ and $R_{\rm phys}(t)$ does not represent an arbitrary mixing of two unrelated length scales. Rather, the GSE is first defined on the causal comoving domain determined by $\chi_p(t)$, and is then converted into a physical density by the usual factor relating comoving and physical volumes.

4.2.1 Causal interaction and comoving GSE density

We introduce two characteristic radii:

$$\chi_p(t) = \int_0^t \frac{c}{a(t')} dt' \qquad \text{(comoving particle horizon)}, \tag{40}$$

$$R_{\rm phys}(t) = a(t)\chi_p(t) \qquad \text{(physical horizon radius)}. \tag{41}$$

The particle horizon $\chi_p(t)$ determines the causal comoving domain whose mass elements have been able to enter causal contact by cosmic time t [18, 35–37]. The physical radius $R_{\rm phys}(t)$, by contrast, gives the actual physical size of that same causal domain at time t.

The mass enclosed in the causal domain can be written equivalently in physical or comoving variables. In physical variables,

$$M(t) = \rho_m(t)\left(\frac{4\pi}{3} R^3_{\rm phys}(t)\right), \tag{42}$$

where $\rho_m(t)$ is the physical matter density. In comoving variables, the same mass is

$$M(t) = \rho_m^{\rm com}(t)\left(\frac{4\pi}{3}\chi_p^3(t)\right), \qquad \rho_m^{\rm com}(t) \equiv a^3(t)\rho_m(t). \tag{43}$$

Since $R_{\rm phys}(t) = a(t)\chi_p(t)$, Eq. (42) and Eq. (43) are identical.

$$M(t) = \rho_m^{com}(t)\left(\frac{4\pi}{3}\chi_p^3(t)\right) = a^3(t)\rho_m(t)\left(\frac{4\pi}{3}\chi_p^3(t)\right) = \rho_m(t)\left(\frac{4\pi}{3}R^3_{phys}(t)\right) \tag{44}$$

Thus the enclosed mass $M(t)$ is independent of the coordinate representation used to evaluate it.

In the MOC framework, the global GSE is evaluated on this causal comoving domain. The leading attractive self-energy contribution is written as

$$U_{gs}(t) = -\beta(t)\frac{GM^2(t)}{\chi_p(t)}. \tag{45}$$

This expression serves as the effective horizon-scale GSE prescription adopted in the MOC framework. The use of $\chi_p(t)$ in Eq. (45) reflects the retarded and accumulated character of the horizon-scale GSE. In a static self-gravitating system, the mass distribution is treated as a pre-existing bound configuration, and the interaction scale is the physical radius of the

system. In an expanding universe, however, the horizon-scale system is built up through causal communication along the past light cone. The particle horizon therefore provides the effective causal scale over which the global GSE contribution is accumulated. Once this global energy is obtained, it is converted into the physical equivalent mass density by dividing by the physical volume $V_{\rm phys}(t) = 4\pi R^3_{\rm phys}(t)/3$.

It is useful to define the corresponding comoving GSE density,

$$\rho^{\rm com}_{\rm GSE}(t) = \frac{U_{\rm GSE}(t)}{c^2 V_\chi(t)}, \qquad V_\chi(t) = \frac{4\pi}{3}\chi_p^3(t). \tag{46}$$

However, the Friedmann equations are sourced by physical energy densities, not by comoving densities [18, 35, 37]. Therefore the density that enters the Friedmann equations is obtained by the standard conversion from comoving volume to physical volume,

$$\rho^{\rm phys}_{\rm GSE}(t) = a^{-3}(t)\rho^{\rm com}_{\rm GSE}(t). \tag{47}$$

Since

$$V_{\rm phys}(t) = \frac{4\pi}{3}R^3_{\rm phys}(t) = a^3(t)V_\chi(t), \tag{48}$$

Eq. (47) is equivalently

$$\rho^{\rm phys}_{\rm GSE}(t) = \frac{U_{\rm GSE}(t)}{c^2 V_{\rm phys}(t)}. \tag{49}$$

This shows explicitly that the MOC prescription does not arbitrarily mix $\chi_p(t)$ and $R_{\rm phys}(t)$. The global GSE is first calculated on the causal comoving domain defined by $\chi_p(t)$. The factor $R_{\rm phys}(t)$ enters only through the conversion of this global energy into the physical density required by the Friedmann equations.

4.2.2 Derivation of GSE densities

We now apply the above prescription to the two components of the total GSE. The attractive Newtonian GSE contribution is $U_{gs}(t) = -\beta(t)\frac{GM^2(t)}{\chi_p(t)}$.

Dividing first by the comoving causal volume gives the comoving equivalent mass density,

$$-\rho^{\rm com}_{gs}(t) = -\frac{1}{c^2}\frac{\beta(t)GM^2(t)/\chi_p(t)}{\frac{4\pi}{3}\chi_p^3(t)} = -\frac{3\beta(t)}{4\pi}\frac{GM^2(t)}{c^2\chi_p^4(t)}. \tag{50}$$

The physical density entering the Friedmann equation is then

$$-\rho_{gs}(t) = a^{-3}(t)\left[-\rho^{\rm com}_{gs}(t)\right] = -\frac{3\beta(t)}{4\pi}\frac{GM^2(t)}{c^2\chi_p(t)R^3_{\rm phys}(t)}. \tag{51}$$

The matter–GSE interaction component is evaluated using the same causal interaction scale:

$$U_{m\text{-}gs}(t) = \frac{5\beta^2(t)}{7}\frac{G^2M^3(t)}{c^2\chi_p^2(t)}. \tag{52}$$

The matter–GSE interaction term contains the same horizon-scale interaction kernel once more, because the equivalent GSE mass generated by U_{gs} interacts gravitationally with the ordinary matter distribution. Therefore, the replacement of the effective interaction scale by $\chi_p(t)$ leads naturally to the squared kernel $1/\chi_p^2(t)$ in the interaction term.

Its comoving equivalent mass density is

$$\rho_{m\text{-}gs}^{\text{com}}(t) = \frac{1}{c^2} \frac{\frac{5\beta^2(t)}{7} \frac{G^2M^3(t)}{c^2\chi_p^2(t)}}{\frac{4\pi}{3}\chi_p^3(t)} = \frac{15\beta^2(t)}{28\pi} \frac{G^2M^3(t)}{c^4\chi_p^5(t)}. \tag{53}$$

Converting this to a physical density gives

$$\rho_{m\text{-}gs}(t) = a^{-3}(t)\rho_{m\text{-}gs}^{\text{com}}(t) = \frac{15\beta^2(t)}{28\pi} \frac{G^2M^3(t)}{c^4\chi_p^2(t)R_{\text{phys}}^3(t)}. \tag{54}$$

The total matter-induced dark energy density is therefore

$$\rho_{\Lambda_m}(t) = \frac{3\beta(t)}{4\pi} \frac{GM^2(t)}{c^2\chi_p(t)R_{\text{phys}}^3(t)} \left[\frac{5\beta(t)}{7} \frac{GM(t)}{c^2\chi_p(t)} - 1 \right]. \tag{55}$$

Using the Schwarzschild radius associated with the causally connected mass, $R_S(t) \equiv \frac{2GM(t)}{c^2}$, this can be written compactly as

$$\boxed{\rho_{\Lambda_m}(t) = \frac{\beta(t)\rho_m(t)}{2} \frac{R_S(t)}{\chi_p(t)} \left[\frac{5\beta(t)}{14} \frac{R_S(t)}{\chi_p(t)} - 1 \right]} \tag{56}$$

where $\rho_m(t)$ is the physical matter density and $M(t) = \rho_m(t)\frac{4\pi}{3}R_{\text{phys}}^3(t)$ is the mass contained in the causal domain.

Equivalently, substituting $M(t) = \rho_m(t)(4\pi/3)R_{\text{phys}}^3(t)$ gives

$$\boxed{\rho_{\Lambda_m} = \frac{4\pi G}{3c^2}\beta a^3\rho_m^2\chi_p^2 \left[\frac{20\pi G}{21c^2}\beta a^3\rho_m\chi_p^2 - 1 \right]} \tag{57}$$

The conceptual meaning of these expressions is as follows. The particle horizon $\chi_p(t)$ defines the causal comoving domain on which the global GSE is computed. If one first divides this global energy by the comoving volume $V_\chi(t)$, the result is a comoving GSE density. To use this quantity as a source in the Friedmann equations, it must be converted into a physical density by multiplying by $a^{-3}(t)$. This conversion is exactly equivalent to dividing the global GSE by the physical volume $V_{\text{phys}}(t) = a^3(t)V_\chi(t)$.

Thus the appearance of both $\chi_p(t)$ and $R_{\text{phys}}(t)$ is not an inconsistency. Rather, it reflects the distinction between causal accumulation and physical density representation. Using $\chi_p^3(t)$ alone as the volume for expressing the final density would leave a comoving density, whereas using $R_{\text{phys}}(t)$ as the interaction scale would treat the GSE as an instantaneous physical-separation energy rather than as a causally accumulated horizon-scale self-energy. The MOC prescription therefore assigns $\chi_p(t)$ and $R_{\text{phys}}(t)$ to distinct but mutually consistent roles.

Effective cosmological term in the MOC framework. In the standard ΛCDM model, the cosmological constant is commonly expressed as

$$\Lambda = \frac{8\pi G}{c^2}\rho_\Lambda = \frac{3H^2}{c^2}\Omega_\Lambda, \tag{58}$$

where ρ_Λ is the dark energy density, $\Omega_\Lambda \equiv \rho_\Lambda/\rho_c$, and

$$\rho_c(t) = \frac{3H^2(t)}{8\pi G} \tag{59}$$

is the critical density. In the MOC framework, dark energy is not an independent component, but is identified with the physical GSE density generated by matter itself, $\rho_{\Lambda_m}(t)$. The corresponding effective cosmological term is therefore

$$\Lambda_m(t) \equiv \frac{8\pi G}{c^2}\rho_{\Lambda_m}(t) = \frac{3H^2(t)}{c^2}\Omega_{\Lambda_m}(t), \tag{60}$$

where

$$\Omega_{\Lambda_m}(t) \equiv \frac{\rho_{\Lambda_m}(t)}{\rho_c(t)}. \tag{61}$$

Using Eq. (56), one obtains

$$\Lambda_m(t) = \frac{8\pi G}{c^2}\frac{\beta(t)\rho_m(t)}{2}\frac{R_S(t)}{\chi_p(t)}\left[\frac{5\beta(t)}{14}\frac{R_S(t)}{\chi_p(t)} - 1\right]. \tag{62}$$

At the present epoch $t = t_0$, this reduces to

$$\Lambda_{m,0} = \frac{3H_0^2}{c^2}\Omega_{\Lambda_m,0}. \tag{63}$$

This expression has the same formal structure as the standard cosmological constant relation. However, its physical interpretation is different: in MOC, $\Lambda_m(t)$ is not a fundamental constant, but a time-dependent effective cosmological term generated by matter through its own gravitational self-energy.

4.2.3 General GSE Framework: The Friedmann equations in expanding space

Before introducing the effective source notation, it is important to clarify the meaning of the GSE contribution. **The GSE contribution introduced here should not be interpreted as a local stress-energy tensor of the gravitational field itself.** In General Relativity, the local energy density of the gravitational field is not uniquely defined in a coordinate-independent manner. The present construction does not rely on such a quantity. Rather, gravitational self-energy is treated as an internal binding energy contribution of a finite matter distribution, analogous to the way electromagnetic binding energy contributes to the invariant mass of a bound atomic system.

Thus, $T^{\mathrm{GSE}}_{\mu\nu}$ **should be understood as an effective decomposition of the total equivalent matter source, not as an additional stress-energy tensor of the gravitational field.** In principle, this contribution belongs to the total mass-energy content of the matter system itself. The notation

$$T^{\mathrm{total}}_{\mu\nu} = T^{\mathrm{matter}}_{\mu\nu} + T^{\mathrm{GSE}}_{\mu\nu}$$

is therefore a bookkeeping decomposition that makes explicit the part of the matter source associated with gravitational self-energy. In an FLRW setting, this contribution is represented as an effective homogeneous component because the Friedmann equations are written in terms of averaged cosmic energy densities.

To formalize this framework, we treat the total GSE as an effective source term in the Einstein field equations,

$$G_{\mu\nu} = \frac{8\pi G}{c^4}\left(T^{\mathrm{matter}}_{\mu\nu} + T^{\mathrm{GSE}}_{\mu\nu}\right), \tag{64}$$

where the GSE contribution is modeled as an effective perfect fluid,

$$T^{\mathrm{GSE}}_{\mu\nu} = \left(\rho_{\Lambda_m} + P_{\Lambda_m}\right)u_\mu u_\nu + P_{\Lambda_m} g_{\mu\nu}. \tag{65}$$

Solving these equations for the standard FLRW metric, substituting the total GSE densities and expressing them in terms of the matter density ρ_m yields the first Friedmann equation in the MOC framework:

$$\boxed{H^2 = \frac{8\pi G\rho_m}{3}\left[1+\frac{\beta}{2}\frac{R_S}{\chi_p}\left(\frac{5\beta}{14}\frac{R_S}{\chi_p}-1\right)\right]-\frac{k}{a^2}} \tag{66}$$

This expression explicitly reveals the scaling with the dimensionless geometric ratio R_S/χ_p, which represents the competition between the gravitational radius and the causal horizon.

The acceleration equation is derived from the total energy-momentum conservation as follows:

$$\frac{\ddot{a}}{a} = -\frac{4\pi G}{3}(\rho_m + \rho_{\Lambda_m} + 3P_T) \approx -\frac{4\pi G}{3}\left[\rho_m + (1+3w_{\Lambda_m})\rho_{\Lambda_m}\right]. \tag{67}$$

Adopting an effective equation of state $w_{\Lambda_m} \approx -1$ for the emergent dark energy component, the acceleration equation reduces to a compact form:

$$\boxed{\frac{\ddot{a}}{a} = -\frac{4\pi G\rho_m}{3}\left[1-\beta\frac{R_S}{\chi_p}\left(\frac{5\beta}{14}\frac{R_S}{\chi_p}-1\right)\right]} \tag{68}$$

This equation demonstrates that the sign of cosmic acceleration is governed by the evolution of the total GSE term. As the causal horizon grows and the balance between the attractive and repulsive self-interaction components shifts, the universe naturally transitions from early-time deceleration to late-time acceleration.

This result encapsulates the central thesis of the MOC framework. Matter is the sole fundamental energy source. Dark energy is not an independent physical entity but an emergent consequence of the GSE of matter and its relativistic self-interaction. In this sense, matter generates dark energy and drives cosmic acceleration through its own gravitational field.

4.2.4 Static GSE Framework: The Friedmann equations in non-expanding space

The MOC framework can also be formally extended to non-expanding and static systems by setting the causal interaction scale and the physical density representation scale equal to a single radius, $\chi_p = R_{\text{phys}} = R$. This identification renders the equations applicable to a wide class of self-gravitating systems beyond cosmology. In this limit, the ratio R_S/χ_p becomes R_S/R.

Substituting the explicit GSE-based expressions, the first Friedmann equation for a static system is expressed as follows:

$$H^2 = \frac{8\pi G\rho_m}{3}\left[1+\frac{\beta}{2}\frac{R_S}{R}\left(\frac{5\beta}{14}\frac{R_S}{R}-1\right)\right]-\frac{k}{a^2}. \tag{69}$$

Expanding the terms inside the bracket highlights the corrections to the Newtonian limit:

$$H^2 = \frac{8\pi G\rho_m}{3}\left(1-\frac{\beta}{2}\frac{R_S}{R}+\frac{5\beta^2}{28}\frac{R_S^2}{R^2}\right)-\frac{k}{a^2}. \tag{70}$$

The curvature term enters in the standard geometric manner and plays the same role as in the ΛCDM model. All nontrivial dynamical effects arise solely from the GSE of the matter distribution.

The corresponding acceleration equation is derived under the assumption $w_{\Lambda_m} \approx -1$:

$$\frac{\ddot{a}}{a} = -\frac{4\pi G\rho_m}{3}\left[1-\beta\frac{R_S}{R}\left(\frac{5\beta}{14}\frac{R_S}{R}-1\right)\right]. \tag{71}$$

In the strictly static limit, the first Friedmann equation reduces to a constraint equation describing the balance of energy densities:

$$\frac{8\pi G\rho_m}{3}\left[1+\frac{\beta}{2}\frac{R_S}{R}\left(\frac{5\beta}{14}\frac{R_S}{R}-1\right)\right]-\frac{k}{R^2}=0. \tag{72}$$

This condition describes the formal equivalent of hydrostatic equilibrium in a self-gravitating sphere. The repulsive component of the GSE can counterbalance gravitational attraction and can in principle oppose gravitational collapse. The acceleration equation similarly simplifies to a form that determines the stability of the system:

$$\ddot{a} \propto -\frac{4\pi G\rho_m}{3}\left[1-\beta\frac{R_S}{R}\left(\frac{5\beta}{14}\frac{R_S}{R}-1\right)\right]. \tag{73}$$

This static formulation provides a powerful analytical tool for various physical scales. For astrophysical objects such as stars or black hole interiors, it offers a framework to model internal energy density structures where repulsive GSE effects may regulate singularity formation. In elementary particle physics, it suggests a novel approach to self-energy problems by treating particles as self-contained gravitationally bound systems whose divergences are naturally regularized by their own GSE [32, 38].

4.3 Origin of negative pressure in the MOC framework

The second Friedmann equation governs cosmic acceleration. In the MOC framework, dark energy is not introduced as an independent fundamental fluid. Instead, it is identified with an effective contribution ρ_{Λ_m} generated by the total GSE of matter, including both the attractive GSE term and its associated interaction contribution.

In this setting, the pressure associated with ρ_{Λ_m} is not imposed axiomatically. Rather, it can be inferred from the conservation of the total effective energy–momentum tensor once the total equivalent mass density is specified.

The total equivalent mass density is defined as

$$\rho_T = \rho_m + \rho_{\Lambda_m}, \tag{74}$$

and the total effective pressure is

$$P_T = P_m + P_{\Lambda_m}. \tag{75}$$

Since the ρ quantities used in the Friedmann equations are equivalent mass densities, the conservation of the total energy content is expressed as

$$\dot{\rho}_T + 3H\left(\rho_T + \frac{P_T}{c^2}\right) = 0. \tag{76}$$

Because ρ_{Λ_m} is not an independent fundamental component but an effective sector induced by the total GSE of matter, the matter sector and the effective GSE sector need not be exactly conserved separately in the full theory. A more general background-level description is therefore

$$\dot{\rho}_m + 3H\left(\rho_m + \frac{P_m}{c^2}\right) = Q, \tag{77}$$

$$\dot{\rho}_{\Lambda_m} + 3H\left(\rho_{\Lambda_m} + \frac{P_{\Lambda_m}}{c^2}\right) = -Q. \tag{78}$$

Adding Eqs. (77) and (78) reproduces Eq. (76). Here Q parametrizes a possible effective exchange of equivalent mass density between the matter sector and the GSE-induced sector at the homogeneous background level.

For pressureless matter one has $P_m = 0$. In the minimal MOC approximation adopted here, this exchange is assumed to be negligible at the background level, $Q \simeq 0$, so that the matter component remains approximately conserved in the standard FRW sense,

$$\dot{\rho}_m + 3H\rho_m \simeq 0 \tag{79}$$

and the effective GSE-induced component approximately satisfies

$$\dot{\rho}_{\Lambda_m} + 3H\left(\rho_{\Lambda_m} + \frac{P_{\Lambda_m}}{c^2}\right) \simeq 0. \tag{80}$$

Solving Eq. (80) for the effective pressure gives

$$P_{\Lambda_m} \simeq -\rho_{\Lambda_m} c^2 - \frac{c^2}{3H}\dot{\rho}_{\Lambda_m}. \tag{81}$$

More generally, if the exchange term is retained explicitly, Eq. (78) gives

$$P_{\Lambda_m} = -\rho_{\Lambda_m} c^2 - \frac{c^2}{3H}\left(\dot{\rho}_{\Lambda_m} + Q\right). \tag{82}$$

Equation (81) is therefore the minimal-background limit of the more general interacting decomposition.

This relation implies that the effective pressure contains two contributions. The first term, $-\rho_{\Lambda_m} c^2$, is vacuum-like in the sense that it reproduces the familiar relation $P = -\rho c^2$ when ρ_{Λ_m} is constant. The second term encodes the dynamical nature of the MOC framework through the time variation of ρ_{Λ_m}. If the exchange term is retained, it also contains the effect of matter–GSE transfer through Q.

To analyze cosmic acceleration within the MOC framework, we define an effective equation-of-state parameter

$$w_{\Lambda_m}(t) \equiv \frac{P_{\Lambda_m}}{\rho_{\Lambda_m} c^2}. \tag{83}$$

Combining this definition with Eq. (82) yields

$$w_{\Lambda_m}(t) = -1 - \frac{\dot{\rho}_{\Lambda_m} + Q}{3H\rho_{\Lambda_m}}. \tag{84}$$

In the minimal approximation $Q \simeq 0$, this reduces to

$$w_{\Lambda_m}(t) \simeq -1 - \frac{\dot{\rho}_{\Lambda_m}}{3H\rho_{\Lambda_m}}. \tag{85}$$

In the MOC framework, $\rho_{\Lambda_m}(t)$ is determined by the total GSE expression given in Eq. (28). Accordingly, $w_{\Lambda_m}(t)$ is generally time dependent, reflecting the evolving balance between the attractive and repulsive contributions inside the total GSE term.

This expression provides a transparent physical interpretation of the effective equation of state. If the total GSE density varies slowly compared to the Hubble expansion rate, such that

$$|\dot{\rho}_{\Lambda_m} + Q| \ll 3H|\rho_{\Lambda_m}|, \tag{86}$$

then the second term is subdominant and $w_{\Lambda_m}(t)$ approaches -1. In the minimal approximation $Q \simeq 0$, this condition reduces to

$$|\dot{\rho}_{\Lambda_m}| \ll 3H|\rho_{\Lambda_m}|. \tag{87}$$

In that regime, the effective pressure satisfies

$$P_{\Lambda_m} \simeq -\rho_{\Lambda_m} c^2 \tag{88}$$

and the GSE contribution behaves similarly to a cosmological constant.

More generally, whenever $\rho_{\Lambda_m}(t)$ evolves sufficiently slowly with cosmic time and the exchange term remains subdominant, the effective equation-of-state parameter remains negative. As a result, the GSE-induced component produces an effective negative pressure. In the MOC framework, cosmic acceleration is thus interpreted as the dynamical consequence of the time-dependent total GSE generated by matter, rather than as the effect of an independent vacuum component.

The total continuity equation employed above is not an additional model-dependent assumption. Rather, it follows from the covariant conservation law for the total energy–momentum tensor,

$$\nabla_\mu T^{\mu\nu}_{\text{total}} = 0 \tag{89}$$

which is required by general relativity [15, 18]. The decomposition into matter and effective GSE sectors with the exchange term Q therefore provides an effective background parametrization of the total conserved source, rather than a statement that the two sectors are fundamentally independent.

4.4 Thermodynamic interpretation of GSE pressure

The thermodynamic derivation in this subsection should be regarded as a complementary consistency check of the sign and magnitude of the effective pressure. The primary definition of P_{Λ_m} in the cosmological background is obtained from the total covariant conservation law.

As such a complementary check, one may introduce the thermodynamic-like relation

$$P_{\Lambda_m} \equiv -\frac{dU_{\text{gs-T}}}{dV_{\text{phys}}} = -\frac{\dot{U}_{\text{gs-T}}}{\dot{V}_{\text{phys}}}, \tag{90}$$

where $V_{\text{phys}}(t) = (4\pi/3)R_{\text{phys}}(t)^3$ represents the physical volume with respect to which the GSE-induced internal energy is expressed and varied. The second equality holds provided that the cosmic time t serves as the unique parameter governing the evolution of the system [35].

We emphasize that Eq. (90) should be interpreted as an effective equation-of-state identification rather than a full equilibrium thermodynamic identity. Standard thermodynamics dictates that pressure is defined as a partial derivative, $P = -(\partial U/\partial V)_{S,N,\ldots}$, taken at fixed entropy and particle number [39]. Consequently, adopting Eq. (90) implies the following idealized assumptions:

1) **Prescribed matter evolution along the horizon.** Unlike a closed thermodynamic system with fixed particle number, the causal domain in our framework is an open system where the enclosed mass M grows with the horizon scale (e.g., via the causal prescription $M(\chi_p)$). Accordingly, the derivative in Eq. (90) is evaluated along this *specific evolutionary trajectory*. It implicitly captures the combined effects of geometric expansion and the causal inflow of matter, effectively treating the horizon-enclosed region as a single dynamic entity.

2) **Negligible non-volumetric work.** We neglect macroscopic work channels other than effective volumetric work. This implies that contributions from chemical potential ($\mu\, dN$), anisotropic stress, or viscous dissipation are either absent or subdominant at the level of this effective description. This simplification is consistent with the standard treatment of the cosmic fluid as a perfect fluid on large scales [15, 37].

3) **Effective adiabaticity for the fluid description.** While horizon growth may in principle be accompanied by entropy production, we model the GSE component as an effective perfect fluid governed by mechanical work. Thus, the derivative in Eq. (90) is taken under the assumption that explicit entropy production terms are either subdominant or can be decoupled from the mechanical equation of state, analogous to the standard adiabatic treatment of cosmic fluids [4].

4) **Phenomenological energy exchange.** If the system exchanges energy with its surroundings (e.g., via radiation during collapse), these microscopic processes are not resolved here. Instead, their net effect is assumed to be encoded phenomenologically in the evolution of $U_{\text{gs-T}}$. Therefore, P_{Λ_m} represents the effective pressure required to reproduce the macroscopic U–V relation, rather than a locally measured microscopic pressure.

Strictly speaking, since the causally connected domain constitutes an open system with causal matter inflow, the direct application of the equilibrium relation Eq. (90) faces formal limitations. However, it is instructive to examine the consequences of this thermodynamic definition as a heuristic probe. Under the assumptions outlined above, Eq. (90) serves as a valuable proxy, providing a useful framework to estimate the sign and magnitude of the effective pressure. This exploratory analysis allows us to evaluate the effective equation-of-state parameter $w_{\Lambda_m} \equiv P_{\Lambda_m}/(\rho_{\Lambda_m} c^2)$ and its contribution to cosmic acceleration ($\rho_{\Lambda_m} + 3P_{\Lambda_m}/c^2$), offering complementary insights to the rigorous gravitational derivation.

4.4.1 Geometric volume factor

We define the physical volume of the causally connected domain as

$$V_{\text{phys}}(t) = \frac{4\pi}{3} R_{\text{phys}}(t)^3 = \frac{4\pi}{3}\big[a(t)\chi_p(t)\big]^3. \tag{91}$$

Differentiating with respect to time yields

$$\frac{dV_{\text{phys}}}{dt} = 4\pi a(t)^3 \chi_p(t)^3 \left(H(t) + \frac{\dot{\chi}_p(t)}{\chi_p(t)}\right). \tag{92}$$

Using the definition of the comoving particle horizon,

$$\chi_p(t) \equiv \int_0^t \frac{c}{a(t')}\, dt' \quad \Longrightarrow \quad \dot{\chi}_p(t) = \frac{c}{a(t)}. \tag{93}$$

and noting that $\chi_p(t) = c\,\eta(t)$ (where η is the conformal time), Eq. (92) can be rewritten in a computationally convenient form.

$$\begin{aligned} \frac{dV_{\text{phys}}}{dt} &= 4\pi a(t)^3 \chi_p(t)^2 \Big(H(t)\chi_p(t) + \dot{\chi}_p(t)\Big) \\ &= 4\pi a(t)^2 \chi_p(t)^2\, c\,\Big(1 + a(t)H(t)\eta(t)\Big). \end{aligned} \tag{94}$$

Since $a > 0$, $\chi_p > 0$, and (for an expanding universe) $H > 0$ and $\dot{\chi}_p > 0$, it follows that $dV_{\text{phys}}/dt > 0$. Therefore, the sign of the effective pressure P_{Λ_m} is determined solely by the sign of the time derivative $dU_{\text{gs-T}}/dt$.

4.4.2 Time derivative of the total GSE

In the MOC framework, the total GSE is taken as

$$U_{\text{gs-T}}(t) = -\beta(t)\frac{GM^2(t)}{\chi_p(t)} + \frac{5}{7}\beta^2(t)\frac{G^2M^3(t)}{c^2\chi_p^2(t)}. \tag{95}$$

Here $M(t)$ denotes the mass enclosed within the causally connected particle-horizon domain. Since $\rho_m(t)$ is the physical matter density, the same enclosed mass can be written equivalently as

$$M(t) = \rho_m(t)\left(\frac{4\pi}{3}R_{\text{phys}}^3(t)\right) = \rho_m^{\text{com}}(t)\left(\frac{4\pi}{3}\chi_p^3(t)\right), \qquad \rho_m^{\text{com}}(t) \equiv a^3(t)\rho_m(t). \tag{96}$$

Thus,

$$M(t) = \frac{4\pi}{3}\rho_m^{\text{com}}(t)\chi_p^3(t). \tag{97}$$

This form makes explicit that the time dependence of $M(t)$ comes from the growth of the causal comoving volume and, more generally, from any evolution of the comoving matter density. Differentiating Eq. (97) gives

$$\dot{M}(t) = \frac{4\pi}{3}\left[\dot{\rho}_m^{\text{com}}(t)\chi_p^3(t) + 3\rho_m^{\text{com}}(t)\chi_p^2(t)\dot{\chi}_p(t)\right]. \tag{98}$$

Equivalently, in terms of the physical matter density,

$$\dot{M}(t) = \frac{4\pi}{3}a^3(t)\chi_p^3(t)\left[\dot{\rho}_m(t) + 3H(t)\rho_m(t) + 3\rho_m(t)\frac{\dot{\chi}_p(t)}{\chi_p(t)}\right]. \tag{99}$$

For pressureless matter satisfying the standard background conservation law, $\dot{\rho}_m + 3H\rho_m = 0$, this reduces to

$$\dot{M}(t) = 4\pi a^3(t)\rho_m(t)\chi_p^2(t)\dot{\chi}_p(t) = 4\pi\rho_m^{\text{com}}(t)\chi_p^2(t)\dot{\chi}_p(t). \tag{100}$$

Therefore the apparent $\dot{a}$ term in the physical-density representation is cancelled by the dilution of $\rho_m(t)$ for conserved pressureless matter.

Treating $U_{\text{gs-T}}(t) = U(\beta(t), M(t), \chi_p(t))$ as a composite function yields

$$\frac{dU_{\text{gs-T}}}{dt} = \frac{\partial U}{\partial \beta}\dot{\beta} + \frac{\partial U}{\partial M}\dot{M} + \frac{\partial U}{\partial \chi_p}\dot{\chi}_p. \tag{101}$$

The partial derivatives are

$$\frac{\partial U}{\partial \beta} = -\frac{GM^2}{\chi_p} + \frac{10}{7}\beta\frac{G^2M^3}{c^2\chi_p^2}, \tag{102}$$

$$\frac{\partial U}{\partial M} = -2\beta\frac{GM}{\chi_p} + \frac{15}{7}\beta^2\frac{G^2M^2}{c^2\chi_p^2}, \tag{103}$$

$$\frac{\partial U}{\partial \chi_p} = \beta\frac{GM^2}{\chi_p^2} - \frac{10}{7}\beta^2\frac{G^2M^3}{c^2\chi_p^3}. \tag{104}$$

Substituting these results into Eq. (101) gives

$$\begin{aligned}\frac{dU_{\text{gs-T}}}{dt} = &\left(-\frac{GM^2}{\chi_p} + \frac{10}{7}\beta\frac{G^2M^3}{c^2\chi_p^2}\right)\dot{\beta} \\ &+ \left(-2\beta\frac{GM}{\chi_p} + \frac{15}{7}\beta^2\frac{G^2M^2}{c^2\chi_p^2}\right)\dot{M} \\ &+ \left(\beta\frac{GM^2}{\chi_p^2} - \frac{10}{7}\beta^2\frac{G^2M^3}{c^2\chi_p^3}\right)\dot{\chi}_p.\end{aligned} \tag{105}$$

Here $M(t)$ and $\dot{M}(t)$ are given by Eqs. (97)–(98), or equivalently by Eqs. (99)–(100) when expressed in terms of the physical matter density.

4.4.3 Final pressure formula in an expanding universe

Combining the thermodynamic relation

$$P_{\Lambda_m}(t) = -\frac{\dot{U}_{\text{gs-T}}(t)}{\dot{V}_{\text{phys}}(t)} \tag{106}$$

with

$$\dot{V}_{\text{phys}}(t) = 4\pi a^3(t)\chi_p^2(t)\big[H(t)\chi_p(t) + \dot{\chi}_p(t)\big], \tag{107}$$

and using Eq. (105), the thermodynamic GSE pressure becomes

$$P_{\Lambda_m}(t) = -\frac{\left(-\frac{GM^2}{\chi_p} + \frac{10}{7}\beta\frac{G^2M^3}{c^2\chi_p^2}\right)\dot{\beta} + \left(-2\beta\frac{GM}{\chi_p} + \frac{15}{7}\beta^2\frac{G^2M^2}{c^2\chi_p^2}\right)\dot{M} + \left(\beta\frac{GM^2}{\chi_p^2} - \frac{10}{7}\beta^2\frac{G^2M^3}{c^2\chi_p^3}\right)\dot{\chi}_p}{4\pi a^3\chi_p^2\left(H\chi_p + \dot{\chi}_p\right)}. \tag{108}$$

Here the enclosed mass is the mass inside the causally connected particle-horizon domain,

$$M(t) = \frac{4\pi}{3}\rho_m^{\text{com}}(t)\chi_p^3(t) = \frac{4\pi}{3}a^3(t)\rho_m(t)\chi_p^3(t), \tag{109}$$

where

$$\rho_m^{\text{com}}(t) \equiv a^3(t)\rho_m(t). \tag{110}$$

Its time derivative is therefore

$$\dot{M}(t) = \frac{4\pi}{3}\Big[\dot{\rho}_m^{\text{com}}(t)\chi_p^3(t) + 3\rho_m^{\text{com}}(t)\chi_p^2(t)\dot{\chi}_p(t)\Big]. \tag{111}$$

Equivalently, in terms of the physical matter density,

$$\dot{M}(t) = \frac{4\pi}{3}a^3(t)\chi_p^3(t)\left[\dot{\rho}_m(t) + 3H(t)\rho_m(t) + 3\rho_m(t)\frac{\dot{\chi}_p(t)}{\chi_p(t)}\right]. \tag{112}$$

1) Optional specialization for conserved pressureless matter. If one further assumes pressureless matter conservation in an FRW background,

$$\dot{\rho}_m(t) + 3H(t)\rho_m(t) = 0, \tag{113}$$

then Eq. (112) reduces to

$$\dot{M}(t) = 4\pi a^3(t)\rho_m(t)\chi_p^2(t)\dot{\chi}_p(t) = 4\pi\rho_m^{\text{com}}(t)\chi_p^2(t)\dot{\chi}_p(t). \tag{114}$$

Thus, the apparent $\dot{a}$ contribution in the physical-density representation is cancelled by the dilution of $\rho_m(t)$ for conserved pressureless matter.

2) Slow evolution of the structure coefficient $\beta(t)$. In the MOC framework, β is a structural coefficient fixed by the matter distribution through the GSE integral. Once the density profile is specified, β is determined by the corresponding gravitational self-energy calculation rather than introduced as an independent dynamical variable. After the formation of large-scale galactic structure, any residual evolution of $\beta(t)$ is expected to be slow compared to the Hubble time, so that β may be approximated as constant for the purpose of the present derivation.

Accordingly, we adopt the quasi-static approximation, $\dot{\beta}(t) \simeq 0$, under which Eq. (108) simplifies to

$$P_{\Lambda_m}(t) = -\frac{\left(-2\beta\,\frac{GM(t)}{\chi_p(t)} + \frac{15}{7}\beta^2\,\frac{G^2M^2(t)}{c^2\chi_p^2(t)}\right)\dot{M}(t) + \left(\beta\,\frac{GM^2(t)}{\chi_p^2(t)} - \frac{10}{7}\beta^2\,\frac{G^2M^3(t)}{c^2\chi_p^3(t)}\right)\dot{\chi}_p(t)}{4\pi a^3(t)\chi_p^2(t)\left[H(t)\chi_p(t) + \dot{\chi}_p(t)\right]}. \tag{115}$$

3) Fully expanded form using the comoving matter density. It is algebraically cleanest to expand the pressure in terms of the comoving matter density $\rho_m^{\rm com}(t) = a^3(t)\rho_m(t)$. Using

$$M(t) = \frac{4\pi}{3}\rho_m^{\rm com}(t)\chi_p^3(t), \qquad \dot{M}(t) = \frac{4\pi}{3}\left[\dot{\rho}_m^{\rm com}(t)\chi_p^3(t) + 3\rho_m^{\rm com}(t)\chi_p^2(t)\dot{\chi}_p(t)\right], \tag{116}$$

Eq. (115) can be written as

$$P_{\Lambda_m}(t) = -\frac{\mathcal{A}_{\rm com}(t)\dot{\rho}_m^{\rm com}(t) + \mathcal{B}_{\rm com}(t)\dot{\chi}_p(t)}{4\pi a^3(t)\chi_p^2(t)\left[H(t)\chi_p(t) + \dot{\chi}_p(t)\right]}, \tag{117}$$

where

$$\mathcal{A}_{\rm com}(t) \equiv \left(\frac{32\pi^2}{9}\right)\beta G\rho_m^{\rm com}(t)\chi_p^5(t)\left[-1 + \left(\frac{10\pi G}{7c^2}\right)\beta\rho_m^{\rm com}(t)\chi_p^2(t)\right], \tag{118}$$

$$\mathcal{B}_{\rm com}(t) \equiv \left(\frac{80\pi^2}{9}\right)\beta G\left[\rho_m^{\rm com}(t)\right]^2\chi_p^4(t)\left[-1 + \left(\frac{4\pi G}{3c^2}\right)\beta\rho_m^{\rm com}(t)\chi_p^2(t)\right]. \tag{119}$$

4) Equivalent representation in terms of the physical matter density. Using

$$\dot{\rho}_m^{\rm com} = a^3\left(\dot{\rho}_m + 3H\rho_m\right), \tag{120}$$

Eq. (117) may be written directly in terms of the physical matter density as

$$P_{\Lambda_m}(t) = -\frac{\mathcal{A}_{\rm phys}(t)\left[\dot{\rho}_m(t) + 3H(t)\rho_m(t)\right] + \mathcal{B}_{\rm phys}(t)\dot{\chi}_p(t)}{4\pi a^3(t)\chi_p^2(t)\left[H(t)\chi_p(t) + \dot{\chi}_p(t)\right]}, \tag{121}$$

where

$$\mathcal{A}_{\rm phys}(t) \equiv \left(\frac{32\pi^2}{9}\right)\beta G a^6(t)\rho_m(t)\chi_p^5(t)\left[-1 + \left(\frac{10\pi G}{7c^2}\right)\beta a^3(t)\rho_m(t)\chi_p^2(t)\right], \tag{122}$$

$$\mathcal{B}_{\rm phys}(t) \equiv \left(\frac{80\pi^2}{9}\right)\beta G a^6(t)\rho_m^2(t)\chi_p^4(t)\left[-1 + \left(\frac{4\pi G}{3c^2}\right)\beta a^3(t)\rho_m(t)\chi_p^2(t)\right]. \tag{123}$$

For conserved pressureless matter,

$$\dot{\rho}_m + 3H\rho_m = 0, \tag{124}$$

and Eq. (121) reduces to

$$P_{\Lambda_m}(t) = -\frac{\mathcal{B}_{\rm phys}(t)\dot{\chi}_p(t)}{4\pi a^3(t)\chi_p^2(t)\left[H(t)\chi_p(t) + \dot{\chi}_p(t)\right]}. \tag{125}$$

5) Equation-of-state form and a present-day estimate. The effective GSE pressure can be written in the standard equation-of-state form

$$P_{\Lambda_m}(t) = w_{\Lambda_m}(t)\rho_{\Lambda_m}(t)c^2, \tag{126}$$

where

$$w_{\Lambda_m}(t) = \frac{P_{\Lambda_m}(t)}{\rho_{\Lambda_m}(t)c^2}. \tag{127}$$

At the present epoch, using the fiducial CMB late-time parameters

$$a(t_0) = 1, \qquad \chi_p(t_0) = 46.114\,\mathrm{Gly}, \qquad \beta(t_0) = 1.6172,$$

$$\Omega_m = 0.3158, \qquad \rho_c \simeq 8.5227 \times 10^{-27}\,\mathrm{kg\,m^{-3}}, \qquad H_0 = 67.360\,\mathrm{km\,s^{-1}\,Mpc^{-1}},$$

together with

$$\dot{\chi}_p(t_0) = c, \qquad \rho_m(t_0) = \Omega_m \rho_c, \tag{128}$$

Eq. (125) gives

$$P_{\Lambda_m}(t_0) \simeq -3.92 \times 10^{-10}\,\mathrm{Pa}. \tag{129}$$

The corresponding present dark energy density is

$$\rho_{\Lambda_m}(t_0) \simeq 5.831 \times 10^{-27}\,\mathrm{kg\,m^{-3}}. \tag{130}$$

Therefore,

$$\boxed{w_{\Lambda_m}(t_0) = \frac{P_{\Lambda_m}(t_0)}{\rho_{\Lambda_m}(t_0)c^2} \simeq -0.749.} \tag{131}$$

This value is noteworthy in light of recent discussions of DESI BAO constraints combined with CMB and Type Ia supernova data, which in some combined fits hint at possible deviations from ΛCDM and may favor dynamical dark energy scenarios with a present-day equation of state satisfying $w_0 > -1$ [11, 12].

4.4.4 Thermodynamic origin and sign transition of GSE pressure

The effective pressure associated with the GSE-induced dark energy is defined thermodynamically by Eq. (90).

In an expanding universe one has $a > 0$, $H > 0$, and $\dot{\chi}_p > 0$. Consequently $dV_{\mathrm{phys}}/dt > 0$. It follows that the sign of P_{Λ_m} is determined entirely by the sign of $dU_{\text{gs-T}}/dt$. The attractive or repulsive character of the effective pressure is therefore controlled by the internal energy structure of the total GSE and is independent of the detailed expansion history beyond the monotonic growth of the physical volume.

$$\mathrm{sign}\big(P_{\Lambda_m}\big) = -\mathrm{sign}\left(\frac{dU_{\text{gs-T}}}{dt}\right). \tag{132}$$

In the MOC framework, the total GSE in the static approximation is given by Eq. (19).

To inspect the structural dependence of the GSE potential $U_{\text{gs-T}}$ on the horizon scale, we adopt a scaling ansatz for the enclosed mass:

$$M(\chi_p) \approx K\,\chi_p^3. \tag{133}$$

where K represents an effective density coefficient. While the actual matter density evolves with time, this power-law relation captures the leading-order geometric scaling of the mass within the causal volume, allowing us to determine the stationary point of the potential.

Substituting Eq. (133) into Eq. (19) yields

$$U_{\text{gs-T}}(\chi_p) = -A\,\chi_p^5 + B\,\chi_p^7. \tag{134}$$

with $A \equiv \beta G K^2$, $B \equiv \frac{5}{7}\beta^2 \frac{G^2K^3}{c^2}$. Taking the derivative with respect to χ_p gives

$$\frac{dU_{\text{gs-T}}}{d\chi_p} = \chi_p^4\big(-5A + 7B\chi_p^2\big). \tag{135}$$

Since $\dot{\chi}_p > 0$, Eqs. (132) and (135) imply that the pressure changes sign when the factor in parentheses vanishes:

$$-5A + 7B\chi_p^2 = 0 \quad \Longleftrightarrow \quad \chi_{p,*}^2 = \frac{c^2}{\beta G K}. \tag{136}$$

Using $M = K\chi_p^3$ and the Schwarzschild radius $R_S = 2GM/c^2$, the transition condition can be written in compact and physically transparent form:

$$\boxed{\frac{R_S}{\chi_p} = \frac{2}{\beta}} \tag{137}$$

Therefore, the effective GSE pressure satisfies

$$P_{\Lambda_m} \gtrless 0 \quad \Longleftrightarrow \quad \frac{R_S}{\chi_p} \lessgtr \frac{2}{\beta}. \tag{138}$$

The dark energy density is defined as $\rho_{\Lambda_m} \equiv \frac{U_{\text{gs-T}}}{V_{\text{phys}}c^2}$. Since $V_{\text{phys}}(t) > 0$, the sign of ρ_{Λ_m} is determined by the sign of $U_{\text{gs-T}}$.

Equation (134) shows that the same competition between the negative Newtonian binding term and the positive relativistic self-interaction term governs both the sign of $U_{\text{gs-T}}$ and the sign of its derivative. However, the transition epochs differ slightly because the two terms carry different powers of χ_p: the pressure turns negative as the system passes the potential minimum ($dU_{\text{gs-T}}/d\chi_p = 0$), whereas the energy density becomes positive only later, when $U_{\text{gs-T}}$ itself crosses zero.

In the regime where the Newtonian binding term dominates, the potential slope is negative ($dU_{\text{gs-T}}/d\chi_p < 0$), resulting in positive pressure $P_{\Lambda_m} > 0$. Once the relativistic term grows sufficiently for the system to pass the transition point defined by Eq. (137), the slope turns positive ($dU_{\text{gs-T}}/d\chi_p > 0$), generating negative pressure $P_{\Lambda_m} < 0$. This repulsive phase emerges naturally from the deep relativistic structure of the gravitational self-energy.

4.4.5 Connection to the sign of the dark energy density

In MOC, the dark energy density is defined as

$$\rho_{\Lambda_m} \equiv \frac{U_{\text{gs-T}}}{V_{\text{phys}}c^2}. \tag{139}$$

Since $V_{\text{phys}} > 0$, the sign of ρ_{Λ_m} is determined by the sign of $U_{\text{gs-T}}$. The total GSE contains two competing contributions. The Newtonian self-binding term is negative, while the relativistic self-interaction term is positive.

At early epochs, when the causally connected domain is small and the enclosed mass is correspondingly limited, the negative binding contribution dominates. In this regime one has

$$U_{\text{gs-T}} < 0 \quad \Longrightarrow \quad \rho_{\Lambda_m} < 0. \tag{140}$$

In the same regime, the thermodynamic pressure analysis implies $P_{\Lambda_m} > 0$. Within the present scaling picture, the same early-time regime is therefore characterized by

$$\rho_{\Lambda_m} < 0 \quad \Longrightarrow \quad P_{\Lambda_m} > 0. \tag{141}$$

As the causal domain grows and the enclosed mass increases, the positive self-interaction contribution eventually dominates the total GSE. One then finds

$$U_{\text{gs-T}} > 0 \quad \Longrightarrow \quad \rho_{\Lambda_m} > 0. \tag{142}$$

In this late-time regime the same thermodynamic analysis implies $P_{\Lambda_m} < 0$.

$$\rho_{\Lambda_m} > 0 \quad \Longrightarrow \quad P_{\Lambda_m} < 0. \tag{143}$$

Equations (141) and (143) summarize a key physical feature of the MOC mechanism. The dark energy component contributes an attractive tendency when its equivalent density is negative and its effective pressure is positive. After the sign transition, it contributes a repulsive tendency once its equivalent density becomes positive and its effective pressure becomes negative. This late-time behavior is the regime relevant for cosmic acceleration in MOC.

The thermodynamic derivation presented here is consistent with the continuity-equation approach. Both routes lead to the same qualitative conclusion in the late universe. The effective pressure becomes negative and the corresponding equation of state approaches $w_{\Lambda_m} \simeq -1$ when the evolution of ρ_{Λ_m} is slow compared to the Hubble rate.

4.5 Applicability to the radiation era

Although the name "Matter-Only Cosmology" emphasizes that the model introduces no independent dark energy fluid, the underlying mechanism is not restricted to nonrelativistic matter. The GSE construction is an energy-budget statement and therefore applies, in principle, to any dominant gravitating component that enters the Friedmann equations.

During the radiation-dominated epoch, the dominant energy component is radiation with energy density ε_r. The corresponding equivalent mass density sourcing gravity is [15, 37]

$$\rho_r \equiv \frac{\varepsilon_r}{c^2}. \tag{144}$$

In this era, the MOC framework is implemented by replacing the matter source ρ_m with the radiation source ρ_r in the GSE expressions. The total equivalent mass density then retains the same structural form:

$$\rho_T = \rho_r + \rho_{\Lambda_r}. \tag{145}$$

Here ρ_{Λ_r} denotes the total GSE contribution induced by the radiation source.

In direct analogy with the matter-era decomposition, it can be written as

$$\rho_{\Lambda_r} = \rho_{r\text{-}gs}(\rho_r) - \rho_{gs}(\rho_r), \tag{146}$$

where the bracket notation emphasizes that both the positive interaction contribution and the negative binding contribution are now sourced by ρ_r.

The principal differences relative to the matter-dominated case are the background density scaling and the background pressure. Radiation satisfies $\rho_r \propto a^{-4}$, reflecting both volume expansion and photon redshift, whereas nonrelativistic matter satisfies $\rho_m \propto a^{-3}$. In addition, the radiation equation-of-state parameter is $w_r = \frac{1}{3}$, whereas for pressureless matter one has $w_m \simeq 0$.

These differences modify the time dependence of $\chi_p(t)$, $R_{\rm phys}(t)$, and the sourced GSE densities, but do not alter the formal structure of the GSE-induced contribution itself.

Consequently, the MOC framework is formally applicable across both the radiation- and matter-dominated epochs, provided that the dominant source term in the GSE expressions is chosen consistently with the cosmic equation of state. In the present work, we focus primarily on quantitative predictions for the post-CMB epoch. The implications of the same mechanism for earlier epochs, including the transition out of inflation, are discussed in Section 10.

4.6 Theoretical consistency: Positive energy density and the origin of repulsion

A central theoretical requirement for any alternative description of cosmic acceleration is to generate repulsive dynamics without introducing known instabilities. Scenarios that rely on genuinely exotic degrees of freedom, such as phantom components with $w < -1$, can exhibit vacuum instabilities or ghostlike excitations and are therefore widely regarded as pathological [40, 41].

In this section we show that the MOC framework avoids these pathologies by maintaining a nonnegative total equivalent mass density ρ_T while producing repulsion through the effective pressure associated with the total GSE contribution.

4.6.1 Stability via nonnegative total energy density

To test whether the total density can become negative, we examine the condition

$$\rho_T = \rho_m + \rho_{\Lambda_m} < 0, \tag{147}$$

which is equivalent to $\rho_{\Lambda_m} < -\rho_m$. Substituting $\rho_m = 3M/(4\pi R^3)$ and the expression for ρ_{Λ_m} from Eq. (28) yields

$$\frac{3\beta}{4\pi}\frac{GM^2}{c^2R^4}\left(\frac{5\beta}{14}\frac{R_S}{R} - 1\right) < -\frac{3M}{4\pi R^3}. \tag{148}$$

Introducing the dimensionless compactness variable, $x \equiv \frac{R_S}{R}$, and using $R_S = 2GM/c^2$ transforms Eq. (148) into the quadratic inequality

$$\frac{5\beta^2}{28}x^2 - \frac{\beta}{2}x + 1 < 0. \tag{149}$$

The discriminant of the quadratic polynomial in Eq. (149) is

$$D = \left(-\frac{\beta}{2}\right)^2 - 4\left(\frac{5\beta^2}{28}\right) = -\frac{13\beta^2}{28}. \tag{150}$$

For any real β, one has $D < 0$ and the leading coefficient is positive. Therefore the quadratic expression is strictly positive for all real x, so the inequality in Eq. (149) has no solution. Equivalently, the total density never becomes negative:

$$\rho_T(R) > 0 \qquad \text{for all } R > 0. \tag{151}$$

In regimes where ρ_{Λ_m} is negative because the binding contribution dominates, its magnitude remains bounded so that ρ_T stays positive. The same conclusion holds when the attractive and repulsive GSE densities are expressed through the general expanding-universe prescriptions in Eqs. (51) and (54), provided M denotes the causally connected mass and $R_{\rm phys}$ the corresponding physical volume scale.

This result implies that the MOC background satisfies the density part of the weak energy condition in the sense that $\rho_T \geq 0$ [18, 36]. Accordingly, the construction avoids the most direct instability associated with genuinely negative total energy density and is not forced into the pathological behavior often associated with explicitly unstable negative-energy or exotic components [40–42].

4.6.2 Repulsion from effective pressure

If the total mass-energy density remains positive, the origin of acceleration must reside in the pressure sector. In an FRW background, the acceleration equation depends on the active gravitational mass density, which contains the combination $\rho + 3P/c^2$. In the MOC framework this may be written as

$$\frac{\ddot{a}}{a} = -\frac{4\pi G}{3}\left(\rho_T + \frac{3P_T}{c^2}\right), \tag{152}$$

where $P_T = P_m + P_{\Lambda_m}$. For pressureless matter one sets $P_m \simeq 0$, so $P_T \simeq P_{\Lambda_m}$.

Although ρ_T remains positive, the total GSE sector induces an effective pressure P_{Λ_m} that can become negative after the sign transition derived in Section 4.4 and in the analysis of the structure coefficient β in Section 3. In the effective-fluid description, this negative pressure is the driver of repulsive dynamics.

Our thermodynamic and continuity-equation derivations show that, in the late universe where $\rho_{\Lambda_m} > 0$, the effective equation-of-state parameter approaches

$$w_{\Lambda_m} \equiv \frac{P_{\Lambda_m}}{\rho_{\Lambda_m} c^2} \simeq -1, \tag{153}$$

so that $P_{\Lambda_m} < 0$ holds in the same regime.

Under these conditions the active gravitational mass density contributed by the GSE sector is negative:

$$\rho_{\Lambda_m} + \frac{3P_{\Lambda_m}}{c^2} \simeq -2\rho_{\Lambda_m} < 0 \tag{154}$$

and the total combination in Eq. (152) can satisfy

$$\rho_T + \frac{3P_T}{c^2} < 0 \tag{155}$$

which yields $\ddot{a} > 0$ and therefore accelerated expansion.

This provides a mechanism for repulsive cosmological dynamics without requiring a negative total energy density or a phantom component with $w < -1$.

- **Ontological stability:** The total equivalent mass density remains positive, $\rho_T > 0$, avoiding the most direct negative-energy pathology and remaining consistent with standard energy-condition expectations for the background density [18, 36].
- **Dynamical repulsion:** The total GSE sector generates an effective negative pressure, $P_{\Lambda_m} < 0$, which can render the active gravitational mass density negative and drive acceleration in agreement with supernova evidence for late-time repulsion [1, 2].

Therefore, within the MOC framework, late-time acceleration can arise as a purely gravitational effect generated by the self-consistent energy structure of the total GSE sector, without introducing additional exotic fields and without invoking phantom instabilities.

4.7 Definition of the GSE framework

The GSE framework asserts that the total energy of a gravitating system can be decomposed into a free-state contribution and a self-gravitating contribution associated with mutual gravitational interactions among the system constituents. In particular, the framework treats the GSE as part of the system energy budget that enters its equivalent mass, consistent with the general relativistic principle that all forms of energy gravitate [14, 15].

Crucially, our construction extends the conventional Newtonian binding energy term by incorporating an additional relativistic interaction contribution that arises once the self-energy itself is included as part of the gravitational source. In other words, the effective source is obtained by replacing the bare enclosed mass with an equivalent mass that includes the self-energy contribution, which generates a second term at order $1/c^2$ in the total GSE. Since all physical entities possess energy and thus generate gravity, the GSE framework is a universal principle applicable to all matter distributions, from elementary particles to the universe at large.

[Classification: general versus static model]

Depending on whether the background spacetime is treated as expanding or effectively time independent on the scales of interest, the framework is formulated in two regimes.

- **The General GSE model:** This formulation applies to an expanding FRW background, where the causal interaction scale is set by the particle horizon $\chi_p(t)$, while the resulting global GSE is expressed as a physical energy density with respect to the physical horizon radius $R_{\rm phys}(t)$. Because $\chi_p(t)$ and $R_{\rm phys}(t)$ can evolve differently, the total GSE density acquires a nontrivial time dependence, which is the relevant regime for cosmological applications and the emergence of a dark energy component.

- **The Static GSE model:** This limiting formulation applies to gravitationally bound systems that are effectively decoupled from cosmic expansion on the scales of interest, including compact astrophysical objects such as stars and black holes, as well as more localized energy-carrying systems such as elementary particles [38]. In this regime, the characteristic interaction length is taken to be commensurate with the physical size of the system, so that the distinction between the causal interaction scale and the physical size can be neglected to leading order. Accordingly, one may set $R_{\rm phys} \simeq \chi_p \simeq R$ within the system and treat the cosmological expansion as a subleading background effect in the internal energy bookkeeping.

  This static approximation is justified not only by spatial scale separation, but also by temporal scale separation. The characteristic dynamical timescales of such bound systems are vastly shorter than the cosmological expansion timescale. As a result, the cosmological background evolves negligibly over the relevant analysis time and can be treated as effectively constant. Background-induced corrections therefore remain parametrically small across the spatial extent of the system and are consistently neglected.

  This static GSE formulation provides a simplified and self-consistent analytic description of internal structure and stability in self-gravitating configurations.

Part II. Cosmological Phenomenology

5 Observational Validation and the Determination of β

In the preceding sections, we established the foundational equations of MOC. In this paradigm, the phenomenon conventionally attributed to dark energy arises from the total GSE of the universe, evaluated in a self-consistent manner.

$$\rho_{\Lambda_m} = \rho_{m\text{-}gs} - \rho_{gs} = \frac{\beta\rho_m}{2}\frac{R_S}{R}\left(\frac{5\beta}{14}\frac{R_S}{R} - 1\right). \tag{156}$$

Here β is a structure coefficient entering the total GSE. It summarizes the dependence of the self-energy on the mass distribution and relativistic compactness. In the full cosmic history, β may in principle vary as the large-scale matter distribution evolves. However, after the onset of substantial structure formation, its residual evolution is expected to be slow, and it can be approximated as constant for the late universe benchmark analysis presented in this section.

The decisive test of this framework is confrontation with empirical anchors. We therefore compare the MOC requirements with constraints from the early universe inferred from the Cosmic Microwave Background (CMB) [5] and with late universe measurements of the local distance ladder such as SH0ES [13].

In principle, β is determined by the matter distribution itself through the GSE integral, and is therefore not an independent free parameter. Once the density profile of the mass distribution is specified, the corresponding value of β is determined by the gravitational self-energy integral. However, a direct calculation would require a detailed large-scale density profile for the present universe, and no unique observationally established form of such a profile is currently available. We therefore determine the effective late-time value of β inversely from the observed present-epoch energy budget and compare it with the reference range suggested by known self-gravitating structures.

We treat the present matter density parameter Ω_m as a variable to be explored rather than as a fixed input. For each baseline, we solve for the value of β that satisfies the present-epoch matching condition

$$\rho_{\Lambda_m}(t_0) = (1-\Omega_m)\rho_c. \tag{157}$$

For the CMB baseline we adopt $H_0 = 67.36\,\mathrm{km\,s^{-1}\,Mpc^{-1}}$, $\rho_c = 8.5227\times10^{-27}\,\mathrm{kg\,m^{-3}}$, $\Omega_m = 0.3158$, and $\chi_p(t_0) = 46.114\,\mathrm{Gly}$ [5]. For the SH0ES baseline we adopt $H_0 = 73.04$ $\mathrm{km\,s^{-1}\,Mpc^{-1}}$ and $\chi_p(t_0) = 43.377\,\mathrm{Gly}$ [13]. We repeat this procedure across a range of matter densities, including scenarios in which the effective matter abundance is modestly higher than the standard CMB inference $\Omega_m = 0.3158$ [5].

The results are summarized in Tables 1 and 2. By comparing the required values of β with reference values inferred from known self-gravitating systems, we can assess whether the required coefficients are structurally reasonable. For reference, a uniform Newtonian sphere yields $\beta = 3/5$, the classical $n = 3$ polytrope gives $\beta = 3/2$, and NFW-like halo profiles give $\beta \simeq 1.0$–1.6 depending on concentration [19, 31]. Relativistic compact-object estimates also commonly use the leading binding-energy scale $E_{\mathrm{grav}} \sim GM^2/R$, indicating that order-unity structure coefficients are physically natural in self-gravitating systems [20, 30].

An examination of Tables 1 and 2 reveals an important implication of the MOC matching procedure. Across a broad span of assumed matter densities, solutions for β exist that reproduce the required present-epoch ρ_{Λ_m}. This indicates that the framework is not restricted to a narrowly tuned matter abundance at t_0.

Matter Incr. (%)	ρ_m ($\times 10^{-27}\,\mathrm{kg\,m^{-3}}$)	ρ_{Λ_m} (Target) ($\times 10^{-27}\,\mathrm{kg\,m^{-3}}$)	**Required β**	$\rho_{m\text{-}gs}$ ($\times 10^{-27}\,\mathrm{kg\,m^{-3}}$)	$-\rho_{gs}$ ($\times 10^{-27}\,\mathrm{kg\,m^{-3}}$)
-20	2.153	6.370	**2.2373**	12.511	-6.141
-10	2.422	6.100	**1.8854**	12.650	-6.550
0	2.691	5.831	**1.6172**	12.767	-6.936
10	2.961	5.562	**1.4071**	12.864	-7.302
20	3.230	5.293	**1.2387**	12.943	-7.650
30	3.499	5.024	**1.1012**	13.005	-7.982
40	3.768	4.755	**0.9871**	13.053	-8.298
50	4.037	4.485	**0.8912**	13.086	-8.600
60	4.306	4.216	**0.8096**	13.105	-8.889

Table 1: **Required Structure Coefficient β for the CMB Baseline ($H_0 = 67.360\,\mathrm{km\,s^{-1}\,Mpc^{-1}}$, $\Omega_m = 0.3158$, $\chi_p(t_0) = R = 46.114\,\mathrm{Gly}$, $\rho_c = 8.5227 \times 10^{-27}\,\mathrm{kg\,m^{-3}}$).** The table lists the values of β required to recover the CMB-baseline target dark energy density across different matter density scenarios. The matter density increment is defined relative to the standard CMB matter abundance $\Omega_m = 0.3158$. For each row, $\rho_{\Lambda_m}^{\text{target}} = \rho_c - \rho_m$ is imposed, the resulting quadratic equation for β is solved, and the obtained value is then inserted back into $\rho_{m\text{-}gs}$ and $-\rho_{gs}$. The equality $\rho_{\Lambda_m} = \rho_{m\text{-}gs} - \rho_{gs}$ is therefore satisfied by construction. The range from -10% to $+30\%$ places the required coefficient within the broad reference interval suggested by known self-gravitating structures, roughly $1.0 \lesssim \beta \lesssim 2.0$. This interval is used as a structural guide rather than as a strict theoretical bound.

Matter Incr. (%)	ρ_m ($\times 10^{-27}\,\mathrm{kg\,m^{-3}}$)	ρ_{Λ_m} (Target) ($\times 10^{-27}\,\mathrm{kg\,m^{-3}}$)	**Required β**	$\rho_{m\text{-}gs}$ ($\times 10^{-27}\,\mathrm{kg\,m^{-3}}$)	$-\rho_{gs}$ ($\times 10^{-27}\,\mathrm{kg\,m^{-3}}$)
-20	2.525	7.496	**2.1587**	14.706	-7.210
-10	2.840	7.180	**1.8197**	14.869	-7.689
0	3.156	6.865	**1.5606**	15.008	-8.143
10	3.472	6.549	**1.3577**	15.123	-8.574
20	3.787	6.233	**1.1954**	15.214	-8.981
30	4.103	5.918	**1.0626**	15.290	-9.372
40	4.418	5.602	**0.9527**	15.344	-9.742
50	4.734	5.287	**0.8601**	15.385	-10.098
60	5.050	4.971	**0.7812**	15.408	-10.437

Table 2: **Required Structure Coefficient β for SH0ES Baseline ($H_0 = 73.04$ km/s/Mpc, $\chi_p(t_0) = R = 43.377$ Gly, $\rho_c \approx 1.002 \times 10^{-26}$ kg/m^3).** The table lists the values of β required to recover the SH0ES-baseline dark energy density across different matter density scenarios. For each row, the matter density first fixes the matter-generated compactness R_S/R; the required value of β is then obtained by solving the quadratic matching equation for ρ_{Λ_m}. The range from -10% to $+30\%$ places the required coefficient within the broad reference interval suggested by known self-gravitating structures, roughly $1.0 \lesssim \beta \lesssim 2.0$.

For the standard 0% matter enhancement rows, the required values are $\beta \simeq 1.6172$ under the CMB baseline and $\beta \simeq 1.5606$ under the SH0ES baseline. These values should not be interpreted as a direct measurement of the time evolution of $\beta(t)$. They are effective structure coefficients inferred under different background calibrations, with different values of H_0, ρ_c, and horizon scale. Both values remain compatible with the reference range suggested by known self-gravitating systems.

The tables also show that a moderate increase in the effective matter abundance lowers the value of β required to reproduce the same present-epoch dark energy density. For example, under the CMB baseline, the required coefficient decreases from $\beta \simeq 1.6172$ at 0% matter enhancement to $\beta \simeq 1.2387$ at +20%. Under the SH0ES baseline, it decreases from $\beta \simeq 1.5606$ to $\beta \simeq 1.1954$ over the same range. This behavior reflects the fact that in MOC the dark energy density is not an independent component, but a derived quantity tied to the matter density, horizon-scale compactness, and the total GSE structure.

In this sense, the comparison between CMB and SH0ES baselines should be understood as a comparison between different effective cosmological calibrations, rather than as direct evidence for a prescribed time evolution of β. Even with fixed β, the MOC dark energy density remains dynamical, because it depends on the matter density and the horizon scale. Therefore, if this total GSE component is forced into a constant-Λ description, early and late universe observations can lead to different inferred expansion histories. This provides a possible MOC interpretation of the Hubble tension without requiring an explicit time-dependent ansatz for $\beta(t)$.

6 Cosmic History of the MOC

6.1 Preface on methodology and comparative strategy

Most currently adopted cosmological parameters and widely used compilation datasets have been established within the standard ΛCDM framework, which has provided the most successful phenomenological description of the observed universe to date by modeling dark energy as a constant energy density represented by a cosmological constant Λ [3–5]. For this reason, any alternative cosmological model must first be tested against the same observational benchmarks that have supported the success of ΛCDM.

The MOC framework departs from the standard paradigm by proposing that the effective dark energy density evolves over time and is generated by the total gravitational self-energy of matter. Precisely because of this conceptual difference, it is both reasonable and necessary to compare MOC, at its present stage of development, with the observational inputs and parameter baselines that have already proved successful in the standard cosmological context.

Accordingly, the primary objective of this paper is to examine whether the core ideas of MOC can reproduce physically meaningful and observationally relevant behavior when evaluated against the same baseline datasets that underlie modern precision cosmology. This comparative strategy provides a transparent and informative first test of the model: if MOC can account for key cosmic features while using the same successful observational anchors, then the framework merits further development and more dedicated future analysis.

The numerical results presented below therefore constitute a comparative and exploratory analysis based on the best available observational benchmarks. Their purpose is not merely to illustrate feasibility under simplified assumptions, but to determine whether MOC can stand in meaningful comparison with the currently most successful cosmological reference model.

6.2 Methods: General framework for MOC cosmic history simulations

6.2.1 Overview: Relation between the causal and physical horizon descriptions

This work develops a MOC framework in which the dark energy density $\rho_{\Lambda_m}(t)$ arises dynamically from the total GSE of the matter sector. Unlike standard ΛCDM, where ρ_Λ is introduced as a constant independent component, MOC treats dark energy as an emergent consequence of the total GSE of matter and the evolving causal structure of the universe.

1) **Causal horizon in comoving coordinates**

   The total GSE is computed for the mass elements that have entered causal contact by cosmic time t. This causal domain is specified by the comoving particle horizon $\chi_p(t)$, which gives the comoving extent of the causally connected region [37]. In the MOC prescription, $\chi_p(t)$ is used to describe the causal range over which the horizon-scale GSE is evaluated.

2) **Physical horizon in proper coordinates**

   The Friedmann equations are sourced by physical energy densities, not by comoving densities [37]. Therefore, after the global GSE has been evaluated for the causal domain, it must be expressed per unit physical volume of that same domain. This physical volume is determined by $V_{\rm phys}(t) = \frac{4\pi}{3} R^3_{\rm phys}(t)$.

   The physical horizon radius therefore does not define a new causal domain; it is the physical coordinate representation of the same domain defined by $\chi_p(t)$.

This formulation does not rely on a special separation mechanism between two independent horizons. Rather, it uses the standard relation $R_{\rm phys}(t) = a(t)\chi_p(t)$ to express the same causally connected region in two coordinate descriptions. The enclosed mass $M(t)$ is the same in both descriptions; only the density volume representation changes. The comoving horizon $\chi_p(t)$ is used to specify the causal domain, while $R_{\rm phys}(t)$ is used to express the resulting GSE as a physical density entering the Friedmann equations.

6.2.2 Mass growth and matter density

The effective gravitational mass $M(t)$ entering the self-energy calculation is defined as the mass enclosed within the causal domain set by the particle horizon. This mass is a coordinate-independent quantity: it is the same enclosed mass whether it is written in comoving variables or in physical variables.

Within the causal bookkeeping prescription used in the simulations, the enclosed mass grows with the comoving causal volume,

$$M(t) = M(t_0, f)\left(\frac{\chi_p(t)}{\chi_p(t_0)}\right)^3. \tag{158}$$

Here, $M(t_0, f)$ denotes the present-epoch enclosed mass corresponding to a matter enhancement factor f relative to the canonical reference $\Omega_m = 0.315$.

The same mass can be written equivalently in physical or comoving form. In physical variables,

$$M(t) = \rho_m(t)\left(\frac{4\pi}{3} R^3_{\rm phys}(t)\right), \tag{159}$$

where $\rho_m(t)$ is the physical matter density. In comoving variables,

$$M(t) = \rho^{\rm com}_m(t)\left(\frac{4\pi}{3}\chi^3_p(t)\right), \qquad \rho^{\rm com}_m(t) = a^3(t)\rho_m(t). \tag{160}$$

Using $R_{\rm phys}(t) = a(t)\chi_p(t)$, these two expressions are identical:

$$M(t) = \rho_m^{\rm com}(t)\left(\frac{4\pi}{3}\chi_p^3(t)\right) = a^3(t)\rho_m(t)\left(\frac{4\pi}{3}\chi_p^3(t)\right) = \rho_m(t)\left(\frac{4\pi}{3}R_{\rm phys}^3(t)\right). \tag{161}$$

Thus $M(t)$ is not changed by the choice of coordinates. What changes is the density volume representation used to describe the same enclosed mass. Since the Friedmann equations are written in terms of physical densities, the matter density entering the background equations is

$$\rho_m(t) = \frac{M(t)}{V_{\rm phys}(t)}, \qquad V_{\rm phys}(t) = \frac{4\pi}{3}R_{\rm phys}^3(t). \tag{162}$$

For pressureless matter in an FRW background, this physical density follows the standard scaling

$$\rho_m(t) = \frac{\rho_m(t_0, f)}{a^3(t)}. \tag{163}$$

6.2.3 Derivation of GSE densities

The General GSE framework prescribes that the total GSE depends on the enclosed mass $M(t)$ and on the causal interaction scale $\chi_p(t)$. At the level of scaling, one has

$$U_{\text{gs-T}}(t) \sim -\frac{GM^2(t)}{\chi_p(t)}. \tag{164}$$

Here $\chi_p(t)$ specifies the causal comoving scale over which the global GSE is accumulated. After the global GSE has been evaluated, the corresponding equivalent mass density entering the Friedmann equations is obtained by expressing this energy per unit physical volume and dividing by c^2.

1) Negative component ($-\rho_{gs}$)

This term represents the classical binding energy contribution generalized by the structure coefficient $\beta(t)$: $U_{gs}(t)$.

The associated physical equivalent mass density is

$$-\rho_{gs}(t) = -\frac{3\beta(t)}{4\pi}\frac{GM^2(t)}{c^2\chi_p(t)R_{\rm phys}^3(t)} = -\frac{\beta(t)}{2}\rho_m(t)\frac{R_S(t)}{\chi_p(t)}. \tag{165}$$

2) Positive component ($\rho_{m\text{-}gs}$)

This term represents the relativistic matter–GSE interaction contribution, in which the GSE itself contributes to the effective gravitational source. Using the same causal interaction scale $\chi_p(t)$, the interaction energy is $U_{m\text{-}gs}(t)$.

The associated physical equivalent mass density is

$$\rho_{m\text{-}gs}(t) = \frac{5\beta^2(t)}{28}\rho_m(t)\left(\frac{R_S(t)}{\chi_p(t)}\right)^2. \tag{166}$$

3) Total dark energy density

The dark energy density is defined as the net total GSE contribution, $\rho_{\Lambda_m}(t)$

Substituting the two components gives

$$\rho_{\Lambda_m}(t) = \frac{\beta(t)\rho_m(t)}{2}\frac{R_S(t)}{\chi_p(t)}\left[\frac{5\beta(t)}{14}\frac{R_S(t)}{\chi_p(t)} - 1\right]. \tag{167}$$

This formulation yields a dynamical evolution in which the causal gravitational network grows through $\chi_p(t)$, while the corresponding GSE contribution is expressed as a physical density using the physical volume determined by $R_{\rm phys}(t)$. Thus, the simultaneous appearance of $\chi_p(t)$ and $R_{\rm phys}(t)$ reflects two distinct roles: causal accumulation of the global GSE and physical density representation in the Friedmann equations.

6.2.4 Reference simulations for the total GSE dynamics

In the full MOC framework, the structure coefficient β may in principle vary slowly over cosmic time, because the large-scale matter distribution evolves through clustering, halo formation, void growth, and virialization [27, 31]. However, after substantial structure formation has occurred, the residual evolution of the effective cosmological structure coefficient is expected to be slow compared with the Hubble time. For this reason, the main simulations presented here first adopt a constant β benchmark over the full time interval under consideration.

This constant β benchmark has two advantages. First, it isolates the intrinsic time dependence of the GSE-induced dark energy density. Even when β is fixed, the MOC dark energy density remains dynamical, because $\rho_{\Lambda_m}(t)$ depends explicitly on the matter density $\rho_m(t)$ and on the horizon-scale mass distribution, represented by $\chi_p(t)$.

Second, the constant β benchmark provides a conservative test of whether the MOC mechanism can reproduce the observed late-time dark energy behavior without using $\beta(t)$ as a freely prescribed time-dependent function. For each baseline and matter density scenario, the constant value of β is fixed by the present-epoch matching condition

$$\rho_m(t_0, f) + \rho_{\Lambda_m}(t_0, f) = \rho_c. \tag{168}$$

Once this value is fixed at $t = t_0$, it is held constant throughout the benchmark simulation. The resulting cosmic history is then determined primarily by the evolution of $\rho_m(t)$ and the horizon scale, rather than by an additional dark energy sector.

The constant β treatment is not the only case considered in this work. In Section 6.4, we also examine explicitly evolving $\beta(t)$ histories around the standard CMB $\Omega_m = 0.315$ case. Those simulations test how a slowly evolving structural coefficient modifies the timing and amplitude of the transition, while preserving the same total GSE density formula. Together, the constant β benchmark and the evolving $\beta(t)$ extension show that the main MOC cosmic sequence is generated by the total GSE structure itself.

6.2.5 Additional assumptions for the simulation background

The cosmic time and scale factor used in the simulation tables are obtained from a flat cosmological background reconstruction including matter and dark energy. For a given baseline value of H_0, we use the standard analytic relation

$$H(a)^2 = H_0^2\left[\Omega_m a^{-3} + \Omega_\Lambda\right], \qquad \Omega_\Lambda = 1 - \Omega_m, \tag{169}$$

neglecting the radiation component over the simulated interval. The corresponding cosmic time is

$$t(a) = \frac{2}{3H_0\sqrt{\Omega_\Lambda}} \sinh^{-1}\left[\sqrt{\frac{\Omega_\Lambda}{\Omega_m}} a^{3/2}\right], \tag{170}$$

or equivalently,

$$a(t) = \left[\sqrt{\frac{\Omega_m}{\Omega_\Lambda}} \sinh\left(\frac{3}{2} H_0 \sqrt{\Omega_\Lambda}\, t\right)\right]^{2/3}. \tag{171}$$

For the CMB-based simulations, we use

$$H_0 = 67.36\,\mathrm{km\,s^{-1}\,Mpc^{-1}}, \qquad \Omega_m = 0.3158, \tag{172}$$

so that

$$\Omega_\Lambda = 1 - \Omega_m \simeq 0.6842. \tag{173}$$

This gives

$$t_0 \simeq 13.795\,\mathrm{Gyr}. \tag{174}$$

This is the present age used in the CMB-based simulation tables [5], rounded to $t_0 \simeq 13.8\,\mathrm{Gyr}$. The particle-horizon scale is normalized to

$$\chi_p(t_0) = 46.114\,\mathrm{Gly},$$

so that the CMB-based simulations are consistent with the present-epoch matching calculation used to determine β.

For the SH0ES-based simulations, we use $H_0 = 73.04\,\mathrm{km\,s^{-1}\,Mpc^{-1}}$, $\Omega_m = 0.315$, which gives

$$t_0 \simeq 12.73\,\mathrm{Gyr}.$$

This is the present age used in the SH0ES-based simulation tables [13]. The corresponding present particle-horizon scale is taken to be

$$\chi_p(t_0) = 43.377\,\mathrm{Gly}.$$

The tabulated earlier times are chosen by stepping backward in approximately 1 Gyr intervals, and the corresponding values of $a(t)$ are computed from the above relation.

Since the earliest times considered in the simulations are of order $t \simeq 0.7$–$0.8\,\mathrm{Gyr}$, corresponding to redshifts of order

$$z = \frac{1}{a} - 1 \simeq 6\text{–}7, \tag{175}$$

the radiation density is already far below the matter density. Indeed,

$$\frac{\rho_r}{\rho_m} = \frac{\Omega_r}{\Omega_m}\frac{1}{a} \tag{176}$$

is below the percent level over the entire simulated interval. We therefore neglect the radiation component in this late-time background reconstruction.

The matter enhancement factor used in the GSE calculation modifies the matter density entering $\rho_m(t)$, $R_S(t)$, and $\rho_{\Lambda_m}(t)$. It does not imply that the background scale-factor history has been re-solved for each matter enhancement case. Thus, the simulations trace how the MOC GSE density evolves on a fixed observationally anchored background for different matter enhancement scenarios.

6.3 MOC cosmic history simulation results

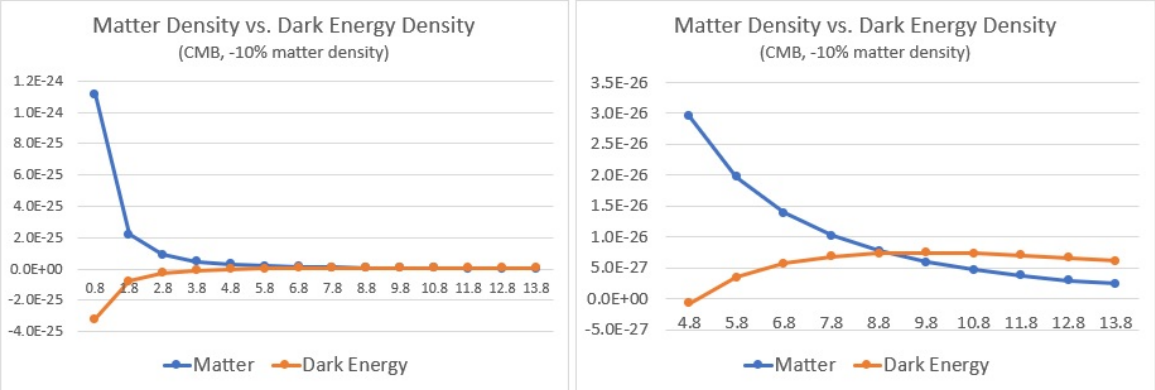

Figure 1: **Matter Density vs. Dark Energy Density (CMB, −10% Matter Enhancement, $\Omega_m \simeq 0.2842$).** The dark energy density is negative for $t \lesssim 4.98\,\mathrm{Gyr}$, enhancing deceleration and supporting the formation of galactic structures. It then becomes positive and drives accelerated expansion from approximately $t \simeq 7.21\,\mathrm{Gyr}$. The dark energy density reaches a broad maximum near $t \simeq 9.71\,\mathrm{Gyr}$ and subsequently decreases slowly toward the present epoch.

Age (Gyr)	Scale $a(t)$	Constant β	Comoving Ho. $\chi_p(t)$ (Gly)	Physical Ho. $R_{\mathrm{phys}}(t)$ (Gly)	**Matter** $\rho_m(t)$	Repulsive $\rho_{m\text{-}gs}(t)$	Attractive $-\rho_{gs}(t)$	**Dark Energy** $\rho_{\Lambda_m}(t)$
					$(10^{-27}\ \mathrm{kg\,m^{-3}})$			
0.8	0.1295	1.8854	17.763	2.300	1115.379	128.240	-447.492	**-319.252**
1.8	0.2226	1.8854	23.521	5.236	219.612	77.628	-154.489	**-76.862**
2.8	0.2998	1.8854	27.369	8.205	89.895	58.252	-85.622	**-27.370**
3.8	0.3694	1.8854	30.368	11.218	48.055	47.200	-56.351	**-9.151**
4.8	0.4346	1.8854	32.862	14.282	29.510	39.744	-40.521	**-0.777**
5.8	0.4972	1.8854	35.013	17.408	19.708	34.205	-30.720	**3.485**
6.8	0.5584	1.8854	36.912	20.612	13.912	29.827	-24.102	**5.724**
7.8	0.6190	1.8854	38.614	23.902	10.213	26.223	-19.363	**6.859**
8.8	0.6796	1.8854	40.156	27.290	7.717	23.175	-15.824	**7.351**
9.8	0.7408	1.8854	41.567	30.793	5.958	20.543	-13.091	**7.452**
10.8	0.8031	1.8854	42.864	34.424	4.677	18.232	-10.925	**7.306**
11.8	0.8668	1.8854	44.064	38.195	3.719	16.194	-9.183	**7.011**
12.8	0.9323	1.8854	45.178	42.119	2.989	14.382	-7.758	**6.624**
13.8	1.0000	1.8854	46.114	46.114	2.422	12.649	-6.549	**6.100**

Table 3: **MOC Cosmic History Simulation (CMB-Based, −10% Matter Enhancement, Constant $\beta = 1.8854$, $\Omega_m \simeq 0.2842$).** CMB-based evolution for a −10% matter enhancement scenario, corresponding to $\Omega_m \simeq 0.2842$, with the present particle-horizon scale normalized to $\chi_p(t_0) = 46.114\,\mathrm{Gly}$. The dark energy density is negative for $t \lesssim 4.98\,\mathrm{Gyr}$, enhancing deceleration and supporting the formation of galactic structures. It changes sign near $t \simeq 4.98\,\mathrm{Gyr}$, becomes positive, and satisfies the acceleration condition $\rho_{\Lambda_m} > \rho_m/2$ near $t \simeq 7.21\,\mathrm{Gyr}$. The dark energy density reaches a broad maximum near $t \simeq 9.71\,\mathrm{Gyr}$ and then decreases slowly toward the present epoch. Although ρ_{Λ_m} is a dynamical dark energy density, it exhibits a clear quasi-constant behavior in the late universe: over the interval $t \simeq 7.8$–$13.8\,\mathrm{Gyr}$, it fluctuates only at about the 10% level around its mean value, while the matter density decreases by about 76% over the same period.

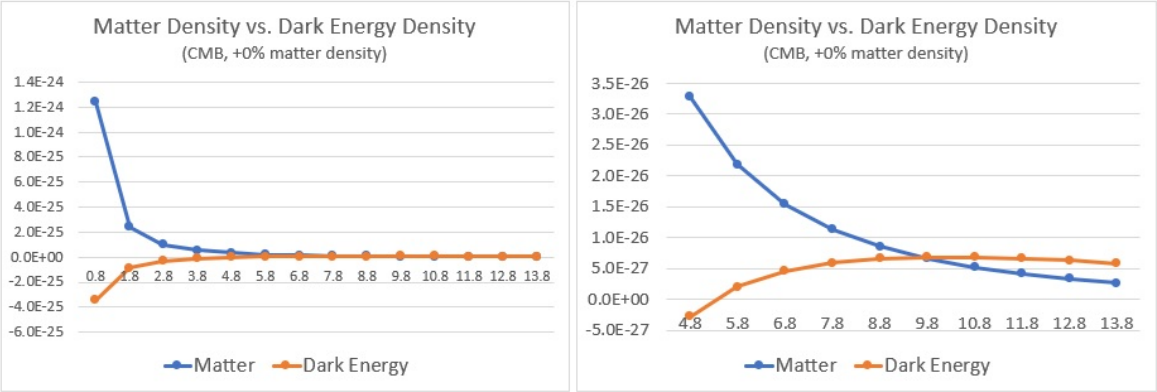

Figure 2: **Matter Density vs. Dark Energy Density (CMB-Based, +0% Matter Enhancement, Constant $\beta = 1.6172$, $\Omega_m \simeq 0.3158$).** For the standard matter abundance case, $\Omega_m \simeq 0.3158$, the dark energy density is negative for $t \lesssim 5.38\,\mathrm{Gyr}$, enhancing deceleration and supporting the formation of galactic structures. It becomes positive after the sign transition and drives accelerated expansion from approximately $t \simeq 7.72\,\mathrm{Gyr}$. The dark energy density reaches a broad maximum over $t \simeq 9.8$–$10.8\,\mathrm{Gyr}$ and then decreases slowly toward the present epoch.

Age (Gyr)	Scale $a(t)$	Constant β	Comoving Ho. $\chi_p(t)$ (Gly)	Physical Ho. $R_{\mathrm{phys}}(t)$ (Gly)	**Matter** $\rho_m(t)$	Repulsive $\rho_{m\text{-}gs}(t)$	Attractive $-\rho_{gs}(t)$	**Dark Energy** $\rho_{\Lambda_m}(t)$
					(10^{-27} kg m^{-3})			
0.8	0.1295	1.6172	17.763	2.300	1239.310	129.425	-473.872	**-344.447**
1.8	0.2226	1.6172	23.521	5.236	244.013	78.345	-163.596	**-85.252**
2.8	0.2998	1.6172	27.369	8.205	99.884	58.790	-90.669	**-31.879**
3.8	0.3694	1.6172	30.368	11.218	53.395	47.636	-59.673	**-12.037**
4.8	0.4346	1.6172	32.862	14.282	32.788	40.111	-42.910	**-2.798**
5.8	0.4972	1.6172	35.013	17.408	21.898	34.521	-32.531	**1.990**
6.8	0.5584	1.6172	36.912	20.612	15.458	30.102	-25.523	**4.579**
7.8	0.6190	1.6172	38.614	23.902	11.348	26.465	-20.505	**5.960**
8.8	0.6796	1.6172	40.156	27.290	8.575	23.389	-16.756	**6.632**
9.8	0.7408	1.6172	41.567	30.793	6.620	20.733	-13.862	**6.870**
10.8	0.8031	1.6172	42.864	34.424	5.196	18.400	-11.569	**6.831**
11.8	0.8668	1.6172	44.064	38.195	4.133	16.343	-9.724	**6.619**
12.8	0.9323	1.6172	45.178	42.119	3.321	14.515	-8.215	**6.299**
13.8	1.0000	1.6172	46.114	46.114	2.691	12.766	-6.935	**5.831**

Table 4: **MOC Cosmic History Simulation (CMB-Based, +0% Matter Enhancement, Constant $\beta = 1.6172$, $\Omega_m \simeq 0.3158$).** The dark energy density is negative for $t \lesssim 5.38\,\mathrm{Gyr}$, enhancing deceleration and supporting the formation of galactic structures. It changes sign near $t \simeq 5.38\,\mathrm{Gyr}$, becomes positive, and satisfies the acceleration condition $\rho_{\Lambda_m} > \rho_m/2$ near $t \simeq 7.72\,\mathrm{Gyr}$. The dark energy density reaches a broad maximum over $t \simeq 9.8$–$10.8\,\mathrm{Gyr}$ and then decreases slowly toward the present epoch. At $t_0 \simeq 13.8\,\mathrm{Gyr}$, the model gives $\rho_{\Lambda_m}(t_0) \simeq 5.831 \times 10^{-27}\,\mathrm{kg\,m^{-3}}$, consistent with $\rho_{\Lambda_m} \simeq 0.684\rho_c$ for $\rho_c \simeq 8.5227 \times 10^{-27}\,\mathrm{kg\,m^{-3}}$. This single equation for $\rho_{\Lambda_m}(t)$ simultaneously accounts for the existence of early massive galaxies, the onset of late-time acceleration, the quasi-constant behavior of dark energy, and recent indications of a mild decline in the dark energy density.

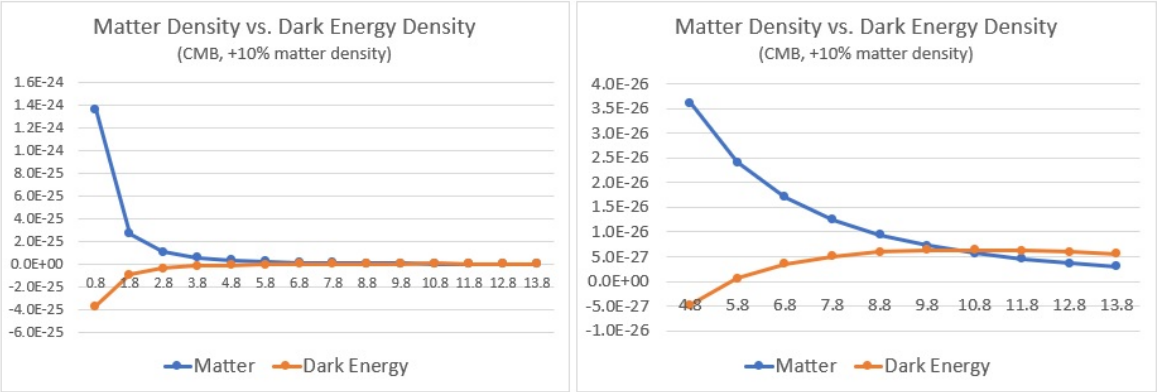

Figure 3: **Matter Density vs. Dark Energy Density (CMB-Based, +10% Matter Enhancement, Constant $\beta = 1.4071$, $\Omega_m \simeq 0.3474$).** For the +10% matter enhancement case, $\Omega_m \simeq 0.3474$, the dark energy density is negative for $t \lesssim 5.79\,\mathrm{Gyr}$, enhancing deceleration and supporting the formation of galactic structures. It becomes positive after the sign transition and drives accelerated expansion from approximately $t \simeq 8.29\,\mathrm{Gyr}$.

Age (Gyr)	Scale $a(t)$	Constant β	Comoving Ho. $\chi_p(t)$ (Gly)	Physical Ho. $R_{\mathrm{phys}}(t)$ (Gly)	**Matter** $\rho_m(t)$	Repulsive $\rho_{m\text{-}gs}(t)$	Attractive $-\rho_{gs}(t)$	**Dark Energy** $\rho_{\Lambda_m}(t)$
					(10^{-27} kg m^{-3})			
0.8	0.1295	1.4071	17.763	2.300	1363.241	130.412	-498.893	**-368.481**
1.8	0.2226	1.4071	23.521	5.236	268.415	78.942	-172.235	**-93.292**
2.8	0.2998	1.4071	27.369	8.205	109.870	59.238	-95.457	**-36.218**
3.8	0.3694	1.4071	30.368	11.218	58.734	47.999	-62.824	**-14.825**
4.8	0.4346	1.4071	32.862	14.282	36.067	40.417	-45.176	**-4.758**
5.8	0.4972	1.4071	35.013	17.408	24.087	34.785	-34.249	**0.535**
6.8	0.5584	1.4071	36.912	20.612	17.004	30.332	-26.871	**3.461**
7.8	0.6190	1.4071	38.614	23.902	12.483	26.667	-21.587	**5.079**
8.8	0.6796	1.4071	40.156	27.290	9.432	23.567	-17.641	**5.926**
9.8	0.7408	1.4071	41.567	30.793	7.282	20.891	-14.594	**6.297**
10.8	0.8031	1.4071	42.864	34.424	5.716	18.541	-12.180	**6.360**
11.8	0.8668	1.4071	44.064	38.195	4.546	16.468	-10.240	**6.230**
12.8	0.9323	1.4071	45.178	42.119	3.654	14.625	-8.649	**5.976**
13.8	1.0000	1.4071	46.114	46.114	2.961	12.863	-7.302	**5.562**

Table 5: **MOC Cosmic History Simulation (CMB-Based, +10% Matter Enhancement, Constant $\beta = 1.4071$, $\Omega_m \simeq 0.3474$).** CMB-based evolution for a +10% matter enhancement scenario, corresponding to $\Omega_m \simeq 0.3474$, with the present particle-horizon scale normalized to $\chi_p(t_0) = 46.114\,\mathrm{Gly}$. The dark energy density is negative for $t \lesssim 5.79\,\mathrm{Gyr}$, enhancing deceleration and supporting the formation of galactic structures. It changes sign near $t \simeq 5.79\,\mathrm{Gyr}$, becomes positive, and satisfies the acceleration condition $\rho_{\Lambda_m} > \rho_m/2$ near $t \simeq 8.29\,\mathrm{Gyr}$. The dark energy density reaches a broad maximum over $t \simeq 9.8$–$11.8\,\mathrm{Gyr}$, centered near $t \simeq 10.8\,\mathrm{Gyr}$, and then decreases slowly toward the present epoch.

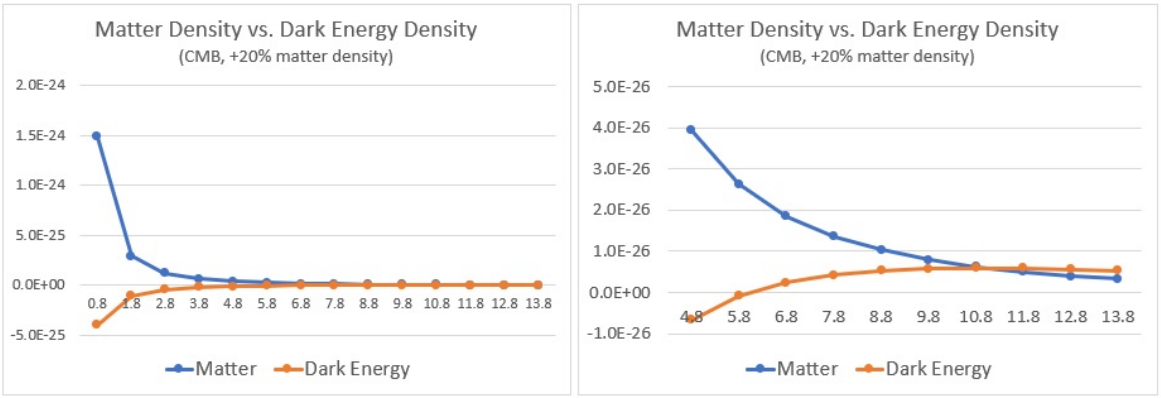

Figure 4: **Matter Density vs. Dark Energy Density (CMB-Based, +20% Matter Enhancement, Constant $\beta = 1.2387$, $\Omega_m \simeq 0.3790$).** For the +20% matter enhancement case, $\Omega_m \simeq 0.3790$, the dark energy density remains negative for $t \lesssim 6.07\,\mathrm{Gyr}$, thereby enhancing deceleration and supporting the formation of galactic structures. After changing sign, it drives accelerated expansion from approximately $t \simeq 8.77\,\mathrm{Gyr}$. The dark energy density then reaches a broad maximum over $t \simeq 10.8$–$11.8\,\mathrm{Gyr}$ and subsequently decreases slowly toward the present epoch.

Age (Gyr)	Scale $a(t)$	Constant β	Comoving Ho. $\chi_p(t)$ (Gly)	Physical Ho. $R_{\mathrm{phys}}(t)$ (Gly)	**Matter** $\rho_m(t)$	Repulsive $\rho_{m\text{-}gs}(t)$	Attractive $-\rho_{gs}(t)$	**Dark Energy** $\rho_{\Lambda_m}(t)$
					$(10^{-27}\ \mathrm{kg\,m^{-3}})$			
0.8	0.1295	1.2387	17.763	2.300	1487.172	131.210	-522.668	**-391.458**
1.8	0.2226	1.2387	23.521	5.236	292.816	79.425	-180.442	**-101.020**
2.8	0.2998	1.2387	27.369	8.205	119.860	59.601	-100.010	**-40.405**
3.8	0.3694	1.2387	30.368	11.218	64.074	48.293	-65.818	**-17.525**
4.8	0.4346	1.2387	32.862	14.282	39.346	40.665	-47.328	**-6.664**
5.8	0.4972	1.2387	35.013	17.408	26.277	34.997	-35.881	**-0.884**
6.8	0.5584	1.2387	36.912	20.612	18.550	30.517	-28.151	**2.366**
7.8	0.6190	1.2387	38.614	23.902	13.618	26.830	-22.616	**4.214**
8.8	0.6796	1.2387	40.156	27.290	10.290	23.711	-18.482	**5.229**
9.8	0.7408	1.2387	41.567	30.793	7.945	21.019	-15.290	**5.729**
10.8	0.8031	1.2387	42.864	34.424	6.235	18.654	-12.761	**5.893**
11.8	0.8668	1.2387	44.064	38.195	4.959	16.569	-10.736	**5.843**
12.8	0.9323	1.2387	45.178	42.119	3.986	14.715	-9.061	**5.653**
13.8	1.0000	1.2387	46.114	46.114	3.230	12.942	-7.650	**5.292**

Table 6: **MOC Cosmic History Simulation (CMB-Based, +20% Matter Enhancement, Constant $\beta = 1.2387$, $\Omega_m \simeq 0.3790$).** CMB-based evolution for a +20% matter enhancement scenario, corresponding to $\Omega_m \simeq 0.3790$, with the present particle-horizon scale normalized to $\chi_p(t_0) = 46.114\,\mathrm{Gly}$. The dark energy density is negative up to $t \simeq 6.07\,\mathrm{Gyr}$, so the early evolution remains decelerating and favorable to structure formation. It becomes positive near $t \simeq 6.07\,\mathrm{Gyr}$, and the acceleration condition $\rho_{\Lambda_m} > \rho_m/2$ is reached near $t \simeq 8.77\,\mathrm{Gyr}$. A broad late-time maximum is realized over $t \simeq 10.8$–$11.8\,\mathrm{Gyr}$, after which ρ_{Λ_m} decreases only slowly, indicating a quasi-constant dark energy behavior over much of the late universe. Compared with the standard +0% CMB case, where the sign transition occurs near $t \simeq 5.38\,\mathrm{Gyr}$ and acceleration begins near $t \simeq 7.72\,\mathrm{Gyr}$, the higher matter abundance delays both transitions. This illustrates the systematic trend that increasing the matter density extends the decelerating structure-formation epoch before the GSE-induced dark energy component becomes dynamically dominant.

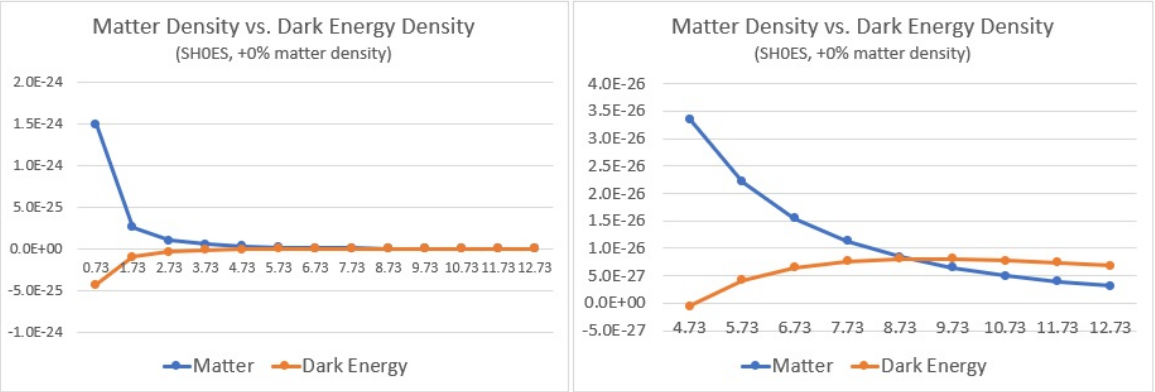

Figure 5: **Matter Density vs. Dark Energy Density (SH0ES-Based, +0% Matter Enhancement, Constant $\beta = 1.5606$, $\Omega_m \simeq 0.315$).** For the standard matter abundance case, $\Omega_m \simeq 0.315$, the dark energy density remains negative for $t \lesssim 4.85\,\mathrm{Gyr}$, enhancing deceleration and supporting the formation of galactic structures. It becomes positive after the sign transition and drives accelerated expansion from approximately $t \simeq 7.11\,\mathrm{Gyr}$. The dark energy density reaches a broad maximum over $t \simeq 8.73$–$9.73\,\mathrm{Gyr}$ and then decreases slowly toward the present epoch.

Age (Gyr)	Scale $a(t)$	Constant β	Comoving Ho. $\chi_p(t)$ (Gly)	Physical Ho. $R_{\mathrm{phys}}(t)$ (Gly)	**Matter** $\rho_m(t)$	Repulsive $\rho_{m\text{-}gs}(t)$	Attractive $-\rho_{gs}(t)$	**Dark Energy** $\rho_{\Lambda_m}(t)$
					(10^{-27} kg m^{-3})			
0.73	0.1283	1.5606	17.082	2.192	1494.613	170.967	-598.103	**-427.136**
1.73	0.2285	1.5606	22.762	5.201	264.576	95.416	-187.993	**-92.577**
2.73	0.3111	1.5606	26.487	8.240	104.836	69.322	-100.866	**-31.544**
3.73	0.3854	1.5606	29.364	11.317	55.141	55.076	-65.204	**-10.130**
4.73	0.4552	1.5606	31.749	14.452	33.466	45.683	-46.263	**-0.580**
5.73	0.5224	1.5606	33.798	17.656	22.141	38.814	-34.686	**4.129**
6.73	0.5883	1.5606	35.599	20.943	15.503	33.450	-26.944	**6.506**
7.73	0.6540	1.5606	37.212	24.337	11.284	29.069	-21.429	**7.640**
8.73	0.7200	1.5606	38.667	27.840	8.457	25.398	-17.341	**8.058**
9.73	0.7871	1.5606	39.995	31.480	6.473	22.252	-14.200	**8.052**
10.73	0.8559	1.5606	41.215	35.276	5.034	19.516	-11.728	**7.788**
11.73	0.9266	1.5606	42.336	39.229	3.968	17.124	-9.753	**7.371**
12.73	1.0000	1.5606	43.377	43.377	3.157	15.013	-8.145	**6.868**

Table 7: **MOC Cosmic History Simulation (SH0ES-Based, +0% Matter Enhancement, Constant $\beta = 1.5606$, $\Omega_m \simeq 0.315$).** SH0ES-based evolution for the standard matter abundance case, with the present particle-horizon scale normalized to $\chi_p(t_0) = 43.377\,\mathrm{Gly}$. Because the SH0ES baseline has a larger Hubble constant than the CMB baseline, the reconstructed present age of the universe is reduced to $t_0 \simeq 12.73\,\mathrm{Gyr}$, about 1 Gyr shorter than the CMB-based value. The dark energy density is negative up to $t \simeq 4.85\,\mathrm{Gyr}$, so the early evolution remains decelerating and favorable to structure formation. It changes sign near $t \simeq 4.85\,\mathrm{Gyr}$, becomes positive, and satisfies the acceleration condition $\rho_{\Lambda_m} > \rho_m/2$ near $t \simeq 7.11\,\mathrm{Gyr}$. The dark energy density reaches a broad maximum over $t \simeq 8.73$–$9.73\,\mathrm{Gyr}$ and then decreases slowly toward the present epoch. This SH0ES-based standard-matter case shows the same qualitative sequence as the CMB-based +0% case: early negative ρ_{Λ_m}, sign transition, onset of accelerated expansion, a broad late-time maximum, and slow decline toward the present.

6.4 Dark energy evolution under an evolving structure coefficient $\beta(t)$

The constant-β simulations show that the total GSE density function alone can generate the main MOC cosmic sequence. However, in the full physical interpretation of the model, β is a structural coefficient associated with the matter distribution. As the universe evolves from a smoother early matter distribution toward a more structured cosmic web of galaxies, clusters, voids, and halo environments, the effective cosmological value of β may also evolve.

For this reason, we also examine explicitly evolving-$\beta(t)$ histories in the standard CMB 0% matter enhancement case. This case is the natural reference background because it corresponds to the standard CMB matter abundance, $\Omega_m \simeq 0.3158$, with the present particle-horizon scale normalized to $\chi_p(t_0) = 46.114\,\mathrm{Gly}$. The present value $\beta(t_0) = 1.6172$ is fixed by the same present-epoch matching condition used in the constant-β CMB baseline.

We consider three representative prescriptions:

$$\beta(t) = 1.6172,$$

$$\beta(t) : 1.4555 \rightarrow 1.6172,$$

and

$$\beta(t) : 1.7789 \rightarrow 1.6172.$$

The latter two cases correspond to monotonic linear evolution from values 10% below and 10% above the present matched value, respectively. They are not independent dark energy functions. Rather, they represent explicit evolving structural coefficients entering the same total GSE density formula, $\rho_{\Lambda_m}(t)$ (Eq. 167).

A linear evolution of $\beta(t)$ provides the simplest first-order representation of slow structural evolution over the simulated interval. This is physically motivated by the fact that β is not an independent field, but an effective GSE coefficient determined by the large-scale organization of matter. The process of structure formation is directional: the matter distribution evolves from an initially smoother state toward a locally clustered, filamentary cosmic web. Therefore, allowing $\beta(t)$ to evolve monotonically provides a natural extension of the constant-β approximation while preserving the same total GSE mechanism.

The results show that the evolving-$\beta(t)$ histories modify the quantitative timing of the transition epochs, but do not change the qualitative cosmic sequence.

The evolving-$\beta(t)$ cases can be summarized as follows.

- **Lower-evolving case:**

  $$\beta(t) : 1.4555 \rightarrow 1.6172.$$

  In this case, the early negative dark energy density is reduced in magnitude compared with the constant-β case. The sign transition is delayed from $t \simeq 5.38\,\mathrm{Gyr}$ to approximately $t \simeq 5.84\,\mathrm{Gyr}$, and the acceleration condition $\rho_{\Lambda_m} > \frac{1}{2}\rho_m$ is reached near $t \simeq 8.29\,\mathrm{Gyr}$.

- **Upper-evolving case:**

  $$\beta(t) : 1.7789 \rightarrow 1.6172.$$

  In this case, the early negative dark energy density is mildly enhanced in magnitude compared with the constant-β case. The sign transition is advanced from $t \simeq 5.38\,\mathrm{Gyr}$ to approximately $t \simeq 4.81\,\mathrm{Gyr}$, and the onset of acceleration is correspondingly advanced to $t \simeq 7.19\,\mathrm{Gyr}$.

Thus, the explicit evolution of $\beta(t)$ changes the detailed timing of the sign transition and acceleration onset, as expected. A larger early value of β makes the repulsive matter–GSE interaction term become important earlier, whereas a smaller early value delays this transition. Nevertheless, all three cases exhibit the same main MOC pattern:

1) an early negative $\rho_{\Lambda_m}(t)$ phase,

2) a transition to positive dark energy at intermediate times,

3) the onset of late-time accelerated expansion,

4) a quasi-constant dark energy behavior in the late-time universe,

5) and a mild weakening trend in the recent universe.

This comparison is important because it shows that the MOC result is not restricted to the constant-β approximation. Even in these evolving-$\beta(t)$ cases, where the structure coefficient is allowed to vary explicitly, the total GSE formula continues to generate the same qualitative cosmic history.

The role of $\beta(t)$ should therefore be understood as limited and structural. The primary source variables of the total GSE are not $\beta(t)$, but the matter density and the length scale over which the mass distribution is defined. In the dark energy density formulation, these are $\rho_m(t)$ and $\chi_p(t)$.

By contrast, $\beta(t)$ is a coefficient entering the GSE integral. It encodes the internal distribution of a given mass within the relevant volume, but **it is not a new source of gravity and not a primary variable comparable to $\rho_m(t)$ or $\chi_p(t)$.** Once the density profile is specified, $\beta(t)$ is fixed by the corresponding gravitational self-energy calculation. Thus, varying $\beta(t)$ can shift the detailed timing and amplitude of the transition, but the origin of the dark energy behavior remains the total GSE structure itself.

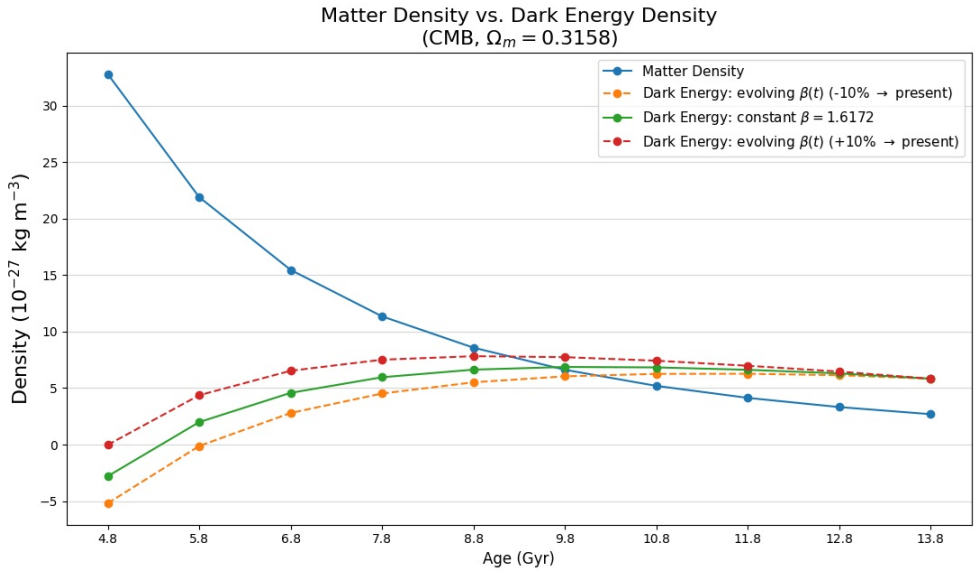

Figure 6: **Matter Density vs. Dark Energy Density (CMB-Based, +0% Matter Enhancement, Evolving β).** The three dark energy curves correspond to $\beta(t)$: 1.4555 → 1.6172, constant $\beta = 1.6172$, and $\beta(t)$: 1.7789 → 1.6172. **All cases retain the same qualitative MOC sequence: sign transition, late-time acceleration, and quasi-constant dark energy.**

Age (Gyr)	Scale $a(t)$	Evolving $\beta(t)$	Comoving Ho. $\chi_p(t)$ (Gly)	Physical Ho. $R_{\text{phys}}(t)$ (Gly)	**Matter** $\rho_m(t)$	Repulsive $\rho_{m\text{-}gs}(t)$	Attractive $-\rho_{gs}(t)$	**Dark Energy** $\rho_{\Lambda_m}(t)$
					(10^{-27} kg m^{-3})			
0.8	0.1295	1.4555	17.763	2.300	1239.310	104.834	-426.485	**-321.650**
1.8	0.2226	1.4679	23.521	5.236	244.013	64.549	-148.495	**-83.947**
2.8	0.2998	1.4804	27.369	8.205	99.884	49.262	-82.997	**-33.736**
3.8	0.3694	1.4928	30.368	11.218	53.395	40.589	-55.083	**-14.494**
4.8	0.4346	1.5052	32.862	14.282	32.788	34.750	-39.939	**-5.189**
5.8	0.4972	1.5177	35.013	17.408	21.898	30.403	-30.529	**-0.126**
6.8	0.5584	1.5301	36.912	20.612	15.458	26.948	-24.149	**2.799**
7.8	0.6190	1.5426	38.614	23.902	11.348	24.078	-19.558	**4.520**
8.8	0.6796	1.5550	40.156	27.290	8.575	21.624	-16.112	**5.512**
9.8	0.7408	1.5674	41.567	30.793	6.620	19.476	-13.436	**6.041**
10.8	0.8031	1.5799	42.864	34.424	5.196	17.561	-11.302	**6.258**
11.8	0.8668	1.5923	44.064	38.195	4.133	15.844	-9.574	**6.270**
12.8	0.9323	1.6048	45.178	42.119	3.321	14.292	-8.152	**6.140**
13.8	1.0000	1.6172	46.114	46.114	2.691	12.766	-6.935	**5.831**

Table 8: **MOC Cosmic History Simulation (CMB-Based, +0% Matter Enhancement, Evolving $\beta(t)$: 1.4555 → 1.6172, $\Omega_m \simeq 0.3158$).** Compared with the constant-$\beta = 1.6172$ case, the lower-evolving $\beta(t)$ mildly reduces the early negative ρ_{Λ_m}, delays the sign transition to $t \simeq 5.84$ Gyr, and delays the acceleration onset to $t \simeq 8.29$ Gyr, while preserving the same late-time quasi-constant behavior.

Age (Gyr)	Scale $a(t)$	Evolving $\beta(t)$	Comoving Ho. $\chi_p(t)$ (Gly)	Physical Ho. $R_{\text{phys}}(t)$ (Gly)	**Matter** $\rho_m(t)$	Repulsive $\rho_{m\text{-}gs}(t)$	Attractive $-\rho_{gs}(t)$	**Dark Energy** $\rho_{\Lambda_m}(t)$
					(10^{-27} kg m^{-3})			
0.8	0.1295	1.7789	17.763	2.300	1239.310	156.604	-521.259	**-364.655**
1.8	0.2226	1.7665	23.521	5.236	244.013	93.476	-178.698	**-85.222**
2.8	0.2998	1.7540	27.369	8.205	99.884	69.160	-98.341	**-29.181**
3.8	0.3694	1.7416	30.368	11.218	53.395	55.247	-64.263	**-9.016**
4.8	0.4346	1.7292	32.862	14.282	32.788	45.858	-45.880	**-0.023**
5.8	0.4972	1.7167	35.013	17.408	21.898	38.901	-34.533	**4.367**
6.8	0.5584	1.7043	36.912	20.612	15.458	33.431	-26.898	**6.533**
7.8	0.6190	1.6918	38.614	23.902	11.348	28.964	-21.451	**7.513**
8.8	0.6796	1.6794	40.156	27.290	8.575	25.222	-17.401	**7.822**
9.8	0.7408	1.6670	41.567	30.793	6.620	22.028	-14.289	**7.739**
10.8	0.8031	1.6545	42.864	34.424	5.196	19.259	-11.836	**7.423**
11.8	0.8668	1.6421	44.064	38.195	4.133	16.850	-9.874	**6.976**
12.8	0.9323	1.6296	45.178	42.119	3.321	14.739	-8.279	**6.460**
13.8	1.0000	1.6172	46.114	46.114	2.691	12.766	-6.935	**5.831**

Table 9: **MOC Cosmic History Simulation (CMB-Based, +0% Matter Enhancement, Evolving $\beta(t)$: 1.7789 → 1.6172, $\Omega_m \simeq 0.3158$).** This simulation uses the standard CMB matter abundance, $\Omega_m \simeq 0.3158$, and linearly evolves the structure coefficient from a value 10% above the present matched value, $\beta(t = 0.8\,\text{Gyr}) = 1.7789$, to $\beta(t_0) = 1.6172$ at $t_0 \simeq 13.8$ Gyr. The sign transition is correspondingly advanced from $t \simeq 5.38$ Gyr to $t \simeq 4.81$ Gyr, and the acceleration condition $\rho_{\Lambda_m} > \rho_m/2$ is advanced from $t \simeq 7.72$ Gyr to $t \simeq 7.19$ Gyr. The dark energy density reaches a broad late-time maximum over $t \simeq 8.8$–9.8 Gyr and then decreases slowly toward the present epoch. Despite these quantitative shifts, the same qualitative MOC sequence persists: an early negative dark energy density, an intermediate transition to positive dark energy, the onset of late-time acceleration, and a quasi-constant late universe behavior.

7 Analysis of the Cosmic History using MOC

We now analyze the cosmic history simulations obtained from the MOC framework. The primary reference set is the CMB-based reconstruction, for which we consider matter density scenarios

$$f = -10\%, \quad 0\%, \quad +10\%, \quad +20\%$$

relative to the standard matter abundance $\Omega_m \simeq 0.315$. The corresponding benchmark simulations are summarized in Tables 3–6. As a late universe comparison, we also present the SH0ES-based standard matter abundance case in Table 7.

In the main benchmark simulations, the structure coefficient β is held fixed within each matter density scenario. This choice is not meant to imply that β is exactly constant over the full cosmic history. Rather, it provides a clean reference reconstruction of the total GSE density evolution. Since β is a structural coefficient in the GSE integral, the dominant physical dependence of $\rho_{\Lambda_m}(t)$ is carried by the matter density and the horizon-scale mass distribution. In the present cosmological formulation, these are represented by $\rho_m(t)$ and $\chi_p(t)$.

We also examine explicitly evolving-$\beta(t)$ cases around the standard CMB 0% matter enhancement case in Section 6.4. Those simulations show that allowing $\beta(t)$ to evolve mildly changes the detailed timing and amplitude of the transition, but preserves the same qualitative MOC sequence. For this reason, the main physical analysis below is based on the constant-β benchmark tables, while the evolving-$\beta(t)$ cases are used to confirm that the characteristic behavior of $\rho_{\Lambda_m}(t)$ is not restricted to the fixed-β choice.

The simulations show that the total GSE density function reproduces the characteristic late-time behavior usually attributed to dark energy. It yields the onset of cosmic acceleration approximately 5–6 Gyr before the present epoch, a quasi-constant late-time regime, and a subsequent mild weakening of $\rho_{\Lambda_m}(t)$. A distinctive feature of the MOC framework, however, is that this late-time behavior is preceded by an early negative dark energy phase and a subsequent sign transition. This differs sharply from the standard ΛCDM model, in which the dark energy density is positive and constant at all times. The early negative phase and sign transition are therefore not merely auxiliary features, but potential observational discriminants of the total GSE interpretation.

Thus, the main time dependence of $\rho_{\Lambda_m}(t)$ arises from the evolution of the matter density and the horizon scale within the total GSE structure, rather than from introducing a separate dark energy sector.

For the CMB-based simulations, the present particle-horizon scale is normalized to

$$\chi_p(t_0) = 46.114\,\text{Gly},$$

with $t_0 \simeq 13.8\,\text{Gyr}$. For the SH0ES-based comparison case, the larger Hubble constant implies a shorter reconstructed age, $t_0 \simeq 12.73\,\text{Gyr}$, and the present particle-horizon scale is normalized to

$$\chi_p(t_0) = 43.377\,\text{Gly}.$$

A coherent picture emerges across all simulated cases. In contrast to the standard ΛCDM scenario, where dark energy is represented by a strict cosmological constant, the MOC framework predicts a matter-induced dynamical dark energy density with a characteristic three-phase evolution:

1) an early phase with negative $\rho_{\Lambda_m}(t)$, acting as an additional attractive contribution and supporting structure formation;

2) an intermediate phase in which $\rho_{\Lambda_m}(t)$ crosses zero and becomes positive;

3) a late phase in which positive $\rho_{\Lambda_m}(t)$ drives accelerated expansion and then varies only mildly, behaving quasi-constantly on Gyr timescales.

Below we quantify this behavior and examine how it changes with the assumed matter abundance.

7.1 Competition between the attractive and repulsive GSE components

The central dynamical mechanism of the MOC framework is the competition between two GSE contributions. The first is the attractive conventional GSE density, denoted by $-\rho_{gs}$. The second is the positive matter–GSE interaction density, denoted by $\rho_{m\text{-}gs}$. The effective dark energy density is their sum,

$$\rho_{\Lambda_m}(t) = \rho_{m\text{-}gs}(t) - \rho_{gs}(t). \tag{177}$$

Using the horizon-scale compactness variable

$$x(t) \equiv \frac{R_S(t)}{\chi_p(t)}, \tag{178}$$

the two terms may be written as

$$-\rho_{gs}(t) = -\frac{\beta\rho_m(t)}{2}x(t), \tag{179}$$

and

$$\rho_{m\text{-}gs}(t) = \rho_m(t)\frac{5\beta^2}{28}x(t)^2. \tag{180}$$

Therefore,

$$\rho_{\Lambda_m}(t) = \frac{\beta\rho_m(t)}{2}x(t)\left[\frac{5\beta}{14}x(t) - 1\right]. \tag{181}$$

This form makes the sign transition transparent. At early times, the compactness $x(t)$ is not yet large enough for the quadratic repulsive term to dominate. The attractive GSE density then exceeds the matter–GSE interaction density in magnitude, and $\rho_{\Lambda_m}(t) < 0$. As the causal horizon grows and the causally connected matter content increases, $x(t)$ grows sufficiently for the x^2-dependent repulsive term to overtake the linear attractive term. The sign change occurs when

$$\frac{5\beta}{14}x(t) = 1, \qquad \text{or equivalently} \qquad x(t) = \frac{14}{5\beta}. \tag{182}$$

Here $x(t) = R_S(t)/\chi_p(t)$ is used as a compact diagnostic, but it is not an independent source variable. Since $R_S(t) = 2GM(t)/c^2$ and $M(t)$ is fixed by the matter density and the horizon-scale volume, the underlying physical inputs are $\rho_m(t)$ and $\chi_p(t)$. The coefficient β enters as a structural coefficient of the GSE integral. Therefore, the sign transition and the later quasi-constant behavior of $\rho_{\Lambda_m}(t)$ arise primarily from the evolution of the matter density and horizon scale within the total GSE structure.

7.2 A possible MOC interpretation of the Hubble tension

One of the most significant challenges in modern cosmology is the "Hubble tension"—the persistent discrepancy between the value of the Hubble constant H_0 inferred from early-universe observations and that measured in the local, late-time universe [10]. Measurements of the Cosmic Microwave Background (CMB) by the Planck satellite infer $H_0 \approx 67.36\,\mathrm{km\,s^{-1}\,Mpc^{-1}}$ [5], whereas local distance ladder measurements, such as those from the SH0ES program, indicate a higher value, $H_0 \approx 73.04\,\mathrm{km\,s^{-1}\,Mpc^{-1}}$ [13]. In the standard ΛCDM model, where dark energy is represented by a strict cosmological constant, this discrepancy has become one of the major tensions in precision cosmology [10, 43].

In the MOC framework, the effective dark energy density is not a fundamental constant. It is a matter-induced quantity determined by the total GSE,

$$\rho_{\Lambda_m}(t) = \frac{\beta\rho_m(t)}{2}\frac{R_S(t)}{\chi_p(t)}\left[\frac{5\beta}{14}\frac{R_S(t)}{\chi_p(t)} - 1\right]. \tag{183}$$

Thus, even when β is held fixed, $\rho_{\Lambda_m}(t)$ remains dynamical because it depends on the matter density and the horizon-scale compactness ratio $R_S(t)/\chi_p(t)$. This is the central difference from ΛCDM: the effective dark energy contribution in MOC evolves with the matter distribution and the causal horizon, rather than being imposed as a strict constant.

From this viewpoint, the Hubble tension may be interpreted as a possible consequence of forcing a dynamical matter-induced dark energy component into a constant-Λ description. Early universe and late universe observations are calibrated against different effective cosmic histories. If the effective dark energy sector evolves with $\rho_m(t)$ and $R_S(t)/\chi_p(t)$, then a single constant-Λ fit can lead to different inferred expansion rates depending on whether the calibration is anchored to the CMB or to late time distance ladder observations.

Therefore, within MOC, the Hubble tension may be understood as a possible consequence of imposing the constant-Λ assumption on a dynamical dark energy sector.

7.3 The emergence of quasi-constant and weakening dark energy

A key quantitative outcome of the MOC simulations is the emergence of a positive dark energy density at late times with only mild evolution on multi-Gyr timescales. This behavior appears across the CMB-based matter enhancement sequence and also in the SH0ES-based standard-matter comparison case. The important point is that this quasi-constant behavior is obtained even though $\rho_{\Lambda_m}(t)$ is not imposed as a cosmological constant. It follows from the total GSE density function itself.

For the CMB-based simulations, the matter enhancement percentage is defined relative to the standard reference abundance $\Omega_m \simeq 0.3158$. The transition epochs are summarized in Table 10. The sign transition is defined by

$$\rho_{\Lambda_m}(t) = 0, \tag{184}$$

while the onset of accelerated expansion is estimated by the diagnostic condition

$$\rho_{\Lambda_m}(t) > \frac{1}{2}\rho_m(t). \tag{185}$$

This condition follows from the standard acceleration equation for pressureless matter and an effective dark energy component with $w \simeq -1$ once ρ_{Λ_m} becomes positive [4]. In the present context, it is used as a diagnostic criterion rather than as an assumption that ρ_{Λ_m} is a strict cosmological constant.

Baseline	Matter enhancement relative to $\Omega_m = 0.3158$	Constant β	Sign transition	Acceleration onset
CMB	-10%	1.8854	$t \simeq 4.98\,\mathrm{Gyr}$	$t \simeq 7.21\,\mathrm{Gyr}$
CMB	0%	1.6172	$t \simeq 5.38\,\mathrm{Gyr}$	$t \simeq 7.72\,\mathrm{Gyr}$
CMB	$+10\%$	1.4071	$t \simeq 5.79\,\mathrm{Gyr}$	$t \simeq 8.29\,\mathrm{Gyr}$
CMB	$+20\%$	1.2387	$t \simeq 6.07\,\mathrm{Gyr}$	$t \simeq 8.77\,\mathrm{Gyr}$
SH0ES	0%	1.5606	$t \simeq 4.85\,\mathrm{Gyr}$	$t \simeq 7.11\,\mathrm{Gyr}$

Table 10: **Transition epochs in the MOC benchmark simulations.** The matter enhancement percentage is defined relative to the standard reference abundance $\Omega_m = 0.3158$. The sign transition is defined by $\rho_{\Lambda_m} = 0$, while the acceleration onset is estimated by $\rho_{\Lambda_m} > \rho_m/2$. The CMB-based cases show that increasing the matter abundance delays both the sign transition and the onset of accelerated expansion. The SH0ES 0% matter enhancement case shows the same qualitative sequence on a shorter reconstructed cosmic age scale.

The standard CMB case, corresponding to 0% matter enhancement relative to $\Omega_m = 0.3158$, provides the reference simulation. In this case, $\rho_{\Lambda_m}(t)$ changes sign near $t \simeq 5.38\,\mathrm{Gyr}$, satisfies the acceleration condition near $t \simeq 7.72\,\mathrm{Gyr}$, reaches a broad maximum over $t \simeq 9.8$–$10.8\,\mathrm{Gyr}$, and then decreases slowly toward the present. The present value is

$$\rho_{\Lambda_m}(t_0) \simeq 5.831 \times 10^{-27}\,\mathrm{kg\,m^{-3}}, \tag{186}$$

consistent with $\rho_{\Lambda_m} \simeq 0.684\rho_c$ for the CMB critical density $\rho_c \simeq 8.5227 \times 10^{-27}\,\mathrm{kg\,m^{-3}}$.

Within the CMB-based sequence, the -10% matter enhancement case reaches its maximum slightly earlier, near $t \simeq 9.71\,\mathrm{Gyr}$. By contrast, the $+10\%$ and $+20\%$ matter enhancement cases exhibit broader late-time maxima extending over $t \simeq 9.8$–$11.8\,\mathrm{Gyr}$ and $t \simeq 10.8$–$11.8\,\mathrm{Gyr}$, respectively. Thus, increasing the matter abundance systematically delays both the sign transition and the onset of acceleration, extending the decelerating structure-formation epoch before the GSE-induced dark energy component becomes dynamically dominant.

Unlike a strict cosmological constant, $\rho_{\Lambda_m}(t)$ is a dynamical density constructed from the total GSE. Nevertheless, after the onset of acceleration it remains nearly constant over several Gyr. For example, in the standard CMB case with 0% matter enhancement, corresponding to $\Omega_m \simeq 0.3158$, $\rho_{\Lambda_m}(t)$ remains quasi-constant over $t \simeq 8.8$–$13.8\,\mathrm{Gyr}$, varying only at the $\sim 10\%$ level around its mean value, while the matter density decreases by about 69% over the same interval. More specifically, after reaching a broad maximum over $t \simeq 9.8$–$10.8\,\mathrm{Gyr}$, $\rho_{\Lambda_m}(t)$ decreases from $\rho_{\Lambda_m}^{\max} \simeq 6.87 \times 10^{-27}\,\mathrm{kg\,m^{-3}}$ to $\rho_{\Lambda_m}(t_0) \simeq 5.83 \times 10^{-27}\,\mathrm{kg\,m^{-3}}$, **corresponding to a mild weakening of about** 15% **relative to the peak value.**

This behavior is qualitatively consistent with recent DESI indications that dark energy may not be strictly constant and may exhibit a mild late-time weakening, although the observational evidence has not yet reached discovery-level significance [11, 12, 44]. In the present MOC framework, such a weakening is not introduced phenomenologically, but follows from the total GSE density function as the matter density and horizon scale evolve.

The SH0ES-based standard-matter case provides a useful comparison. Because the SH0ES baseline has a larger Hubble constant than the CMB baseline, its reconstructed present age is shorter, $t_0 \simeq 12.73\,\mathrm{Gyr}$. Nevertheless, the same qualitative sequence appears: early negative ρ_{Λ_m}, sign transition, onset of accelerated expansion, a broad late-time maximum over

$t \simeq 8.73$–$9.73\,\mathrm{Gyr}$, and slow decline toward the present. This supports the interpretation that the three-phase MOC cosmic history is not an artifact of a particular H_0 baseline, but a robust consequence of the total GSE dynamics.

The resulting picture is therefore neither a strictly constant dark energy model nor a rapidly varying dark energy model. Instead, MOC produces a dynamical $\rho_{\Lambda_m}(t)$ that is negative during the early structure-formation era, becomes positive at intermediate times, drives late-time acceleration, and then behaves quasi-constantly with a mild weakening trend in the recent universe.

7.4 Possible implications for early–universe structure anomalies

One of the most distinctive features of the MOC simulations is the appearance of a negative effective dark energy density in the early universe. In this phase, $\rho_{\Lambda_m}(t) < 0$ acts as an additional attractive contribution rather than as a repulsive component. This provides a natural pathway for enhanced early structure growth and may help alleviate several early-structure anomalies, including the rapid assembly of massive galaxies reported by JWST [45, 46] and the structure-growth tensions indicated by Euclid, KiDS, and related surveys [47, 48].

In the CMB-based benchmark simulations, the early value of ρ_{Λ_m} at $t = 0.8\,\mathrm{Gyr}$ is significantly negative in all four matter enhancement scenarios:

- $f = -10\%$: $\rho_{\Lambda_m} \simeq -3.19 \times 10^{-25}\,\mathrm{kg\,m^{-3}}$,
- $f = 0\%$: $\rho_{\Lambda_m} \simeq -3.44 \times 10^{-25}\,\mathrm{kg\,m^{-3}}$,
- $f = +10\%$: $\rho_{\Lambda_m} \simeq -3.68 \times 10^{-25}\,\mathrm{kg\,m^{-3}}$,
- $f = +20\%$: $\rho_{\Lambda_m} \simeq -3.91 \times 10^{-25}\,\mathrm{kg\,m^{-3}}$.

These values are substantial compared with the corresponding matter density at the same epoch, typically at the level of roughly 26–29% of $\rho_m(t)$ in magnitude. They therefore represent a non-negligible attractive component generated by the total GSE, rather than by an exotic new matter species.

Physically, this early negative phase increases the effective attractive contribution in the background evolution and can support the rapid formation of massive bound structures. It therefore offers a possible background level explanation for why massive galaxies and black-hole seeds may appear earlier than expected in a standard ΛCDM interpretation [45, 46, 49, 50]. A complete treatment of structure formation requires perturbation level and N-body analyses. Nevertheless, the background evolution already shows the key qualitative feature: MOC naturally supplies an early attractive phase without introducing a separate early dark energy sector.

The subsequent sign transition is equally important. After $\rho_{\Lambda_m}(t)$ crosses zero, the same total GSE mechanism produces a positive dark energy density that drives late-time accelerated expansion. Thus, within a single GSE-based framework, MOC connects two phenomena that are usually treated separately: enhanced early structure growth and late-time cosmic acceleration.

7.5 The cosmological constant coincidence problem

A long-standing conceptual puzzle in the standard ΛCDM framework is the cosmological constant coincidence problem [3, 4, 8]: why is the dark energy density observed today of the same

order of magnitude as the matter density, despite their different physical origins and different redshift scalings? In ΛCDM, the matter density decreases as the universe expands, while the cosmological constant remains fixed. The near equality $\rho_m \sim \rho_\Lambda$ therefore occurs only within a limited temporal window, motivating fine-tuning or anthropic arguments in parts of the literature [3, 8].

In the MOC framework, this near equality is not accidental. The effective dark energy density $\rho_{\Lambda_m}(t)$ is not an independent vacuum component. It is generated from the total GSE of matter and is therefore linked to the same matter distribution that determines $\rho_m(t)$. Equivalently, when the characteristic radius of the mass distribution is denoted by R, the dark energy density can be expressed as a function of the matter density and the mass distribution scale:

$$\rho_{\Lambda_m}(\rho_m, R) = c_1 \beta \rho_m^2 R^2 \left(c_2 \beta \rho_m R^2 - 1\right), \tag{187}$$

where c_1 and c_2 are fixed constants defined by G and c. Thus, apart from the structural coefficient β, the relevant physical dependence is carried by ρ_m and the length scale R, or by $\rho_m(t)$ and the particle-horizon scale $\chi_p(t)$ in the cosmological application.

This relation explains why the matter density and the effective dark energy density can remain comparable over a substantial fraction of late cosmic history. In the standard CMB case with 0% matter enhancement, for example, ρ_{Λ_m} becomes comparable to ρ_m during the late universe. At $t = 7.8\,\mathrm{Gyr}$, one has

$$\rho_m \simeq 11.348, \qquad \rho_{\Lambda_m} \simeq 5.960,$$

while near $t = 9.8\,\mathrm{Gyr}$,

$$\rho_m \simeq 6.620, \qquad \rho_{\Lambda_m} \simeq 6.870,$$

in units of $10^{-27}\,\mathrm{kg\,m^{-3}}$. At the present epoch,

$$\rho_m(t_0) \simeq 2.691, \qquad \rho_{\Lambda_m}(t_0) \simeq 5.831,$$

so the two densities remain within the same order of magnitude.

From this perspective, the present-day relation $\rho_m \sim \rho_{\Lambda_m}$ is not a coincidence between two unrelated components. It is a consequence of the fact that both quantities originate from the same underlying matter distribution. What appears as an unnatural coincidence in ΛCDM is reinterpreted in MOC as a natural outcome of total GSE dynamics: the effective dark energy density is generated by matter itself, becomes positive only after a sign transition, remains quasi-constant over the late universe, and shows a mild weakening trend toward the present epoch.

7.6 Describing the dynamics of the universe without new free parameters or fields

The MOC framework describes the observed dark energy phenomenology without introducing new fundamental scalar fields or an additional independent dark energy fluid. In this framework, the effective dark energy density is generated by the total gravitational self-energy of matter itself. The primary physical inputs are the matter density and the length scale over which the mass distribution is defined.

This point is most transparent when the dark energy density is written directly as a function of the matter density and the characteristic radius of the mass distribution. With

$$c_1 \equiv \frac{4\pi G}{3c^2}, \qquad c_2 \equiv \frac{20\pi G}{21c^2}, \tag{188}$$

the total GSE dark energy density can be written as

$$\rho_{\Lambda_m}(\rho_m, R) = c_1 \beta \rho_m^2 R^2 \left(c_2 \beta \rho_m R^2 - 1\right). \tag{189}$$

Thus, apart from the structural coefficient β, the functional dependence is carried by ρ_m and R. The dark energy density is therefore not introduced as a new component of the cosmic inventory, but is obtained from the matter distribution itself.

In the horizon-scale cosmological application, the same relation may be expressed as

$$\rho_{\Lambda_m}(t) = \frac{\beta \rho_m(t)}{2} \frac{R_S(t)}{\chi_p(t)} \left[\frac{5\beta}{14} \frac{R_S(t)}{\chi_p(t)} - 1\right]. \tag{190}$$

Here $R_S(t) = 2GM(t)/c^2$, and $M(t)$ is determined by the matter density and the horizon-scale volume. Therefore, the compactness ratio $R_S(t)/\chi_p(t)$ is a useful derived quantity, but the underlying physical inputs are still $\rho_m(t)$ and the horizon scale $\chi_p(t)$.

The benchmark simulations make this point explicit. Across the CMB-based matter enhancement sequence, $-10\%, 0\%, +10\%, +20\%$, and also in the SH0ES-based 0% comparison case, the same qualitative cosmic history appears:

1) an early negative $\rho_{\Lambda_m}(t)$ phase,

2) a sign transition at intermediate cosmic time,

3) the onset of late-time accelerated expansion,

4) quasi-constant dark energy behavior in the late universe,

5) and a mild weakening trend toward the present epoch.

This behavior is already obtained when β is kept fixed within each benchmark simulation. The explicitly evolving-$\beta(t)$ cases discussed in Section 6.4 show the same qualitative sequence, with only shifts in the detailed timing and amplitude. Therefore, the emergence of dynamical dark energy in MOC is not driven by prescribing a separate dark energy function, but by the total GSE density function itself.

This is especially important for the late universe. Although $\rho_{\Lambda_m}(t)$ is dynamical, it naturally exhibits a quasi-constant behavior after the onset of acceleration. For example, in the standard CMB case with 0% matter enhancement, corresponding to $\Omega_m \simeq 0.3158$, $\rho_{\Lambda_m}(t)$ remains quasi-constant over $t \simeq 8.8$–$13.8\,\mathrm{Gyr}$, varying only at the $\sim 10\%$ level, while the matter density decreases by about 69% over the same interval. Thus, the quasi-constant appearance of dark energy does not have to be imposed as a strict cosmological constant. It emerges as a late-time property of the total GSE dynamics.

The coefficient β is not a new field, nor a separately evolving dark energy degree of freedom. It is a structural coefficient in the gravitational self-energy integral. It specifies how a given mass distribution contributes to the total GSE, but it is not a primary gravitational source comparable to ρ_m or the mass distribution scale R. Once the density profile is specified, the corresponding value of β is fixed by the gravitational self-energy calculation.

A more structure-resolved treatment could determine β directly from the matter distribution itself. Large-scale N-body simulations of structure formation [33, 34], combined with observed galaxy and cluster-scale statistics, provide a concrete route for extracting the effective cosmological value of β by relating simulated density profiles, halo concentrations, void structure, and clustering to the total GSE over the causally connected volume. In this sense,

β is not an arbitrary fitting function, but a structural coefficient tied to the organization of matter.

Consequently, the MOC framework moves toward a reduced-parameter description of dark energy. The total GSE of matter itself generates the main cosmic sequence, including early attraction, sign transition, late acceleration, quasi-constant behavior, and mild weakening, without adding new dark energy fields or imposing a separate time-dependent dark energy sector.

8 Effective Equation of State $w_{\Lambda_m}(t)$ and Key Transition Points in the MOC

8.1 Effective equation of state $w_{\Lambda_m}(t)$

In the MOC framework, the effective equation of state of the matter-induced dark energy component is not fixed at $w = -1$. Instead, it can be reconstructed as an effective diagnostic from the time evolution of $\rho_{\Lambda_m}(t)$. Here we use the updated standard CMB-based 0% matter enhancement simulation shown in Table 4, corresponding to $\Omega_m \simeq 0.3158$ and constant $\beta = 1.6172$, as the reference case.

Assuming that w_{Λ_m} varies slowly across a single time step, we estimate it from the continuity relation for an effective dark energy component:

$$w_{\Lambda_m}(t_i) \approx -1 - \frac{1}{3}\frac{\ln\left[\rho_{\Lambda_m}(t_{i+1})/\rho_{\Lambda_m}(t_i)\right]}{\ln[a(t_{i+1})/a(t_i)]}. \tag{191}$$

This estimator is meaningful only after ρ_{Λ_m} has become positive. In the updated standard CMB case, the sign transition occurs near $t \simeq 5.38\,\mathrm{Gyr}$, so w_{Λ_m} is not assigned to the earlier negative-ρ_{Λ_m} phase.

Interval (Gyr)	**Estimated w_{Λ_m}**
6.8–7.8	≈ -1.85
7.8–8.8	≈ -1.38
8.8–9.8	≈ -1.14
9.8–10.8	≈ -0.98
10.8–11.8	≈ -0.86
11.8–12.8	≈ -0.77
12.8–13.8	≈ -0.63

Table 11: **Estimated effective equation of state $w_{\Lambda_m}(t)$ for the updated CMB-based 0% matter enhancement simulation $\Omega_m \simeq 0.3158$.** The values are reconstructed using the finite-difference continuity estimator after ρ_{Λ_m} becomes positive. The simulation uses $\Omega_m \simeq 0.3158$, $\chi_p(t_0) = 46.114\,\mathrm{Gly}$, and constant $\beta = 1.6172$. The effective equation of state evolves from $w_{\Lambda_m} < -1$ shortly after the sign transition, approaches $w_{\Lambda_m} \simeq -1$ near the broad maximum of $\rho_{\Lambda_m}(t)$, and then moves into the $w_{\Lambda_m} > -1$ regime as the dark energy density weakens toward the present epoch.

As summarized in Table 11, the effective equation of state is highly dynamical. Immediately after the sign transition, $\rho_{\Lambda_m}(t)$ grows rapidly, giving $w_{\Lambda_m} < -1$. This should not be interpreted

as a fundamental phantom field; rather, it is an effective description of the rapid increase of the GSE-induced dark energy density after it becomes positive.

Near the broad maximum of $\rho_{\Lambda_m}(t)$, over $t \simeq 9.8$–$10.8\,\mathrm{Gyr}$, the estimated value approaches $w_{\Lambda_m} \simeq -1$. This is the epoch in which the MOC dark energy density most closely mimics a cosmological constant. After the maximum, $\rho_{\Lambda_m}(t)$ begins to decline slowly, and the effective equation of state moves into the $w_{\Lambda_m} > -1$ regime. Thus, the MOC framework naturally produces a transition from an early phantom-like effective behavior, through a near-Λ phase, into a late-time weakening phase.

This late-time behavior is consistent with the quasi-constant but mildly weakening dark energy trend found in the updated CMB benchmark simulation. In particular, over $t \simeq 8.8$–$13.8\,\mathrm{Gyr}$, $\rho_{\Lambda_m}(t)$ varies only at the $\sim 10\%$ level around its mean value, while the matter density decreases by about 69%. The effective equation-of-state reconstruction therefore reinforces the main MOC result: the apparent cosmological-constant-like behavior is not imposed, but emerges from the total GSE density function. The subsequent $w_{\Lambda_m} > -1$ behavior is also qualitatively consistent with recent observational analyses that allow for a mild late-time weakening of dark energy [11, 12, 44].

8.2 Key transition points in the MOC model

Using the updated CMB-based standard simulation, corresponding to 0% matter enhancement, $\Omega_m \simeq 0.3158$, and constant $\beta = 1.6172$, we identify two transition epochs that characterize the emergence of matter-induced dark energy and the onset of late-time acceleration. Transition times are obtained via linear interpolation between discrete simulation points. Importantly, the emergence of positive, repulsive dark energy does not immediately lead to cosmic acceleration.

Transition	**Definition**	**Interval**	t **(Gyr)**	z	**Notes**
Sign Crossover	$\rho_{\Lambda_m} = 0$	4.8→5.8	≈ 5.38	≈ 1.12	Dark energy changes sign from attractive to repulsive.
Acceleration Onset	$\rho_{\Lambda_m} \approx \frac{1}{2}\rho_m$	6.8→7.8	≈ 7.72	≈ 0.63	Repulsive dark energy becomes strong enough to compete with matter and trigger global acceleration.

Table 12: **Key transition epochs for the updated CMB-based standard simulation.** The simulation uses 0% matter enhancement, $\Omega_m \simeq 0.3158$, $\chi_p(t_0) = 46.114\,\mathrm{Gly}$, and constant $\beta = 1.6172$. A characteristic feature of the MOC model is the delay between the sign transition of ρ_{Λ_m}, occurring near $t \simeq 5.38\,\mathrm{Gyr}$ ($z \simeq 1.12$), and the onset of accelerated expansion, occurring near $t \simeq 7.72\,\mathrm{Gyr}$ ($z \simeq 0.63$).

The early negative phase, $t \lesssim 5.38\,\mathrm{Gyr}$, enhances structure formation by providing an additional gravitationally attractive contribution to the cosmic energy budget. However, the mere appearance of positive dark energy does not immediately induce cosmic acceleration. Only after the condition

$$\rho_{\Lambda_m} \gtrsim \frac{1}{2}\rho_m$$

is met at $t \simeq 7.72\,\mathrm{Gyr}$ does the universe transition into an accelerating phase.

In the updated CMB standard simulation, the dark energy density reaches a broad maximum over $t \simeq 9.8$–$10.8\,\mathrm{Gyr}$ and then slowly declines toward the present epoch. This behavior indicates a quasi-constant but mildly weakening dark energy component, rather than a strict cosmological constant [11, 44].

Thus, the standard CMB-based MOC simulation exhibits the characteristic three-phase sequence: an early attractive phase with $\rho_{\Lambda_m} < 0$, an intermediate transition to positive dark energy, and a late-time repulsive phase that drives accelerated expansion while remaining quasi-constant over several Gyr.

9 The Future of the Universe in the MOC

In the MOC framework, the long-term fate of the universe is governed not by a fixed vacuum energy, but by the dynamical structure of the total GSE. Unlike ΛCDM, where dark energy is introduced as an independent constant [3, 4, 8], the MOC model treats the dark energy density as a quantity determined by the interplay between the physical matter density and the causal horizon structure. In particular, the dark energy density depends explicitly on the matter density ρ_m and the dimensionless geometric ratio R_S/χ_p as follows:

$$\rho_{\Lambda_m} = \frac{\beta\rho_m}{2}\frac{R_S}{\chi_p}\left(\frac{5\beta}{14}\frac{R_S}{\chi_p} - 1\right). \tag{192}$$

This expression follows directly from the generalized horizon formulation of the GSE densities. Here $R_S = 2GM/c^2$ is the Schwarzschild radius associated with the total mass $M = \rho_m V_{\text{phys}}$ contained within the causally connected region, while the particle horizon χ_p sets the causal interaction scale governing the formation of GSE.

The sign of cosmic acceleration is therefore determined by the evolution of the combination $\rho_m(R_S/\chi_p)$. While the matter density scales as $\rho_m \propto a^{-3}$ in an expanding universe [15, 37], the Schwarzschild radius R_S grows with the total mass enclosed within the particle horizon as $R_S \propto \chi_p^3\rho_m \propto \chi_p^3 a^{-3}$. Consequently, the term R_S/χ_p scales as $\chi_p^2 a^{-3}$. During the epoch of late-time acceleration, the growth of the particle horizon $\chi_p(t)$ is logarithmic or slower relative to the scale factor $a(t)$. This implies that the factor $\rho_m(R_S/\chi_p)$ will eventually decrease in the far future, suggesting that the repulsive phase defined by $\rho_{\Lambda_m} > 0$ cannot persist indefinitely. A future transition toward a weaker dark energy density is therefore a natural consequence of the model.

Quantitatively, the updated CMB-based simulations indicate that the dark energy density has already passed its maximum value. Across all four matter realizations (−10%, 0%, +10%, +20%), the dark energy density $\rho_{\Lambda_m}(t)$ increases after its sign transition, reaches a broad maximum over approximately $t \simeq 9.7$–$11.8\,\text{Gyr}$, and then decreases toward the present epoch. At $z = 0$, the predicted values converge to

$$\rho_{\Lambda_m}(t_0) \simeq (5.29\text{–}6.10) \times 10^{-27}\,\text{kg}\,\text{m}^{-3},$$

consistent with the expectation that the late-time dynamics is relatively insensitive to detailed microphysical parameters [3, 4].

Although the present simulation window does not yet show a full turnover to negative ρ_{Λ_m}, the post-peak decline is clearly visible in all cases. This behavior implies that the effective equation of state has already crossed into the quintessence regime ($w > -1$) and is evolving away from the de Sitter limit [8]. The gradual decrease of ρ_{Λ_m} provides physical motivation for a future transition toward weaker acceleration and potentially toward deceleration in a later epoch.

9.1 Self-regulation of cosmic expansion: A natural feedback cycle

A key structural feature of the MOC framework is the feedback between the expansion history and the GSE term itself. This feedback is mediated by the distinct evolution of the matter

density ρ_m and the geometric ratio R_S/χ_p.

- During **accelerated expansion**, the rapid growth of the scale factor $a(t)$ leads to a rapid decrease in the matter density ρ_m. This suppression of the factor $\rho_m(R_S/\chi_p)$ weakens the repulsive GSE contribution. In the simulations, this behavior appears as a flattening and eventual decline of $\rho_{\Lambda_m}(t)$ after it reaches a finite maximum.
- During **decelerated expansion**, ρ_m decreases more slowly, while the particle horizon $\chi_p(t)$ can evolve comparatively more effectively. Consequently, the quantity $\rho_m(R_S/\chi_p)$ decreases less rapidly than in the accelerated phase, allowing the repulsive GSE component to recover relative importance. This process pushes $\rho_{\Lambda_m}(t)$ back toward more positive values and can re-enable acceleration.

This qualitative feedback structure resembles that of a damped oscillator. The system can overshoot the neutral point defined by $\rho_{\Lambda_m} = 0$, while the amplitude of each excursion is reduced as the overall energy scale continues to dilute in an expanding background.

9.2 Entry into a decelerating phase in the near future

The MOC framework links the sign of cosmic acceleration to the evolution of the same controlling combination that appears in the total GSE expression. Equivalently, the sign of ρ_{Λ_m} is governed by the bracketed factor

$$\frac{5\beta}{14}\frac{R_S}{\chi_p} - 1. \tag{193}$$

As the universe accelerates, the physical volume increases rapidly and the physical matter density ρ_m correspondingly decreases. As a result, the ratio R_S/χ_p decreases, leading the above factor toward zero. The updated CMB-based simulations indicate that the sign transition $\rho_{\Lambda_m} = 0$ occurred in the past at $t \simeq 4.98$–$6.07\,\mathrm{Gyr}$, depending on the matter content. All models subsequently exhibit a finite maximum of ρ_{Λ_m} followed by a gradual decline.

These trends suggest that the universe may eventually enter a new decelerating expansion phase if $\rho_{\Lambda_m}(t)$ continues to decrease from its post-peak values.

This expectation is reinforced by the decline of the quantity $\rho_m(R_S/\chi_p)$ in the late-time regime and by the intrinsic feedback between the expansion history and the GSE term.

9.3 Long-term behavior: Damped oscillatory evolution

Because ρ_{Λ_m} depends on the evolving quantity $\frac{5\beta}{14}\frac{R_S}{\chi_p} - 1$, the MOC framework naturally allows repeated sign changes of the GSE contribution. Once the feedback between the expansion history and the horizon scales becomes active, this can give rise to alternating phases of accelerated and decelerated expansion. As the matter density continues to dilute, each successive cycle is expected to exhibit a smaller amplitude. The characteristic timescale of the oscillation may also increase at late epochs, as the effective driving term evolves more slowly. This behavior is typical of a damped dynamical system, analogous to the feedback mechanisms discussed in nonlinear cosmic structure formation.

Importantly, the early stages of this damped evolution are, in principle, observationally testable. In particular, a gradual weakening of dark energy, a transition toward $w > -1$, and the eventual onset of a decelerating phase constitute concrete predictions of the MOC framework. Future high-precision measurements of $w(a)$ and its time dependence, for example from LSST, DESI, and Euclid, can therefore directly probe this regime.

The universe thus evolves toward a damped, slowly varying expansion history, rather than eternal acceleration or an abrupt recollapse. The oscillatory description here should be understood as an effective characterization of the intermediate and late-time dynamics, prior to the exhaustion of causal structure formation.

9.4 Ultimate fate of the universe after horizon saturation

Beyond the observationally accessible regime, the MOC framework also provides a well-defined prediction for the ultimate fate of the universe. This fate is governed by the saturation of the comoving particle horizon and the consequent termination of causal matter inflow.

Once the particle horizon approaches its asymptotic limit, which is approximately

$$\chi_p(t) \to \chi_{\rm lim} \simeq 62.8\ {\rm Gly} \tag{194}$$

for the updated CMB calibration

$$H_0 = 67.360\,{\rm km\,s^{-1}\,Mpc^{-1}}, \qquad \Omega_m \simeq 0.3158, \qquad \chi_p(t_0) = 46.114\,{\rm Gly},$$

no additional comoving matter shells can enter the causally connected region [51, 52]. As a direct consequence, the total mass enclosed within the particle horizon, $M(t)$, asymptotically approaches a finite limiting value, $M_{\rm max}$.

While the mass sourcing the GSE ceases to grow, the scale factor $a(t)$ continues to increase due to the inertia of the cosmic expansion [4]. Since the Schwarzschild radius R_S is proportional to the enclosed mass, it also approaches a constant value $R_{S,\infty}$. However, the matter density ρ_m continues to dilute as a^{-3}. As a result, the controlling combination $\rho_m(R_S/\chi_p)$ decreases monotonically in the post-saturation regime.

Within the MOC dark energy expression, this monotonic decrease inevitably drives the bracketed factor controlling the sign of ρ_{Λ_m} toward negative values. The repulsive phase of matter-induced dark energy therefore cannot persist indefinitely. After the current post-peak epoch, the universe is expected to transition into a purely decelerating expansion phase. This deceleration does not imply a recollapse or a Big Crunch scenario. Because the total enclosed mass remains finite and the expansion rate remains positive, the universe continues to expand, albeit with steadily decreasing acceleration. The expansion does not reverse; instead, it asymptotically approaches a slow, matter-dominated expansion state.

The long-term cosmological outcome in the MOC framework is thus neither eternal acceleration nor catastrophic collapse, but a gradual approach to a thermodynamically cold and dilute state. In this sense, the ultimate fate of the universe resembles a form of cosmic heat death, characterized by ever-expanding physical scales, diminishing interaction rates, and a vanishingly small dark energy density [4]. The same GSE mechanism that generates cosmic acceleration at intermediate epochs therefore also guarantees its eventual shutdown once causal structure formation is exhausted.

Part III. Extensions

10 A Unified Physical Origin for Cosmic Acceleration

The standard ΛCDM model treats primordial inflation and late-time acceleration as disconnected phenomena, typically driven by independent scalar fields [53–56]. The GSE framework in MOC unifies both via a single, intuitive principle. The dark energy density arises from the total GSE of the contents of the causal horizon, expressed elegantly in terms of its compactness ratio as follows:

$$\rho_{\Lambda_m} = \frac{\beta\rho_m}{2}\frac{R_S}{\chi_p}\left(\frac{5\beta}{14}\frac{R_S}{\chi_p} - 1\right). \tag{195}$$

In the General GSE framework, this single equation reveals a fundamental **Density-Scale Duality**. Repulsive gravity ($\rho_{\Lambda_m} > 0$) is driven by extreme density at small scales during inflation and by extreme scale geometric factors at low densities in the late-time dark energy epoch.

10.1 Inflation: Acceleration at extreme density

We quantify the dark energy density at the Planck epoch. In the radiation-dominated early universe, the causal scale χ_p and the physical scale $R_{\rm phys}$ are tightly coupled and comparable such that $R_{\rm phys} \approx \chi_p \approx R$. Under these conditions, the MOC expression becomes a function of the local density and the compactness ratio.

$$\rho_{\Lambda_m} \approx \frac{\beta\rho_m}{2}\frac{R_S}{R}\left(\frac{5\beta}{14}\frac{R_S}{R} - 1\right). \tag{196}$$

We take $\rho_m \simeq \rho_{\rm pl}$ and $R \simeq l_{\rm pl}$ at this epoch. For an illustrative high-compactness estimate, we adopt $\beta \simeq 2$, which is close to the static compact-object reference scale discussed in Sec. 3.1. This choice is not required for the onset of accelerated expansion. Even for more conservative choices such as $\beta = 1.5$ or $\beta = 1$, the Planck-scale compactness $R_S/R = 8\pi/3$ gives $\rho_{\Lambda_m} > \rho_m$, and therefore the GSE term is already sufficient to generate accelerated expansion. The value $\beta \simeq 2$ is used only to illustrate the high-density limit of the mechanism.

The compactness ratio at the Planck scale is calculated using the Planck density as follows

$$\frac{R_S}{R} = \frac{2GM}{c^2R} = \frac{2G(\frac{4}{3}\pi R^3\rho_{pl})}{c^2R} = \frac{8\pi G\rho_{pl}l_{pl}^2}{3c^2} = \frac{8\pi}{3} \approx 8.38. \tag{197}$$

Substituting these values into the MOC expression for ρ_{Λ_m} yields

$$\rho_{\Lambda_m} \approx \frac{2\rho_{\rm pl}}{2}(8.38)\left(\frac{5(2)}{14}(8.38) - 1\right) \approx 8.38 \times (5.99 - 1). \tag{198}$$

This calculation gives a dark energy density of

$$\rho_{\Lambda_m} \approx 8.38 \times 4.99 \approx 41.8\rho_{\rm pl}. \tag{199}$$

To assess whether this GSE-induced dark energy drives accelerated expansion, we use the general FRW acceleration equation as a diagnostic tool

$$\frac{\ddot{a}}{a} = -\frac{4\pi G}{3}\sum_i\left(\rho_i + 3p_i/c^2\right). \tag{200}$$

For radiation, the equation of state is $p_r = \rho_r c^2/3$, so that

$$\rho_r + 3p_r/c^2 = 2\rho_r. \tag{201}$$

For the GSE dark energy component, we adopt an effective equation of state $p_{\Lambda_m} \simeq -\rho_{\Lambda_m} c^2$ over the relevant interval, yielding

$$\rho_{\Lambda_m} + 3p_{\Lambda_m}/c^2 \approx -2\rho_{\Lambda_m}. \tag{202}$$

The acceleration equation therefore reduces to

$$\frac{\ddot{a}}{a} \approx -\frac{8\pi G}{3}\left(\rho_r - \rho_{\Lambda_m}\right). \tag{203}$$

Assuming an effective equation of state $w \approx -1$ for this dark energy component, the acceleration equation at the Planck epoch becomes

$$\frac{\ddot{a}}{a} \approx -\frac{8\pi G}{3}(\rho_{\rm pl} - \rho_{\Lambda_m}) = -\frac{8\pi G}{3}(\rho_{\rm pl} - 41.8\rho_{\rm pl}) > 0. \tag{204}$$

This strongly negative effective source term in the acceleration equation leads to a powerful accelerated expansion, providing a natural mechanism to address the horizon and flatness problems without the need for additional scalar fields.

Energy Density & Hierarchy With $\rho_{\rm pl} \simeq 5.16 \times 10^{96}\,\mathrm{kg/m^3}$, the calculated dark energy density is

$$\rho_{\Lambda_m} \approx 2.16 \times 10^{98}\,\mathrm{kg/m^3}, \tag{205}$$

$$E_{\Lambda_m} = \rho_{\Lambda_m} c^2 \approx 1.94 \times 10^{115}\,\mathrm{J/m^3}, \tag{206}$$

$$E_{\Lambda_m}^{(\mathrm{Planck})} \sim 10^{115}\ \mathrm{J/m^3}. \tag{207}$$

which is of Planck-scale order and is therefore compatible with the extremely high vacuum-energy scale typically associated with an inflationary phase.

Using the observed late-time dark energy density $\rho_{\Lambda\text{-obs}} \simeq 7 \times 10^{-27}\,\mathrm{kg/m^3}$ (i.e., $E_{\Lambda\text{-obs}} \simeq 6 \times 10^{-10}\,\mathrm{J/m^3}$) [5],

$$\frac{\rho_{\Lambda_m}^{(\mathrm{Planck})}}{\rho_{\Lambda\text{-obs}}} \approx \frac{2.16 \times 10^{98}}{7 \times 10^{-27}} \simeq 3 \times 10^{124}. \tag{208}$$

Equivalently $E_{\Lambda_m}^{(\mathrm{Planck})}/E_{\Lambda\text{-obs}} \sim 10^{124}$. Thus, MOC naturally attains an inflationary-scale energy density while explaining the tiny late-time value through the same density–size GSE mechanism, without introducing new fields.

10.2 Inflation triggered by GSE: Consistency with standard inflation scales

In the MOC framework, primordial inflation is not postulated as an independent dynamical sector. Instead, inflation can emerge when the matter-induced dark energy generated by total GSE becomes comparable to the dominant radiation component.

10.2.1 Acceleration condition in a radiation background

For a radiation component with equation of state $w_r = 1/3$ and a dark energy-like component with $w_{\Lambda_m} \simeq -1$ during the repulsive phase, the acceleration equation reduces to [4, 15]

$$\frac{\ddot{a}}{a} \approx -\frac{8\pi G}{3}\left(\rho_r - \rho_{\Lambda_m}\right). \tag{209}$$

Inflation begins when the right-hand side becomes positive, which is approximately the condition

$$\rho_{\Lambda_m} = \rho_r. \tag{210}$$

10.2.2 Causal regime at very early times

At sufficiently early times, causality enforces a single characteristic scale for the size of the causally connected region. Independently of whether accelerated expansion has already started, one can take

$$\chi_p \approx R_{\rm phys} \approx R \tag{211}$$

and, at the level of an order-of-magnitude trigger estimate, adopt

$$R \approx ct. \tag{212}$$

In this causal regime, the MOC GSE expression can be written in terms of the compactness ratio as

$$\rho_{\Lambda_m} = \frac{\beta\rho_r}{2}\frac{R_S}{R}\left(\frac{5\beta}{14}\frac{R_S}{R} - 1\right) \tag{213}$$

where the Schwarzschild radius is defined by $R_S = \frac{2GM}{c^2}$, and the enclosed mass within radius R is approximated by

$$M = \frac{4\pi}{3}R^3\rho_r. \tag{214}$$

10.2.3 Ratio form and the time–density trigger

Dividing Eq. (213) by ρ_r gives

$$\frac{\rho_{\Lambda_m}}{\rho_r} = \frac{\beta}{2}\frac{R_S}{R}\left(\frac{5\beta}{14}\frac{R_S}{R} - 1\right). \tag{215}$$

For the early-universe configuration emphasized in this paper, we take $\beta \simeq 2$, which yields

$$\frac{\rho_{\Lambda_m}}{\rho_r} \approx \frac{R_S}{R}\left(\frac{5}{7}\frac{R_S}{R} - 1\right). \tag{216}$$

Using Eq.(214), the compactness ratio becomes

$$\frac{R_S}{R} = \frac{2GM}{c^2R} = \frac{8\pi G}{3}\frac{R^2\rho_r}{c^2}. \tag{217}$$

With the causal estimate $R \approx ct$, this simplifies to

$$\frac{R_S}{R} \approx \frac{8\pi G}{3}t^2\rho_r. \tag{218}$$

Substituting Eq. (218) into Eq. (216) gives

$$\frac{\rho_{\Lambda_m}}{\rho_r} \approx \frac{8\pi G}{3}t^2\rho_r\left(\frac{40\pi G}{21}t^2\rho_r - 1\right). \tag{219}$$

Imposing the inflation condition $\rho_{\Lambda_m} = \rho_r$ from Eq. (210) yields a quadratic equation for the combination $t^2\rho_r$. The physically relevant solution can be written as

$$\boxed{t^2\rho_r \simeq 3.71 \times 10^9} \tag{220}$$

10.2.4 Numerical implications at $t \simeq 10^{-36}$ s and $t \simeq 10^{-35}$ s

Equation (220) implies the following two equivalent interpretations.

Inflation time ⇒ density scale. If inflation begins at $t \simeq 10^{-36}\,\mathrm{s}$, then Eq. (220) predicts

$$\rho_r(t \simeq 10^{-36}\,\mathrm{s}) \simeq 3.71 \times 10^{81}\,\mathrm{kg\,m^{-3}} \tag{221}$$

which lies within the standard inflationary onset window commonly discussed in early inflationary models [54–56].

Likewise, if one considers a later onset time $t \simeq 10^{-35}\,\mathrm{s}$, the required density decreases as $\rho_r \propto t^{-2}$, giving

$$\rho_r(t \simeq 10^{-35}\,\mathrm{s}) \simeq 3.71 \times 10^{79}\,\mathrm{kg\,m^{-3}} \tag{222}$$

Density scale ⇒ inflation time. Conversely, if the early universe is characterized by a nearly homogeneous radiation density of order $\rho_r \sim 10^{81}\,\mathrm{kg\,m^{-3}}$, then Eq. (220) implies that the GSE trigger $\rho_{\Lambda_m} = \rho_r$ is reached automatically at $t \sim 10^{-36}\,\mathrm{s}$.

The MOC GSE trigger relation in Eq. (220) provides a direct mapping between a characteristic inflation onset time and a characteristic early-universe mean radiation density. In this sense, the MOC framework can reproduce the usual inflationary scale window without introducing an additional inflaton field or a fine-tuned potential. Inflation emerges as a gravitational phenomenon driven by the compactness of the causally connected region and the resulting total GSE.

10.2.5 Why $\rho_r \sim 10^{79}$–$10^{81}\,\mathrm{kg\,m^{-3}}$ is physically motivated in standard inflation

In standard inflationary phenomenology, the relevant scale is often expressed by the inflationary potential energy density V. A conventional relation links the energy scale $V^{1/4}$ to the tensor-to-scalar ratio r, schematically yielding $V^{1/4}$ in the ballpark of 10^{15}–$10^{16}\,\mathrm{GeV}$ for observationally allowed r values [57]. Because an energy scale $V^{1/4} \sim 10^{15}$–$10^{16}\,\mathrm{GeV}$ corresponds to an enormous energy density $V \sim (10^{15}$–$10^{16}\,\mathrm{GeV})^4$, this translates to mass density scales of order 10^{79}–$10^{81}\,\mathrm{kg\,m^{-3}}$ when converted to SI units.

Therefore, the density level required by the GSE trigger relation in Eq. (220) is not an ad hoc insertion. It lies in the same broad magnitude range that is typically invoked when one parametrizes inflation by a high inflationary energy scale, constrained by the observed amplitude of primordial perturbations and the upper bounds on primordial tensor modes [57].

10.2.6 Initial near-thermal state and its implications for early accelerated expansion

The conventional "horizon problem" is often phrased as a causal objection to the near-uniform CMB temperature observed across widely separated directions on the sky [54–56]. Here we adopt a different viewpoint that is natural within a matter-only, GSE-driven cosmology.

If the universe originates from a single underlying physical mechanism, it is not compelling to assume that widely separated regions are "prepared" with substantially different temperatures or macroscopic states at birth. Rather, in the absence of detailed information about microscopic initial conditions, the most natural macroscopic description of the primordial state is a near-thermal configuration, with deviations that are small and statistically characterized [15].

In this picture, the early accelerated expansion driven by the total GSE proceeds from an initially hot, nearly equilibrated state. As the universe expands and the interactions effectively differentiate through successive dynamical processes, including gravitational instability and phase transitions, the system generically departs from perfect equilibrium. The observed CMB anisotropy at the level of $\Delta T/T \sim 10^{-5}$ is then interpreted not as evidence for a highly non-thermal primordial preparation, but as the expected residual imprint of a nearly equilibrated origin that becomes gradually perturbed by subsequent dynamics [5].

Under this near-thermal initial condition, the conceptual role of primordial acceleration is altered. In contrast to the standard inflationary argument, the accelerated expansion is not required to enforce global causal contact across the entire last-scattering surface. Instead, accelerated expansion occurs because the total GSE energy is positive. The initial accelerated phase (inflation) is therefore a natural dynamical response driven by the negative pressure associated with the GSE.

The resulting dynamics naturally suppress primordial curvature, dilute relic abundances, and can provide initial conditions compatible with the observed near scale-invariant perturbation spectrum [54, 55, 57], without invoking any teleological principle. In this framework, the conventional single-patch requirement is relaxed. If the primordial state is already characterized by a nearly uniform thermal configuration, the number of e-folds required during the early accelerated phase is not dictated by the need to causally synchronize the entire observable universe. Rather, it is determined by dynamical considerations such as the onset of perturbation generation, the stabilization of spatial flatness, and the smooth transition into the subsequent radiation-dominated epoch.

Consequently, a moderately reduced amount of accelerated expansion, compared to that assumed in standard inflationary scenarios, is sufficient within the MOC framework. The accelerated phase driven by the total GSE acts to preserve and gently amplify an already near-equilibrated initial state, rather than to manufacture large-scale homogeneity from an initially uncorrelated configuration.

Because the universe remains hot throughout this process and transitions smoothly into the radiation-dominated phase, the role traditionally played by excessive exponential expansion is replaced by thermal continuity and causal evolution.

As a result, MOC inflation does not need to generate an arbitrarily large number of e-folds. The required expansion factor is fixed by the adiabatic cooling needed to connect the inflationary exit scale, corresponding to a temperature scale of order 10^{15}–10^{16} GeV, to the onset of Big Bang Nucleosynthesis at $T_{\rm BBN} \sim 10^9$ K [4]. This corresponds to a finite expansion of order 10^{19}–10^{20}, which appears sufficient to establish the observed thermal history without invoking superfluous exponential growth.

10.3 The self-terminating mechanism of MOC inflation

A longstanding difficulty in standard inflationary cosmology is the graceful-exit problem and the reheating problem [58,59]. In conventional models, inflation is driven by an external scalar inflaton field whose potential energy dominates the cosmic energy budget. Once inflation ends, the universe is left in a supercooled state due to the enormous exponential expansion required to solve the horizon and flatness problems. Recovering a hot, radiation-dominated universe therefore necessitates an additional reheating phase, in which the inflaton field decays into standard model particles through model-dependent microphysical processes.

In the MOC framework, this entire structure is replaced by a single gravitational mechanism. Inflation is not sourced by an independent scalar field but emerges dynamically when the matter-induced dark energy generated by total GSE becomes comparable to, and then exceeds, the radiation density. As a consequence, the termination of inflation is not a separate dynamical event but follows directly from the same gravitational term that initiates the accelerated expansion.

The sign of the dark energy density in MOC is governed by the following dimensionless factor:

$$\Gamma(R) \equiv \left(\frac{5\beta}{14}\frac{R_S}{R} - 1\right) = \left(\frac{5\beta}{14}\frac{2GM}{c^2 R} - 1\right) \tag{223}$$

which appears explicitly in the total GSE contribution.

Using the mass density relation $M = \frac{4\pi}{3}R^3\rho$, this factor can be rewritten as

$$\Gamma(R) = \left(\frac{20\pi\beta G}{21c^2}\,\rho R^2 - 1\right). \tag{224}$$

During this initial phase, the universe is radiation-dominated, meaning its energy density scales with the size of the causal patch R as $\rho \propto R^{-4}$. Substituting this scaling relation $\rho(R) = \rho_i(R_i/R)^4$ into the equation reveals the inherent evolution of the acceleration driver.

$$\Gamma(R) = \left(\frac{20\pi\beta G}{21c^2}\,\rho_{\rm i} R_i^4\,\frac{1}{R^2} - 1\right) \equiv \left(\frac{C}{R^2} - 1\right) \tag{225}$$

where C is a positive constant fixed by the initial conditions.

This expression makes the termination mechanism transparent. At extremely early times, corresponding to the high-density regime emphasized in standard inflationary phenomenology, the compactness of the causally connected region implies that $\Gamma(R) \gg 0$. The resulting positive dark energy density generates strong repulsive gravity and drives rapid accelerated expansion. However, the same expansion that characterizes inflation inevitably increases the characteristic scale R. Because the leading contribution to $\Gamma(R)$ scales as R^{-2}, the repulsive term decays as the universe expands.

At a finite value of R, the condition $\Gamma(R) = 0$ is reached. Beyond this point, $\Gamma(R)$ becomes negative, causing the effective matter-induced dark energy density ρ_{Λ_m} to change sign from positive to negative. The repulsive gravitational effect therefore shuts off automatically and is replaced by an attractive contribution. Inflation thus terminates smoothly as a direct consequence of the expansion itself, without invoking an external decay channel or additional tuning. This provides a built-in graceful-exit mechanism, rather than requiring a separate exit process as in conventional inflaton-based models.

10.4 A solution to the reheating problem

The resolution of the reheating problem in the MOC framework must be discussed consistently with the inflationary trigger scale established in the preceding section. As shown above, the onset and termination of inflation occur naturally when the matter-induced dark energy becomes comparable to the radiation background at

$$t \sim 10^{-36}\,\mathrm{s}, \qquad \rho_r \sim 10^{79}\text{–}10^{81}\,\mathrm{kg\,m^{-3}} \tag{226}$$

which lies in the characteristic energy density window usually invoked in standard inflationary phenomenology [57].

In conventional inflation, the exponential expansion following this epoch typically dilutes the universe to an extremely cold and effectively empty state. A separate reheating phase is therefore introduced, in which the inflaton field decays into standard model particles through model-dependent microphysics [58, 59]. In this picture, the temperature after inflation is not determined by the expansion history itself but by the efficiency of inflaton decay.

In contrast, inflation in the MOC framework corresponds to an early phase of accelerated but finite power-law expansion driven by total GSE. Once the compactness condition governing the sign of ρ_{Λ_m} is no longer satisfied, the effective repulsive contribution automatically shuts off and the universe transitions smoothly into a radiation-dominated expansion. Within the present MOC framework, no separate decay or reheating mechanism is required.

The thermal evolution after the end of MOC inflation therefore follows directly from adiabatic expansion. Taking the characteristic temperature at the onset of inflation to be $T_{\rm end} \sim 10^{15}$–10^{16} GeV consistent with the density scale derived at $t \sim 10^{-36}$ s, the subsequent cooling proceeds continuously toward the Big Bang Nucleosynthesis scale, $T_{\rm BBN} \sim 10^{9}$ K.

For adiabatic expansion of a radiation-dominated plasma, the temperature scales as $T \propto a^{-1}$. The required expansion factor between the end of inflation and the onset of nucleosynthesis is therefore

$$\frac{T_{\rm end}}{T_{\rm BBN}} \sim 10^{19}\text{–}10^{20}. \tag{227}$$

This corresponds to a decrease in radiation energy density of

$$\frac{\rho_{\rm end}}{\rho_{\rm BBN}} \sim \left(\frac{T_{\rm end}}{T_{\rm BBN}}\right)^4 \sim 10^{76}\text{–}10^{80}, \tag{228}$$

which is fully consistent with the standard thermal history connecting the inflationary epoch to Big Bang Nucleosynthesis.

Neither the exponential expansion factor commonly invoked in standard inflation ($e^{60} \sim 10^{26}$) [54–56] nor the finite expansion factor in MOC ($\sim 10^{19}$–10^{20}) is directly observed. Both represent model-dependent requirements needed to connect the early universe to the observed cosmological state. The difference is that in MOC the required expansion is determined internally by GSE and thermal continuity, rather than imposed to solve horizon-scale problems.

MOC inflation does not cool the universe to a vacuum state. It ends while the universe is still extremely hot, and the subsequent adiabatic expansion alone naturally connects the inflationary epoch to Big Bang Nucleosynthesis.

In this framework, the reheating problem is substantially reformulated: because the universe is not driven into an empty supercooled state by an external inflaton potential, the transition to the radiation-dominated phase may occur through thermal continuity rather than through a separate inflaton-decay reheating stage.

10.5 Dark energy: Acceleration at extreme scale

In the late matter-dominated era, the same total GSE framework governs the cosmic dynamics. However, the physical origin of acceleration is now controlled by extreme scale rather than extreme density. The relevant dimensionless compactness factor appearing in the GSE term can be written as

$$\frac{5\beta}{14}\frac{R_S(t)}{\chi_p(t)} = \frac{5\beta}{14}\frac{2GM(t)}{c^2\chi_p(t)} \propto \beta(t)\rho_m(t)\frac{R_{\rm phys}(t)^3}{\chi_p(t)}, \tag{229}$$

where $M(t) = \frac{4\pi}{3}\rho_m(t)R_{\rm phys}(t)^3$ is the total mass contained within the causally connected region.

At late times, a competition emerges between two opposing effects. The matter density $\rho_m(t)$ decreases as $a(t)^{-3}$ due to cosmic expansion [15, 37], while the geometric factor $R_{\rm phys}(t)^3/\chi_p(t)$ grows monotonically as the causal domain expands. This structure reflects the relation between the causal interaction scale $\chi_p(t)$ and the physical-volume scale $R_{\rm phys}(t)$, which is used to express the GSE contribution as a physical density.

Our numerical simulations show that after an initial period in which the attractive component dominates, the growth of the scale-dependent factor eventually overcomes the decay of the matter density. As a result, the effective GSE contribution crosses the critical threshold and becomes repulsive. This transition marks the onset of late-time cosmic acceleration.

In this regime, the dark energy density evolves slowly and remains close to a quasi-constant value. Rather than representing a true cosmological constant, the observed dark energy [11, 12, 44] is interpreted as the outcome of a slowly varying balance in which the combination $\beta\rho_m(t)\left[R_{\rm phys}(t)^3/\chi_p(t)\right]$ maintains a small net repulsive contribution over cosmological timescales.

10.6 Two accelerations, one physical origin

The total GSE framework provides a unified physical explanation for both primordial inflation and late-time cosmic acceleration. In the early universe, accelerated expansion arises whenever the total GSE becomes positive within a causally connected region. This condition is controlled by the local energy density and does not single out a unique microscopic timescale.

Instead, accelerated expansion can naturally occur across a range of early epochs between the Planck scale and the standard inflationary window, provided that the radiation density satisfies the GSE trigger condition derived in Sec. 10.2. In this sense, MOC is capable of reproducing inflationary behavior at the conventional $t \sim 10^{-36}$–10^{-35} s scale, while remaining equally consistent with earlier onset times approaching the Planck regime.

Primordial inflation in MOC is therefore not tied to a uniquely specified moment in time, but is a density-driven phenomenon. The onset time is selected dynamically by the value of the radiation density rather than imposed by an external field or a fine-tuned potential. The same underlying mechanism can accommodate a continuous range of early-universe conditions, from Planck-scale densities to those conventionally associated with standard inflation.

In contrast, late-time cosmic acceleration emerges from the identical GSE mechanism operating at extreme scale rather than extreme density, when the causally connected region has grown to cosmological dimensions of order $R \sim 46$ Gly. The density–scale duality of the GSE is thus encoded in a single dimensionless compactness factor that controls the GSE regime across cosmic history. At early times this factor is driven by high density, while at late times it is controlled by the growth of the causal scale.

The enormous hierarchy between the Planck-scale vacuum energy density and the present-day effective dark energy, often quoted as $\sim 10^{124}$, arises naturally from evaluating the same physical quantity at different points along cosmic evolution. In this picture, primordial inflation and late-time acceleration are not separate phenomena but two limits of a single gravitational mechanism.

Unlike other unified dark energy models [60], the MOC framework introduces no new fields and requires no modification of General Relativity. It offers a predictive and falsifiable description of cosmic acceleration grounded in the GSE of matter.

11 Resolution of the Black Hole Singularity in MOC

One of the most profound challenges in modern physics is the singularity predicted to exist at the heart of a black hole [61–63]. MOC offers a novel and consistent resolution to this problem. Here, we extend the GSE framework from the cosmos to the core of a collapsing star, demonstrating that the same physical principle that drives cosmic acceleration naturally averts the formation of a singularity.

11.1 Gravitational dynamics in a collapsing object

While the TOV equation describes static stellar structures [28], the dynamical collapse inside a black hole is more naturally analyzed with a Friedmann-type evolution equation. Unlike the TOV equation, which applies strictly to static configurations, the dynamical interior of a collapsing object can be effectively described by a Friedmann-type evolution equation under the assumption of spherical symmetry and homogeneous radial collapse. This correspondence is illustrated by the Oppenheimer–Snyder solution, which shows that the interior of a pressureless collapsing sphere is mathematically equivalent to a time-reversed Friedmann universe [29]. Accordingly, we adopt the Friedmann acceleration equation as an effective tool to analyze whether the collapse proceeds toward a singularity or is dynamically halted.

Unlike the expanding universe where the effective mass depends on the evolving particle horizon, a collapsing star is a localized system residing well within the cosmic causal limit ($R \ll \chi_p$). In the compact regime relevant for a collapsing object, the matter component is pressureless to leading order, $P_m \approx 0$, while the GSE-induced component satisfies an effective equation of state $w_{\Lambda_m} \approx -1$. The active gravitational source term in the acceleration equation therefore reduces to

$$\rho_T + 3P_T \approx \rho_m - 2\rho_{\Lambda_m}. \tag{230}$$

The sign of this term dictates the net gravitational force. To analyze this term, we use the GSE-derived expression for ρ_{Λ_m}, specialized here to a compact object of radius R:

$$\rho_{\Lambda_m} \approx \frac{\beta\rho_m}{2}\frac{R_S}{R}\left(\frac{5\beta}{14}\frac{R_S}{R} - 1\right). \tag{231}$$

11.2 The sign-transition radius and the emergence of repulsion

Equation (231) reveals a characteristic transition scale in the dynamics of gravitational collapse, determined by the ratio of the object's radius R to its Schwarzschild radius R_S. The sign-transition point occurs when the bracketed factor vanishes.

$$\frac{5\beta}{14}\frac{R_S}{R} - 1 = 0 \quad \Rightarrow \quad R_{\text{tran}} = \frac{5\beta}{14}R_S. \tag{232}$$

Here R_{tran} denotes the radius at which the matter-induced dark energy changes sign, $\rho_{\Lambda_m} = 0$. This radius should be distinguished from the critical radius R_{crit}, which is defined separately by the acceleration-balance condition $\ddot{a} = 0$.

Given that the collapsing core represents an extremely dense and centrally concentrated configuration, we adopt a representative structure coefficient value $\beta \approx 1.5$. This choice is consistent with relativistic self-gravitating systems near maximal compactness and lies within the plausible range suggested by TOV-like compact configurations and by our analysis of high-density regimes. In this regime, the sign-transition radius becomes

$$R_{\text{tran}} \approx \frac{7.5}{14}R_S \approx 0.54R_S. \tag{233}$$

- **Phase 1: Accelerated collapse ($R > R_{\text{tran}}$)**
  For a collapsing object with $R > R_{\text{tran}}$, the bracketed term is negative, making $\rho_{\Lambda_m} < 0$. This means the dark energy acts as an attractive force, enhancing gravity. Thus, in the MOC framework, the initial stages of black hole formation can proceed more rapidly than in the standard purely attractive picture.

- **Phase 2: The sign transition ($R = R_{\text{tran}}$)**
  At the specific radius $R \approx 0.54R_S$ (assuming $\beta \approx 1.5$), the dark energy density vanishes. This marks the boundary between the attractive exterior and the repulsive interior.

- **Phase 3: The repulsive core ($R < R_{\text{tran}}$)**
  As the collapse proceeds past this transition radius, ρ_{Λ_m} flips sign and becomes positive. The active gravitational source term now contains a powerful repulsive component. Modeling the GSE component with an effective equation of state $w \approx -1$, or more generally with any negative-pressure condition satisfying $w < -1/3$, this positive energy density generates a repulsive gravitational effect that counteracts the collapse. The repulsive contribution scales more steeply with decreasing radius than the attractive matter term. Specifically, the dominant GSE repulsive term grows as R^{-5}, while the matter contribution scales as R^{-3}. This difference in scaling implies that, below a finite radius, the repulsive effect tends to dominate over the attractive matter term, without requiring the total mass to be Planckian. A singularity, which would require attraction to dominate all the way down to $R = 0$, is therefore dynamically avoided in this framework. The formation of a finite, non-singular core eliminates the spacetime singularity and removes the primary obstruction to unitary evolution. This provides a natural pathway toward resolving the black hole information problem within the MOC framework, without invoking quantum gravity effects at the Planck scale.

11.3 The critical point: A singularity averted

The collapse is halted when the net gravitational force on the collapsing matter becomes zero. For simplicity, we can approximate the equilibrium condition using the general relativistic constraint for accelerated expansion, $\rho_m + \rho_{\Lambda_m} + 3P_{\Lambda_m} = 0$. Using the approximation $w_{\Lambda_m} \approx -1$ for the GSE component, this simplifies to $\rho_m \approx 2\rho_{\Lambda_m}$.

We can now solve for the critical radius, R_{crit}. Substituting the expressions for ρ_m and our GSE-derived ρ_{Λ_m} (Eq. 231), we derive a quadratic equation for the dimensionless variable $X = R_S/R$.

$$\frac{5\beta^2}{14}X^2 - \beta X - 1 = 0. \tag{234}$$

Solving for the positive root gives the critical ratio:

$$\frac{R_S}{R_{\text{crit}}} = \frac{14\beta + \sqrt{196\beta^2 + 280\beta^2}}{10\beta^2} = \frac{7 + \sqrt{119}}{5\beta}. \tag{235}$$

Therefore, the critical radius is

$$R_{\text{crit}} = \left(\frac{5\beta}{7 + \sqrt{119}}\right) R_S \approx 0.28\beta R_S. \tag{236}$$

Assuming $\beta \approx 1.5$ for the high-density core environment, we find

$$R_{\text{crit}} \approx 0.42 R_S. \tag{237}$$

The collapse is thus stabilized at a finite radius of approximately $0.42R_S$, well inside the event horizon but long before the Planck scale. For a stellar black hole of 3 solar masses ($R_S \approx 9$ km), our model predicts that its core would stabilize at a macroscopic critical radius of $R_{\text{crit}} \approx 3.8$ km. **This demonstrates that the singularity is resolved not at the Planck scale, but at a concrete astrophysical scale through classical GSE dynamics alone.**

11.4 Observational validation: The cosmic connection

A common objection to any proposal about black hole interiors is that the relevant physics is hidden behind an event horizon and is therefore not testable. In the MOC framework, the situation is fundamentally different. The mechanism responsible for singularity avoidance is

not introduced as an ad hoc ingredient that acts only inside black holes. It is the same total GSE contribution that is already required to account for the observed acceleration of the universe.

In the cosmological setting, the GSE-induced dark energy density takes the explicit form

$$\rho_{\Lambda_m} = \frac{\beta \rho_m}{2} \frac{R_S}{\chi_p} \left(\frac{5\beta}{14} \frac{R_S}{\chi_p} - 1 \right). \tag{238}$$

where χ_p denotes the particle (comoving) horizon and $R_{\rm phys}$ is the corresponding physical horizon scale. The sign of the dark energy density is governed entirely by the dimensionless compactness factor $\frac{5\beta}{14}\frac{R_S}{\chi_p}$ which directly measures the gravitational compactness of the causally connected universe.

For the representative value $\beta = 1.5$ adopted throughout this work, the sign transition of ρ_{Λ_m} occurs when

$$\left(\frac{5\beta}{14} \frac{R_S}{\chi_p} - 1 \right) = 0 \tag{239}$$

corresponding to the sign-transition scale

$$\chi_p^{\rm tran} \simeq 0.54 R_S. \tag{240}$$

This result demonstrates that the emergence of the repulsive GSE contribution in cosmology is governed by gravitational physics at a sub-horizon scale, $\chi_p^{\rm tran} \simeq 0.54 R_S$, well inside the Schwarzschild radius.

The observational fact that the universe is currently undergoing accelerated expansion implies that the cosmological evolution has entered the regime in which the GSE-induced component satisfies $w_{\Lambda_m} < -1/3$ [1, 2, 44, 64]. Within MOC, this observation empirically confirms the existence and sign of the same GSE mechanism whose Schwarzschild-scale transition is responsible for halting gravitational collapse inside black holes.

Cosmological observations fix the allowed parameter regime of the GSE contribution, including the sign transition near $\chi_p^{\rm tran} \sim 0.54 R_S$. Because the same dimensionless compactness structure governs both cosmology and compact objects, the prediction of a repulsive, non-singular black hole core follows as a derived and testable consequence of the same equations. Remarkably, cosmic acceleration occurs because we exist inside a cosmological black hole.

In this sense, **the accelerating universe and the non-singular black hole are two manifestations of a single Schwarzschild-scale gravitational mechanism.**

11.5 A macroscopic non-singular core and the information paradox

The MOC framework naturally resolves the black hole singularity. Instead of a point of infinite density, the model predicts a finite, macroscopic, non-singular core at the heart of the black hole. As matter collapses past the sign-transition radius ($R_{\rm tran} \approx 0.54 R_S$), the powerful repulsive force generated by the positive ρ_{Λ_m} grows until it precisely counter-balances the attractive force of matter at $R_{\rm crit} \approx 0.42 R_S$, thereby forming a stable macroscopic core.

By replacing the singularity with a stable, **macroscopic** physical structure, this model offers a compelling resolution to the black hole information paradox [63, 65, 66]. The paradox arises because the destruction of information at a singularity violates the fundamental principle of unitarity in quantum mechanics. In our model, this conflict is entirely avoided. Information falling into the black hole is not destroyed; it is encoded in the physical state of this **macroscopic non-singular black hole core**.

Because causality is preserved within this finite, macroscopic structure, the principles of quantum mechanics remain intact throughout the black hole's life and eventual evaporation.

The information can, in principle, be returned to the universe as the black hole radiates away its mass via Hawking radiation, ensuring that the process is unitary. MOC thus provides a classical mechanism that removes one of the deepest paradoxes in modern physics, offering a complete and self-consistent picture of a black hole from its event horizon to its very core.

12 Observational Tests and Falsifiability of MOC

12.1 Test 1: The sign-switch of dark energy

Prediction. A generic prediction of the MOC framework is that the dark energy density was negative (attractive) during an extended early epoch. Using the updated CMB-based simulations with $H_0 = 67.360\,\mathrm{km\,s^{-1}\,Mpc^{-1}}$, $\Omega_m = 0.3158$, and $\chi_p(t_0) = 46.114\,\mathrm{Gly}$ (Tables 3–6), the transition to positive values occurs in the range

$$t_{\mathrm{tran}} \approx 4.98\text{–}6.07\ \mathrm{Gyr}, \qquad z_{\mathrm{tran}} \approx 0.95\text{–}1.24$$

depending on the assumed matter enhancement scenario. This contrasts sharply with the ΛCDM expectation of a strictly positive and constant ρ_Λ at all redshifts.

Test. This prediction can be tested through model-independent reconstructions of $H(z)$ and $\rho_{\mathrm{DE}}(z)$ using supernovae (Pantheon+), BAO, and cosmic chronometers [11,67,68]. MOC would be falsified if future data from DESI, Euclid, or LSST demonstrate with high statistical confidence that $\rho_{\mathrm{DE}}(z)$ has remained strictly positive for all epochs $z \lesssim 1.5$ (corresponding to cosmic times $t \gtrsim 4\,\mathrm{Gyr}$), with no indication of an earlier attractive phase.

12.2 Test 2: Enhanced early structure growth

Prediction. Because ρ_{Λ_m} is negative for all $t \lesssim 4.98\text{–}6.07\,\mathrm{Gyr}$ (i.e., $z \gtrsim 0.95\text{–}1.24$), the early universe experiences an additional attractive contribution to the energy budget. This is expected to enhance the growth of density perturbations and to yield a systematically larger value of the growth-rate observable $f\sigma_8(z)$ at intermediate and high redshifts relative to ΛCDM.

Test. Measurements of $f\sigma_8(z)$ from redshift-space distortions and weak-lensing surveys provide a direct probe of this prediction [69,70]. If high-redshift data ($z \gtrsim 1.0$) from DESI or Euclid find a growth history fully consistent with, or weaker than, the ΛCDM expectation, the MOC prediction of an early attractive phase would be strongly disfavored.

12.3 Test 3: The post–crossover evolution of ρ_{Λ_m}

Prediction. In all updated CMB-based simulations, $\rho_{\Lambda_m}(t)$ exhibits a rapid increase immediately after the sign-switch, reaches a peak in the range $t \approx 9.7\text{–}11.8\,\mathrm{Gyr}$ depending on the matter enhancement scenario, and subsequently shows a gradual decline toward the present epoch. Recall the dark energy density derived in Eq. (32):

$$\rho_{\Lambda_m} = \frac{\beta\rho_m}{2}\frac{R_S}{\chi_p}\left(\frac{5\beta}{14}\frac{R_S}{\chi_p} - 1\right). \tag{241}$$

This characteristic "rise-and-fall" behavior follows directly from this expression, which ties the dark energy density to the evolving combination $\rho_m(R_S/\chi_p)$.

During the post-crossover era, the enclosed mass and thus R_S increase only slowly, while the physical matter density $\rho_m(t)$ continues to decrease as the universe expands and the particle horizon $\chi_p(t)$ grows. As a result, the combination $\rho_m(R_S/\chi_p)$ initially increases, reaches a maximum, and eventually begins to decrease.

This naturally generates a finite peak in $\rho_{\Lambda_m}(t)$, followed by a gradual decline once the decrease in $\rho_m(t)$ and the growth of $\chi_p(t)$ dominate over the increase in R_S. Thus MOC predicts a dynamic dark energy density that is distinct both from the constant ρ_Λ of the standard ΛCDM model and from the simple monotonic evolution typical of quintessence scenarios [3, 64].

Test. Reconstruction of $\rho_{\rm DE}(z)$ using SNe, BAO, and cosmic chronometers can reveal whether dark energy flattens or begins to weaken at late times ($z \lesssim 0.5$) [68]. MOC would be falsified if the reconstructed $\rho_{\rm DE}(z)$ shows a strictly monotonic increase for all $z \lesssim 1.0$ with no sign of flattening or turnover, or if it remains exactly constant to high precision across the entire redshift range. Conversely, any detected late-time evolution of dark energy density, i.e. $w > -1$ at low z, as tentatively suggested by recent DESI analyses and by the supernova-based interpretation of Son et al. [11, 44], would strongly support the MOC scenario.

12.4 Test 4: Extensive falsifiability from an explicit functional origin

The Prediction: Unlike phenomenological dark energy models, MOC provides a fully explicit functional origin for the dark energy density ρ_{Λ_m}, specifying its dependence on cosmic variables (e.g., ρ_m, χ_p) in analytic form. This functional transparency renders the model highly and systematically falsifiable in principle: any discrepancy in the detailed time/redshift evolution, scale dependence, or internal parameter relationships can serve as a direct test of the theory.

The Test: The analytical form of $\rho_{\Lambda_m}(t)$ is known, enabling comprehensive comparisons with high-precision observations for all detailed properties of functional evolution, as well as global features (sign conversion, peak, decline). Future advances in reconstructing the cosmic expansion history, horizon scale, and matter density (from DESI, Euclid, JWST, SKA, and beyond) will allow a continually expanding set of new and increasingly precise tests of the model. This falsifiability, made possible by MOC's explicit predictive formalism, provides a transparent link between theory and observation and offers a particularly direct framework for empirical testing.

13 Discussion

In this work, we have presented a mechanism in which the GSE of matter reproduces the phenomenology normally attributed to dark energy. While our primary analysis focused on the β-normalized model (where the interaction term scales with β^2), it is crucial to examine the robustness of this result against alternative choices of interaction coefficients and to address current observational uncertainties.

13.1 Role of the structure coefficient β and model robustness

In deriving the interaction energy between the matter distribution and the equivalent negative mass associated with the GSE, we introduced the structure coefficient β not as an independent dynamical degree of freedom, but as a geometric coefficient to describe the physical state of matter. Since the cosmic matter distribution is neither perfectly uniform nor static, the calculation of the GSE within any given shell inherently depends on this structural descriptor, as defined via $U_{gs}(r) = -\beta GM(r)^2/r$. This single coefficient serves as an effective structural descriptor of the mass distribution. Known reference systems indicate that β can naturally vary across values of order unity: $\beta = 3/5$ for an ideal Newtonian uniform sphere, $\beta = 3/2$ for the classical $n = 3$ polytrope [19], and $\beta \simeq 1.0$–1.6 for NFW-like halo profiles, depending on the concentration parameter [20, 30, 31].

Our simulations demonstrate that once galaxy-scale structures have formed ($t \gtrsim 1\,\mathrm{Gyr}$), the evolution of β becomes very slow, effectively acting as a quasi-constant coefficient for the remainder of cosmic history. This implies that the detailed time-evolution of $\beta(t)$ is not critical for the emergence of cosmic acceleration.

Consequently, the choice of how the interaction term scales with β (e.g., linear β vs. quadratic β^2) becomes a question of matching the effective coupling strength to the assumed background matter density. In our β^2-scaled formulation, which propagates the structural information consistently, the CMB based MOC solutions with matter enhancements of $\{-10\%, 0\%, +10\%, +20\%\}$ yield present-epoch coefficients spanning the range from $\beta(t_0) \simeq 1.2387$ for the +20% model, to 1.4071 for the +10% model, to 1.6172 for the 0% model, and to 1.8854 for the −10% model. These values are broadly consistent with the reference range suggested by known self-gravitating structures.

By contrast, if one adopts a linear interaction scaling, in which the interaction term carries only one power of the structure coefficient rather than β^2, the present SH0ES baseline with $\Omega_m = 0.315$ requires a substantially larger effective coefficient, $\beta \simeq 7.37$, in order to reproduce the observed late-time cosmic acceleration. Such a large value lies well outside the reference range suggested by known self-gravitating systems, such as polytropic and NFW-like configurations. The linear scaling therefore appears less economical under the current baseline assumptions.

However, the required coefficient in the linear formulation decreases if the effective cosmic matter density is higher. For sufficiently enhanced matter abundance, for example $\Omega_m \gtrsim 0.35$, the required value of β can return to the broad reference range associated with known self-gravitating structures. Thus, the linear interaction scaling is not excluded as a possible comparison formulation, but in the present analysis the β^2-scaled formulation provides the more natural and compact description of the observed late-time dark energy density.

13.2 Observational uncertainties and future constraints

First, there is a significant tension in the value of Ω_m across different dataset combinations. As highlighted in recent analyses [44], the inferred matter density can vary substantially, spanning $\Omega_m \approx 0.21$ to $\Omega_m \approx 0.36$, depending on whether SN Ia age-bias corrections are applied and which probes (CMB, BAO, SNe) are combined. Because the structure coefficient β is defined through the matter distribution, this observational scatter in Ω_m directly propagates into an uncertainty range for β. The four CMB-anchored MOC simulations with matter modifications of $\{-10\%, 0\%, +10\%, +20\%\}$ demonstrate the corresponding inferred values of $\beta(t_0)$ as Ω_m varies. In all of these scenarios, however, $\beta(t)$ remains quasi-constant after the epoch of early structure formation, and the MOC model continues to reproduce the observed expansion history even under substantial matter enhancement variations.

Second, and perhaps more fundamentally, nearly all existing cosmological datasets are reduced and calibrated under the assumption of the standard ΛCDM model. There is currently no comprehensive dataset processed specifically within the context of the MOC. Since the MOC model fundamentally reinterprets the source of cosmic acceleration as a GSE effect rather than a vacuum energy, it may ultimately require a re-analysis of raw observational data.

As the MOC framework is still at an early stage, future studies that build dedicated datasets and likelihoods within this alternative paradigm may help break these degeneracies. Once such datasets are established, the MOC framework can be subjected to more stringent observational tests, allowing its viability as a physically motivated alternative to ΛCDM to be assessed more conclusively.

14 Conclusion: A Unified Cosmology from Total Gravitational Self-Energy

The standard cosmological model treats inflation and late-time acceleration as conceptually disconnected phenomena, typically driven by independent scalar fields [53–56, 64]. The GSE framework in Matter-Only Cosmology (MOC) unifies both via a single, intuitive principle.

The matter-induced dark energy density arises from the total GSE of the contents of the causal horizon. Within the total GSE framework, this is expressed as

$$\rho_{\Lambda_m} = \frac{\beta \rho_m}{2} \frac{R_S}{\chi_p} \left(\frac{5\beta}{14} \frac{R_S}{\chi_p} - 1 \right), \tag{242}$$

where ρ_m is the physical matter density defined with respect to the physical volume V_{phys}, and $R_S = \frac{2GM}{c^2}$ is the Schwarzschild radius associated with the total matter mass $M = \rho_m V_{\text{phys}}$ enclosed within the causally connected region.

The same point becomes more transparent when the dark energy density is written directly as a function of the matter density and the characteristic radius of the mass distribution. With $c_1 \equiv \frac{4\pi G}{3c^2}$, $c_2 \equiv \frac{20\pi G}{21c^2}$, the total GSE dark energy density can equivalently be written as

$$\rho_{\Lambda_m}(\rho_m, R) = c_1 \beta \rho_m^2 R^2 \left(c_2 \beta \rho_m R^2 - 1 \right). \tag{243}$$

Thus, apart from the structural coefficient β, the functional dependence is carried by ρ_m and R. Here β is not a new gravitational source or an independent dark energy degree of freedom, but the structural coefficient arising from the GSE integral for a given matter distribution. The dark energy density is therefore not introduced as a new component of the cosmic inventory, but is obtained from the matter distribution itself.

This single total GSE relation encapsulates a fundamental **density–scale duality**: repulsive gravity, $\rho_{\Lambda_m} > 0$, can arise both from extreme density at small scales, as in the inflationary regime, and from the large-scale balance between matter density and horizon growth at low densities, as in the late-time dark energy regime.

In essence, the dynamical interactions governed by this single GSE principle determine the entire history of cosmic expansion, from the onset and natural termination of inflation, to the long epoch of deceleration, to the acceleration phase we observe today, and potentially to a future era of damped oscillatory stability.

By rigorously accounting for the GSE of matter and its contribution to the source of gravity, MOC offers a more complete, self-consistent, and physically motivated description of our universe. It replaces a series of disconnected puzzles with a unified framework and provides a rich set of falsifiable predictions. The next step is clear: to confront this model with the wealth of forthcoming observational data. The journey into the dark sector requires neither new particles nor new forces, but a deeper understanding of gravitational self-interaction within General Relativity.

Finally, the universality of the GSE principle suggests broader implications beyond cosmology. The validity of this self-energy principle is not confined to the macroscopic cosmos. When applied to the microscopic realm, the total GSE dynamics inherently suppresses the gravitational interaction strength near the Planck scale. This suggests that the same framework resolving black hole singularities may also eliminate ultraviolet divergences (UV completion), offering a unified pathway toward the long-sought and definitive "**Completion of Quantum Gravity**" [38, 71].

Puzzle	MOC's Resolution	Key Prediction / Feature
Dark Energy	Replaces the static Λ with a dynamic dark energy density $\rho_{\Lambda_m}(t)$ generated by the GSE of matter.	Predicts a dynamic sequence: **an early negative dark energy density (attractive)**, a current positive dark energy density (repulsive), and a future return to deceleration due to the evolving horizon ratio.
Hubble Tension	Reframes the tension as a measurement of evolving cosmic structure, encapsulated in a time-varying structure coefficient $\beta(t)$.	Naturally explains why CMB ($z \sim 1100$) and local ($z \sim 0$) measurements of H_0 differ, as they probe different epochs with different β values.
Unification of Inflation & Dark Energy	The same GSE mechanism drives both **inflation (high-density repulsion)** and **late-time acceleration (scale-driven repulsion)**.	Naturally explains the 10^{124} energy-scale hierarchy between the two epochs via the geometric scaling of GSE across cosmic evolution.
Cosmic Fate	**Dynamics governed by the competition between matter density and horizon growth.**	Predicts a **damped oscillatory evolution**, preventing eternal acceleration and leading to a stabilized, slowly varying expansion.

Table 13: Summary of cosmological puzzles addressed by MOC. The simulations indicate that these predictions remain qualitatively robust across the scenarios examined, including the predicted future transition to a decelerating phase.

Acknowledgements. All original scientific ideas, physical interpretations, and theoretical proposals presented in this work are the author's own. In particular, the total GSE formula and its physical interpretation, the dark energy density formula and its physical interpretation, Matter-Only Cosmology, the concept of repulsive gravity below the critical radius, the concept of a macroscopic non-singular core, and the unification of inflation and dark energy were all conceived by the author. Generative AI was used during the drafting and editing process to assist with exposition and language refinement. The final manuscript was independently verified by the author, who assumes full responsibility for all content.

A Appendix A: A Re-examination of the Energy Components of a Gravitating System

Theoretical motivation

In this paper, we have developed a cosmological model based on a fundamental principle of General Relativity: *all forms of energy, including gravitational potential energy, must act as sources of gravity [15, 17].* Standard cosmological models typically treat the mass density ρ_m as the sole source of gravity, implicitly assuming that the self-energy of the system is either negligible or already absorbed into the matter sector. However, on cosmological scales, the GSE of the universe becomes significant and cannot be ignored.

We argue that the process of assembling mass M naturally induces a negative GSE component ($-M_{gs}$) and, consequently, a mutual interaction energy ($+M_{m-gs}$) between the matter distribution and the equivalent negative mass associated with its own GSE field. This appendix introduces an approach that explicitly demonstrates that the ρ_{m-gs} term derived from the GSE mechanism is an interaction term between the matter distribution and the equivalent mass associated with the GSE.

$$\rho_{\Lambda_m} = \rho_{m-gs} - \rho_{gs} = \frac{3\beta}{4\pi}\frac{GM^2}{c^2R^4}\left(\frac{5\beta}{14}\frac{R_S}{R} - 1\right). \tag{244}$$

Here, the term $-\rho_{gs}$ represents the traditional negative GSE density, while ρ_{m-gs} represents the positive interaction-energy density arising from the coupling between the matter M and the equivalent negative mass associated with its GSE, $-M_{gs}$. This decomposition reveals that what we observe as "dark energy" is not an exotic addition, but an intrinsic property of a self-gravitating system.

A.1 Total energy components of a gravitating system

In conventional energy accounting of a physical system, it is typically assumed that all forms of energy are implicitly incorporated into an equivalent-mass representation. However, a more careful examination reveals that a dynamical system composed of an extended mass distribution is not a simple single-body system. Instead, it is effectively a composite system that includes an additional negative equivalent mass, $-M_{gs}$, arising from the system's own gravitational potential energy.

A crucial physical effect arises here: when two distinct energy components coexist, a mutual gravitational interaction term U_{m-gs} necessarily appears.

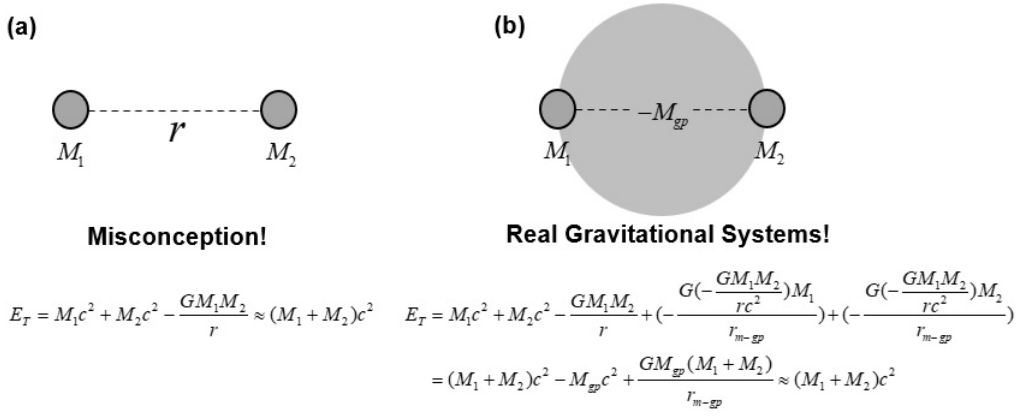

Figure 7: Conceptual diagram illustrating the composite nature of a gravitating system. The system consists of the free mass M_{fr} and the negative equivalent mass of its GSE, $-M_{gs}$. This configuration necessitates an interaction energy term U_{m-gs}, which manifests as a positive energy density.

The total mass-energy of the system is thus

$$M_T \approx M_{fr} + \frac{U_{gs}}{c^2} + \frac{U_{m-gs}}{c^2} = M_{fr} + (-M_{gs}) + M_{m-gs} \tag{245}$$

where $-M_{gs}$ and $+M_{m-gs}$ are the equivalent masses of the GSE and of the interaction energy U_{m-gs}, respectively.

Since the gravitational potential energy between a positive mass ($+M_{fr}$) and a negative equivalent mass ($-M_{gs}$) takes a positive form (repulsive interaction), the interaction energy is given by

$$U_{m-gs} = -\frac{G(+M_{fr})(-M_{gs})}{r} = +\frac{GM_{fr}M_{gs}}{r} > 0. \tag{246}$$

Consequently, the equivalent mass density obtained by dividing this interaction energy by volume, $+\rho_{m-gs}$, carries a positive energy density. The total mass density of the object is therefore

$$\rho_{Total} = \rho_{fr} + \rho_{m-gs} - \rho_{gs} \approx \rho_m + \rho_{m-gs} - \rho_{gs}. \tag{247}$$

1) **Matter (ρ_m):** Strictly speaking, ρ_m is the net result of the free-state mass density ρ_{fr} together with the GSE correction terms, namely the negative GSE term $-\rho_{gs}$ and the interaction term $+\rho_{m-gs}$. Thus, $\rho_m = \rho_{fr} - (\rho_{m-gs} - \rho_{gs})$. In a weak field, $(\rho_{m-gs} - \rho_{gs})$ is negligible, thus $\rho_m \approx \rho_{fr}$. This matter distribution is the ultimate source of all subsequent gravitational effects.

2) **GSE ($-\rho_{gs}$):** The mass-equivalent of the system's own negative binding energy (U_{gs}). Taken in isolation, the negative GSE density plays an attractive role. In cosmology, however, it is more appropriate to interpret the effective behavior through the combined quantity $\rho_{\Lambda_m} = \rho_{m-gs} - \rho_{gs}$ rather than through the $-\rho_{gs}$ term alone.

3) **Interaction energy ($+\rho_{m-gs}$):** The mass-equivalent of the positive GPE that arises from the interaction between the matter field (M) and its own negative GSE field ($-M_{gs}$). Taken in isolation, the positive interaction-energy density tends to contribute repulsively. In cosmology, however, it is more appropriate to characterize the effective behavior through the combined quantity $\rho_{\Lambda_m} = \rho_{m-gs} - \rho_{gs}$ rather than through the ρ_{m-gs} term alone.

In standard astrophysical contexts, the term $(\rho_{m-gs} - \rho_{gs})$ is negligible compared to ρ_m, justifying the approximation $\rho_{Total} \approx \rho_m$. However, on the cosmological scale, these terms are no longer negligible. The net GSE-related contribution, $\rho_{\Lambda_m} = \rho_{m-gs} - \rho_{gs}$, becomes the dominant component driving cosmic acceleration.

$$\rho_{\Lambda_m} = \rho_{m-gs} - \rho_{gs}. \tag{248}$$

A.2 Derivation of the matter-induced dark energy density

Having established the conceptual basis of MOC and the General GSE Framework, we now derive the explicit form of the dark energy density, ρ_{Λ_m}. The derivation uses a physical picture in which the relevant interaction scale is identified with the causal scale, taken here to be the comoving horizon χ_p. The resulting global GSE is then expressed as an energy density with respect to the physical volume V_{phys} [15, 35, 37].

The total energy density entering the Friedmann equation is given by $\rho_T = \rho_m + \rho_{m-gs} - \rho_{gs}$. The latter two terms, arising purely from gravitational interactions, constitute the matter-induced dark energy density.

The entire derivation originates from the GSE of the total mass $M(t)$ contained within the causal horizon. While the classical form scales as $1/R$, in our General GSE framework, the characteristic interaction length scale is the comoving horizon $\chi_p(t)$.

$$U_{gs,\text{General}} = -\beta(t)\frac{GM(t)^2}{\chi_p(t)}. \tag{249}$$

Here, $\beta(t)$ encapsulates the necessary relativistic and structural corrections, evolving as the universe transitions from homogeneity to a structured state.

A.2.1 The negative-energy component: $-\rho_{gs}$

The first component, $-\rho_{gs}$, represents the equivalent mass density of the system's own gravitational binding energy. This binding energy corresponds to a mass defect, effectively creating a negative equivalent mass component, $-M_{gs}$, within the total energy budget [17, 18, 36].

$$-M_{gs} = \frac{U_{gs,\text{General}}}{c^2} = -\frac{\beta G M(t)^2}{c^2 \chi_p(t)}. \tag{250}$$

Distributing this negative equivalent mass over the physical volume $V_{\text{phys}}(t) = \frac{4\pi}{3} R_{\text{phys}}(t)^3$ yields the negative energy density component.

$$-\rho_{gs}(t) = \frac{-M_{gs}}{V_{\text{phys}}(t)} = -\frac{3\beta(t)}{4\pi} \frac{G M(t)^2}{c^2 \chi_p(t) R_{\text{phys}}(t)^3}. \tag{251}$$

A.2.2 The positive-energy component: $+\rho_{m-gs}$

The existence of the negative equivalent mass component ($-M_{gs}$) within the region containing the positive mass M necessitates an interaction term. The interaction energy U_{m-gs} arises from the gravitational coupling between the matter distribution M and the effective negative-mass component $-M_{gs}$. Here, we make a critical choice for the interaction coefficient.

A.2.3 A Note on the Interaction Coefficient

In the main text, the total GSE is formulated using a single effective structure coefficient β. The same coefficient is used for the conventional GSE contribution and for the matter–GSE interaction term. This gives the most compact form of the framework and is motivated by the fact that both terms arise from the same self-gravitating mass distribution and the same GSE source-completion principle.

More generally, however, one may distinguish two structural roles.

The first coefficient, denoted here by β_1, characterizes the conventional GSE contribution that enters the equivalent GSE mass, $M_{gs} = \beta_1 \frac{GM(t)^2}{c^2 \chi_p(t)}$.

The second coefficient, denoted by β_2, may be assigned to the structural normalization of the integral in which the equivalent source mass interacts with the ordinary matter shell. Such a two-coefficient description represents a more detailed parametrization of the same GSE framework, rather than a different physical principle.

The main text adopts the single-coefficient formulation $\beta_1 = \beta_2 \equiv \beta$. This is the minimal model analyzed in this work.

For comparison, this appendix also considers the unit-interaction normalization. In this convention, the interaction normalization is set to unity, while the GSE structure coefficient is retained in the equivalent GSE mass.

With this convention, the interaction energy in the General GSE framework is written as

$$U_{m\text{-}gs} \approx -\frac{GM(t)(-M_{gs})}{\chi_p(t)} = +\frac{GM(t)M_{gs}}{\chi_p(t)}. \tag{252}$$

Substituting

$$M_{gs} = \beta \frac{GM(t)^2}{c^2 \chi_p(t)} \tag{253}$$

gives

$$U_{m\text{-}gs} = +\beta \frac{G^2 M(t)^3}{c^2 \chi_p(t)^2}. \tag{254}$$

The corresponding positive equivalent mass density is therefore

$$\rho_{m\text{-}gs}(t) = \frac{U_{m\text{-}gs}}{V_{\text{phys}}(t)c^2} = \frac{3\beta(t)}{4\pi} \frac{G^2 M(t)^3}{c^4 \chi_p(t)^2 R_{\text{phys}}(t)^3}. \tag{255}$$

A.3 The complete expression for ρ_{Λ_m}

Combining the positive and negative energy density components, we arrive at the final expression for the dark energy density in the present working model with $\beta_2 = 1$.

$$\rho_{\Lambda_m}(t) = \rho_{m-gs}(t) - \rho_{gs}(t) = \frac{3\beta}{4\pi} \frac{G^2 M^3}{c^4 \chi_p^2 R_{\text{phys}}^3} - \frac{3\beta}{4\pi} \frac{GM^2}{c^2 \chi_p R_{\text{phys}}^3}. \tag{256}$$

To reveal its physical significance, we factor this equation and express the bracketed term using the Schwarzschild radius of the total causal mass, $R_S(t) = 2GM(t)/c^2$.

$$\rho_{\Lambda_m}(t) = \frac{3\beta(t)}{4\pi} \frac{GM(t)^2}{c^2 \chi_p(t) R_{\text{phys}}(t)^3} \left(\frac{GM(t)}{c^2 \chi_p(t)} - 1 \right), \tag{257}$$

$$\rho_{\Lambda_m}(t) = \frac{\beta \rho_m}{2} \frac{R_S}{\chi_p} \left(\frac{1}{2} \frac{R_S}{\chi_p} - 1 \right). \tag{258}$$

This result demonstrates that under the assumption of a unity interaction coefficient, the sign change of ρ_{Λ_m} is governed purely by the ratio of the Schwarzschild radius to the comoving horizon, $\frac{R_S}{2\chi_p} > 1$, without an additional β factor inside the bracketed term.

A.4 Observational validation and the evolution of β

Here we briefly recall the role of the structure coefficient β entering the total GSE expression. It summarizes the dependence of the GSE on the mass distribution and relativistic compactness. Although β may vary over the full cosmic history, its residual evolution after substantial structure formation is expected to be modest, so that an effective late-time constant value can be used in the benchmark analysis.

An important consistency check is obtained by comparing the MOC requirements with empirical anchors from the Cosmic Microwave Background (CMB) [5] and from late universe distance-ladder measurements such as SH0ES [13]. Since the present analytic treatment does not uniquely predict the cosmological value of β from first principles, we infer the value required to reproduce the observed present-day dark energy density under each baseline and compare it with the broad structural range suggested by gravitationally bound systems, roughly $\beta \simeq 0.6$–2.

The results summarized in Tables 14 and 15 provide auxiliary benchmarks for the structural viability of the MOC framework. The appendix tables are retained as qualitative consistency checks. In particular, the original SH0ES auxiliary run used $\chi_p(t_0) = 43.337\,\text{Gly}$, whereas the updated main-text benchmark uses $\chi_p(t_0) = 43.377\,\text{Gly}$; the difference is below 0.1%, and the main parameter determination follows the updated benchmark values in the main text.

A.5 Computer simulation results

Matter Incr. (%)	ρ_m ($\times 10^{-27}$ kg/m^3)	ρ_{Λ_m}	**Required β**	$\rho_{m\text{-}gs}$ ($\times 10^{-27}$ kg/m^3)	$-\rho_{gs}$
-20	2.150	6.383	**10.2792**	35.186	-28.803
-10	2.419	6.114	**4.6990**	24.264	-18.150
+0	2.688	5.845	**2.6295**	18.573	-12.728
+10	2.957	5.576	**1.6388**	15.001	-9.425
+20	3.225	5.308	**1.0824**	12.520	-7.212
+30	3.494	5.039	**0.7445**	10.684	-5.645
+40	3.763	4.770	**0.5269**	9.262	-4.492
+50	4.032	4.501	**0.3808**	8.132	-3.631

Table 14: CMB baseline ($H_0 = 67.4$ km/s/Mpc, $R = 46.5$ Gly). Required β and GSE components computed from $\rho_{\Lambda_m} = \beta\left(\frac{4\pi G}{3c^2}\rho_m^2 R^2\right)\left(\frac{4\pi G}{3c^2}\rho_m R^2 - 1\right)$.

Matter Incr. (%)	ρ_m ($\times 10^{-27}$ kg/m^3)	ρ_{Λ_m}	**Required β**	$\rho_{m\text{-}gs}$ ($\times 10^{-27}$ kg/m^3)	$-\rho_{gs}$
-20	2.525	7.495	**7.0184**	30.893	-23.398
-10	2.841	7.178	**3.5026**	21.961	-14.783
+0	3.156	6.864	**2.0267**	17.419	-10.555
+10	3.472	6.548	**1.2738**	14.577	-8.029
+20	3.788	6.232	**0.8469**	12.586	-6.354
+30	4.103	5.917	**0.5868**	11.083	-5.166
+40	4.419	5.601	**0.4185**	9.874	-4.273
+50	4.734	5.286	**0.3057**	8.869	-3.583

Table 15: SH0ES baseline ($H_0 = 73.04$ km/s/Mpc, $R = 43.337$ Gly). Required β and GSE components computed from $\rho_{\Lambda_m} = \beta\left(\frac{4\pi G}{3c^2}\rho_m^2 R^2\right)\left(\frac{4\pi G}{3c^2}\rho_m R^2 - 1\right)$.

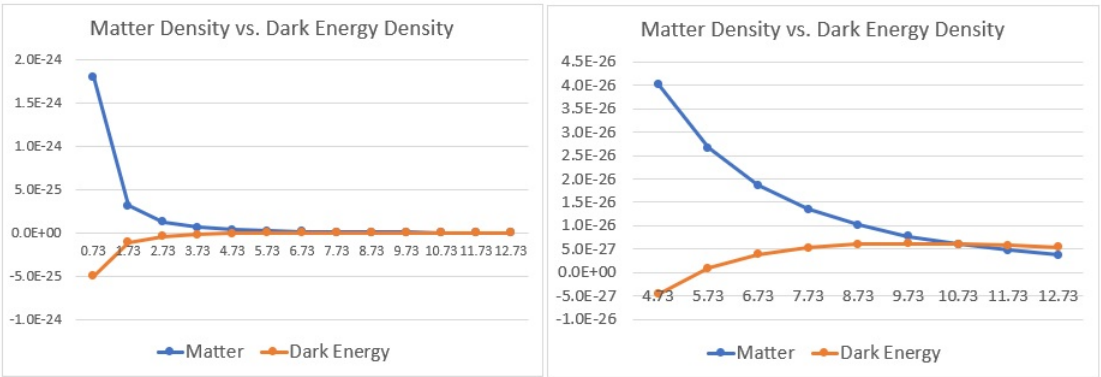

Figure 8: **Matter Density vs. Dark Energy Density (SH0ES baseline, Model-2, +10% Matter Enhancement):** $\Omega_m = 0.347$. In the early universe, the dark energy density is negative and promotes structure formation. It changes sign near $t \approx 5$ Gyr, after which it contributes to the accelerated expansion of the universe. At approximately $t \approx 7.5$ Gyr, the matter density and dark energy density become comparable, and the dark energy density reaches a maximum near $t \approx 8.7$ Gyr before gradually decreasing.

Age (Gyr)	Scale $a(t)$	Evolving $\beta(t)$	Comoving Ho. $\chi_p(t)$ (Gly)	Physical Ho. $R_{\rm phys}(t)$ (Gly)	**Matter** $\rho_m(t)$	Repulsive $\rho_{m-gs}(t)$	Attractive $-\rho_{gs}(t)$	**Dark Energy** $\rho_{\Lambda_m}(t)$
					(10^{-27} kg m^{-3})			
0.73	0.1283	1.6388	17.080	2.191	1645.27	214.737	-760.898	**-546.161**
1.73	0.2285	1.6084	22.764	5.202	291.245	117.716	-234.819	**-117.103**
2.73	0.3111	1.5780	26.487	8.240	115.403	83.876	-123.586	**-39.710**
3.73	0.3854	1.5476	29.365	11.317	60.699	65.364	-78.356	**-12.992**
4.73	0.4552	1.5171	31.748	14.452	36.839	53.136	-54.495	**-1.359**
5.73	0.5224	1.4867	33.797	17.656	24.373	44.243	-40.039	4.204
6.73	0.5883	1.4563	35.599	20.943	17.066	37.352	-30.467	6.885
7.73	0.6540	1.4259	37.211	24.336	12.422	31.779	-23.725	8.054
8.73	0.7200	1.3955	38.668	27.841	9.309	27.179	-18.790	8.389
9.73	0.7871	1.3651	39.996	31.481	7.126	23.293	-15.052	8.241
10.73	0.8559	1.3346	41.214	35.275	5.542	19.970	-12.153	7.817
11.73	0.9266	1.3042	42.337	39.229	4.368	17.126	-9.877	7.249
12.73	1.0000	1.2738	43.337	43.337	3.475	14.610	-8.041	6.569

Table 16: **MOC Cosmic History Simulation (SH0ES baseline, Model-2, +10% Matter Enhancement).** Results obtained using the Model-2 interaction-coefficient choice ($\beta_2 = 1$) discussed in the Appendix. The structure coefficient evolves linearly from $\beta(0.73\,\text{Gyr}) = 1.6388$ to $\beta(12.73\,\text{Gyr}) = 1.2738$. Even with the reduced magnitude of the repulsive term (proportional to β rather than β^2), the model still exhibits a transition of the dark energy density from negative to positive values near $t \approx 5.0\,\text{Gyr}$, illustrating the robustness of the GSE-driven acceleration mechanism.

Age (Gyr)	Scale $a(t)$	Evolving $\beta(t)$	Comoving Ho. $\chi_p(t)$ (Gly)	Physical Ho. $R_{\rm phys}(t)$ (Gly)	**Matter** $\rho_m(t)$	Repulsive $\rho_{m-gs}(t)$	Attractive $-\rho_{gs}(t)$	**Dark Energy** $\rho_{\Lambda_m}(t)$
					(10^{-27} kg m^{-3})			
0.73	0.1283	1.0824	17.080	2.191	1794.84	184.134	-598.089	**-413.955**
1.73	0.2285	1.0628	22.764	5.202	317.722	100.984	-184.655	**-83.672**
2.73	0.3111	1.0432	26.487	8.240	125.894	71.987	-97.229	**-25.242**
3.73	0.3854	1.0235	29.365	11.317	66.217	56.125	-61.674	**-5.549**
4.73	0.4552	1.0039	31.748	14.452	40.188	45.648	-42.914	2.734
5.73	0.5224	0.9843	33.797	17.656	26.589	38.027	-31.546	6.481
6.73	0.5883	0.9647	35.599	20.943	18.617	32.122	-24.018	8.104
7.73	0.6540	0.9450	37.211	24.336	13.551	27.345	-18.713	8.632
8.73	0.7200	0.9254	38.668	27.841	10.156	23.400	-14.829	8.571
9.73	0.7871	0.9058	39.996	31.481	7.773	20.066	-11.886	8.180
10.73	0.8559	0.8862	41.214	35.275	6.046	17.214	-9.603	7.611
11.73	0.9266	0.8665	42.337	39.229	4.765	14.773	-7.810	6.963
12.73	1.0000	0.8469	43.337	43.337	3.791	12.611	-6.363	6.248

Table 17: **MOC Cosmic History Simulation (SH0ES baseline, Model-2, +20% Matter Enhancement).** Results obtained using the Model-2 assumption ($\beta_2 = 1$). The structure coefficient evolves linearly from $\beta(0.73\,\text{Gyr}) = 1.0824$ to $\beta(12.73\,\text{Gyr}) = 0.8469$. In this case, the dark energy density changes sign between $t = 3.73$ and $4.73\,\text{Gyr}$, corresponding to a transition near $t \approx 4.4\,\text{Gyr}$, reflecting the effect of the enhanced matter density. The dark energy density then reaches a maximum near $t \approx 7.7$–$8.0\,\text{Gyr}$ and subsequently decreases slowly, illustrating the dynamic character of the GSE mechanism.

References

[1] A. G. Riess *et al.* (Supernova Search Team), "Observational Evidence from Supernovae for an Accelerating Universe and a Cosmological Constant," Astron. J. **116**, 1009 (1998).

[2] S. Perlmutter *et al.* (Supernova Cosmology Project), "Measurements of Ω and Λ from 42 High-Redshift Supernovae," Astrophys. J. **517**, 565 (1999).

[3] P. J. E. Peebles and B. Ratra, "The cosmological constant and dark energy," Rev. Mod. Phys. **75**, 559 (2003).

[4] S. Dodelson and F. Schmidt, *Modern Cosmology*, 2nd ed. (Academic Press, 2020).

[5] N. Aghanim *et al.* (Planck Collaboration), "Planck 2018 results. VI. Cosmological parameters," Astron. Astrophys. **641**, A6 (2020).

[6] P. Bull *et al.*, "Beyond ΛCDM: Problems, solutions, and the road ahead," Phys. Dark Universe **12**, 56–99 (2016).

[7] S. Weinberg, "The cosmological constant problem," Rev. Mod. Phys. **61**, 1 (1989).

[8] S. M. Carroll, "The Cosmological Constant," Living Rev. Relativ. **4**, 1 (2001).

[9] I. Zlatev, L.-M. Wang, and P. J. Steinhardt, "Quintessence, Cosmic Coincidence, and the Cosmological Constant," Phys. Rev. Lett. **82**, 896–899 (1999).

[10] E. Di Valentino *et al.*, "In the realm of the Hubble tension: A review of solutions," Class. Quantum Grav. **38**, 153001 (2021).

[11] A. G. Adame *et al.* (DESI Collaboration), "DESI 2024 VI: Cosmological Constraints from the Measurements of Baryon Acoustic Oscillations," arXiv:2404.03002 [astro-ph.CO] (2024).

[12] T. M. C. Abbott *et al.* (DES Collaboration), "The Dark Energy Survey: Cosmology Results with ∼1500 New High-redshift Type Ia Supernovae Using the Full 5-year Dataset," Astrophys. J. Lett. **973**, L14 (2024).

[13] A. G. Riess *et al.*, "Large Magellanic Cloud Cepheid Standards Provide a 1% Foundation for the Determination of the Hubble Constant and Stronger Evidence for Physics beyond ΛCDM," Astrophys. J. **876**, 85 (2019).

[14] C. W. Misner, K. S. Thorne, and J. A. Wheeler, *Gravitation* (W. H. Freeman, 1973).

[15] S. Weinberg, *Gravitation and Cosmology: Principles and Applications of the General Theory of Relativity* (John Wiley & Sons, 1972).

[16] H. C. Ohanian and R. Ruffini, *Gravitation and Spacetime*, 3rd ed. (Cambridge University Press, 2013).

[17] A. Einstein, "Die Grundlage der allgemeinen Relativitätstheorie," Ann. Phys. **354**, 769–822 (1916).

[18] R. M. Wald, *General Relativity* (University of Chicago Press, 1984).

[19] S. Chandrasekhar, *An Introduction to the Study of Stellar Structure* (University of Chicago Press, 1939).

[20] E. Alécian and S. M. Morsink, "The Effect of Neutron Star Gravitational-Binding Energy on Gravitational-Radiation-Driven Mass-Transfer Binaries," Astrophys. J. **614**, 914–921 (2004), arXiv:astro-ph/0302219.

[21] H. Choi, "Dark Energy is Gravitational Potential Energy or Energy of the Gravitational Field," preprint (2022). Available at: https://www.researchgate.net/publication/360096238.

[22] S. Chandrasekhar, "The Post-Newtonian Equations of Hydrodynamics in General Relativity," Astrophys. J. **142**, 1488–1512 (1965).

[23] H. A. Buchdahl, "General Relativistic Fluid Spheres," Phys. Rev. **116**, 1027–1034 (1959).

[24] M. S. R. Delgaty and K. Lake, "Physical Acceptability of Isolated, Static, Spherically Symmetric, Perfect Fluid Solutions of Einstein's Equations," Comput. Phys. Commun. **115**, 395–415 (1998).

[25] W. H. McCrea and E. A. Milne, "Newtonian Universes and the Curvature of Space," Q. J. Math. **5**, 73–80 (1934).

[26] S. L. Shapiro and S. A. Teukolsky, *Black Holes, White Dwarfs, and Neutron Stars: The Physics of Compact Objects* (John Wiley & Sons, 1983).

[27] J. Binney and S. Tremaine, *Galactic Dynamics*, 2nd ed. (Princeton University Press, 2008).

[28] R. C. Tolman, "Static Solutions of Einstein's Field Equations for Spheres of Fluid," Phys. Rev. **55**, 364 (1939).

[29] J. R. Oppenheimer and G. M. Volkoff, "On Massive Neutron Cores," Phys. Rev. **55**, 374 (1939).

[30] S. Rosswog, "SPH Methods in the Modelling of Compact Objects," Living Rev. Comput. Astrophys. **1**, 1 (2015), arXiv:1406.4224 [astro-ph.IM].

[31] A. A. Dutton and A. V. Macciò, "Cold dark matter haloes in the Planck era: evolution of structural parameters for Einasto and NFW profiles," Mon. Not. R. Astron. Soc. **441**, 3359–3374 (2014).

[32] H. Choi, "Sphere Theory: Completing Quantum Gravity through Gravitational Self-Energy," preprint (2025). Available at: https://www.researchgate.net/publication/388995044.

[33] M. Boylan-Kolchin, V. Springel, S. D. M. White, A. Jenkins, and G. Lemson, "Resolving cosmic structure formation with the Millennium-II Simulation," Mon. Not. R. Astron. Soc. **398**, 1150–1164 (2009).

[34] A. Pillepich *et al.*, "First results from the IllustrisTNG simulations: the stellar mass content of groups and clusters of galaxies," Mon. Not. R. Astron. Soc. **473**, 4077–4106 (2018).

[35] P. J. E. Peebles, *Principles of Physical Cosmology* (Princeton University Press, 1993).

[36] S. W. Hawking and G. F. R. Ellis, *The Large Scale Structure of Space-Time* (Cambridge University Press, 1973).

[37] V. F. Mukhanov, *Physical Foundations of Cosmology* (Cambridge University Press, 2005).

[38] H. Choi, "The Klein-Gordon-Choi Equation: A Unified Resolution of the Divergences in Quantum Gravity and QED," preprint (2025). Available at: https://www.researchgate.net/publication/398285103.

[39] H. B. Callen, *Thermodynamics and an Introduction to Thermostatistics*, 2nd ed. (John Wiley & Sons, New York, 1985).

[40] S. M. Carroll, M. Hoffman, and M. Trodden, "Can the dark energy be a phantom?," Phys. Rev. D **68**, 023509 (2003).

[41] J. M. Cline, S. Jeon, and G. D. Moore, "The phantom menaced: Constraints on low-energy effective ghosts," Phys. Rev. D **70**, 043543 (2004).

[42] R. V. Buniy and S. D. H. Hsu, "Instabilities and the null energy condition," Phys. Lett. B **632**, 543–546 (2006).

[43] E. Abdalla *et al.*, "Cosmology intertwined: A review of the particle physics, astrophysics, and cosmology associated with the cosmological tensions and anomalies," J. High Energy Astrophys. **34**, 49–211 (2022).

[44] J. Son, Y.-W. Lee, C. Chung, S. Park, and H. Cho, "Strong progenitor age bias in supernova cosmology – II. Alignment with DESI BAO and signs of a non-accelerating universe," Mon. Not. R. Astron. Soc. **544**, 975–987 (2025).

[45] I. Labbé *et al.*, "A population of red candidate massive galaxies at $z > 10$," Nature **616**, 266–269 (2023).

[46] M. Boylan-Kolchin, "Stress testing ΛCDM with high-redshift galaxy candidates," Nat. Astron. **7**, 731–735 (2023).

[47] T. Saifollahi *et al.* (Euclid Collaboration), "Euclid: Early Release Observations – Globular clusters in the Fornax galaxy cluster, from dwarf galaxies to the intracluster field," arXiv:2405.13500 [astro-ph.GA] (2024).

[48] P. A. Burger *et al.* (KiDS-1000 Collaboration), "KiDS-1000 cosmology: Constraints from density split statistics," Astron. Astrophys. **669**, A69 (2023).

[49] X. Fan *et al.*, "Constraining the Evolution of the Ionizing Background and the Epoch of Reionization with $z \sim 6$ Quasars," Astron. J. **132**, 117 (2006).

[50] K. Inayoshi, E. Visbal, and Z. Haiman, "The Assembly of the First Massive Black Holes," Annu. Rev. Astron. Astrophys. **58**, 27–97 (2020).

[51] B. Ryden, *Introduction to Cosmology* (Addison-Wesley, 2003).

[52] T. M. Davis and C. H. Lineweaver, "Expanding Confusion: Common Misconceptions of Cosmological Horizons and the Superluminal Expansion of the Universe," Publ. Astron. Soc. Aust. **21**, 97–109 (2004), arXiv:astro-ph/0310808.

[53] A. A. Starobinsky, "A new type of isotropic cosmological models without singularity," Phys. Lett. B **91**, 99 (1980).

[54] A. H. Guth, "Inflationary universe: A possible solution to the horizon and flatness problems," Phys. Rev. D **23**, 347 (1981).

[55] A. D. Linde, "A new inflationary universe scenario: A possible solution of the horizon, flatness, homogeneity, isotropy and primordial monopole problems," Phys. Lett. B **108**, 389 (1982).

[56] A. Albrecht and P. J. Steinhardt, "Cosmology for Grand Unified Theories with Radiatively Induced Symmetry Breaking," Phys. Rev. Lett. **48**, 1220 (1982).

[57] D. Baumann, "TASI Lectures on Inflation," arXiv:0907.5424 [hep-th] (2009).

[58] L. Kofman, A. D. Linde, and A. A. Starobinsky, "Reheating after inflation," Phys. Rev. Lett. **73**, 3195 (1994).

[59] B. A. Bassett, S. Tsujikawa, and D. Wands, "Inflation dynamics and reheating," Rev. Mod. Phys. **78**, 537–589 (2006).

[60] S. Nojiri and S. D. Odintsov, "Unifying phantom inflation with late-time acceleration: Scalar phantom-non-phantom transition phase and generalized holographic dark energy," Gen. Relativ. Gravit. **38**, 1285–1304 (2006).

[61] R. Penrose, "Gravitational Collapse and Space-Time Singularities," Phys. Rev. Lett. **14**, 57–59 (1965).

[62] S. W. Hawking and R. Penrose, "The Singularities of Gravitational Collapse and Cosmology," Proc. R. Soc. Lond. A **314**, 529–548 (1970).

[63] S. W. Hawking, "Breakdown of predictability in gravitational collapse," Phys. Rev. D **14**, 2460–2473 (1976).

[64] J. A. Frieman, M. S. Turner, and D. Huterer, "Dark Energy and the Accelerating Universe," Annu. Rev. Astron. Astrophys. **46**, 385–432 (2008).

[65] J. Preskill, "Do Black Holes Destroy Information?," arXiv:hep-th/9209058 (1992).

[66] L. Susskind, L. Thorlacius, and J. Uglum, "The Stretched Horizon and Black Hole Complementarity," Phys. Rev. D **48**, 3743–3761 (1993), arXiv:hep-th/9306069.

[67] D. Scolnic *et al.* (Pantheon+ Collaboration), "The Pantheon+ Analysis: The Full Data Set and Light-curve Release," Astrophys. J. **938**, 113 (2022).

[68] R. Jimenez and A. Loeb, "Constraining Cosmological Parameters Based on Relative Galaxy Ages," Astrophys. J. **573**, 37 (2002).

[69] R. C. Nunes and S. Vagnozzi, "Arbitrating the S_8 discrepancy with growth rate measurements from redshift-space distortions," Mon. Not. R. Astron. Soc. **505**, 5427–5437 (2021).

[70] N. Kaiser, "Clustering in real space and in redshift space," Mon. Not. R. Astron. Soc. **227**, 1–21 (1987).

[71] H. Choi, "The Physical Origin of the Planck Scale Cutoff and Completion of Perturbative Quantum Gravity," preprint (2025). Available at: https://www.researchgate.net/publication/397952460.